

**CHARACTERIZATION OF POLY(LACTIC ACID)
COMPOSITE REINFORCED WITH CELLULOSE AND
KERATIN TREATED WITH 1-BUTYL-3-
METHYLIMIDAZOLIUM CHLORIDE**

KHAW YING YING

**FACULTY OF ENGINEERING
UNIVERSITY OF MALAYA
KUALA LUMPUR**

2019

**CHARACTERIZATION OF POLY(LACTIC ACID)
COMPOSITE REINFORCED WITH CELLULOSE AND
KERATIN TREATED WITH 1-BUTYL-3-
METHYLIMIDAZOLIUM CHLORIDE**

KHAW YING YING

**DISSERTATION SUBMITTED IN FULFILMENT OF
THE REQUIREMENTS FOR THE DEGREE OF MASTER
OF ENGINEERING SCIENCE**

**FACULTY OF ENGINEERING
UNIVERSITY OF MALAYA
KUALA LUMPUR**

2019

UNIVERSITY OF MALAYA
ORIGINAL LITERARY WORK DECLARATION

Name of Candidate: Khaw Ying Ying _____

Matric No: KGA 160041

Name of Degree: Master of Engineering Science

Title of Dissertation:

Characterization of Poly(Lactic Acid) Composite Reinforced with Cellulose and Keratin Treated with 1-Butyl-3-Methylimidazolium Chloride

Field of Study: Advanced Materials & Technology

I do solemnly and sincerely declare that:

- (1) I am the sole author/writer of this Work;
- (2) This Work is original;
- (3) Any use of any work in which copyright exists was done by way of fair dealing and for permitted purposes and any excerpt or extract from, or reference to or reproduction of any copyright work has been disclosed expressly and sufficiently and the title of the Work and its authorship have been acknowledged in this Work;
- (4) I do not have any actual knowledge nor do I ought reasonably to know that the making of this work constitutes an infringement of any copyright work;
- (5) I hereby assign all and every rights in the copyright to this Work to the University of Malaya ("UM"), who henceforth shall be owner of the copyright in this Work and that any reproduction or use in any form or by any means whatsoever is prohibited without the written consent of UM having been first had and obtained;
- (6) I am fully aware that if in the course of making this Work I have infringed any copyright whether intentionally or otherwise, I may be subject to legal action or any other action as may be determined by UM.

Candidate's Signature

Date:

Subscribed and solemnly declared before,

Witness's Signature

Date:

Name:

Designation:

**CHARACTERIZATION OF POLY(LACTIC ACID) COMPOSITE
REINFORCED WITH CELLULOSE AND KERATIN TREATED WITH 1-
BUTYL-3-METHYLIMIDAZOLIUM CHLORIDE**

ABSTRACT

Biodegradable polymers such as poly(lactic acid) (PLA) were receiving much attention in the recent years due to the plastic pollution that filled up the ocean, causing harm to the marine biodiversity. Due to the relative high cost and poor mechanical properties of biodegradable polymers, microcrystalline cellulose (MCC) and keratin from chicken feather fibers (CFF) reinforcements were introduced in PLA to determine the effect of these fillers to the thermal, mechanical and morphological properties to the composites. Dissolution of fillers in ionic liquid (IL) of 1-butyl-3-methylimidazolium chloride (BMIMCl) were implemented to investigate its enhancement of CFF and MCC dispersion in PLA matrices. The PLA composites films were fabricated *via* measuring mixer and compression molding at 180 °C with 1 wt% of fillers consist of 5 compositions of CFF to MCC, namely 100/0, 70/30, 50/50, 30/70 and 0/100 respectively. High intensity of the composite absorption peaks in Fourier transform infrared spectra confirmed that the polymer blends were unaffected by the high temperature processing and ionic liquid (IL). As CFF/MCC ratio increased in the composites without IL, glass transition temperature, T_g decreased. The T_g further declined with BMIMCl added composites due to the chain flexibility increment and shortening of polymer chain length. This was in contrast to the increase in Vickers hardness and thermal stability as CFF composition increased in the presence of BMIMCl. Incorporation of BMIMCl in the composites produced porous structure in the PLA matrices as seen in scanning electron microscope (SEM) images which corresponded to their relative reduction in T_g , melting temperature (T_m) and thermal

stability as compared to composites without IL. Apart from no phase separation observed in SEM, BMIMCl were able to enhance the composite compatibility by reducing double T_g to single T_g in 0/100 and 100/0 samples. Although PLA-CFF₇₀MCC₃₀IL obtained the highest crystallinity, χ_c of 46 % in differential scanning calorimetry (DSC), X-ray diffraction patterns showed that PLA-CFF₇₀MCC₃₀ was in turn to achieve the highest crystallinity index (CI) of 41 %. Despite the effect of BMIMCl to the composites were more significant than fillers compositions, 70/30 ratio was the best in attaining optimum compatibility and polymer chain flexibility.

Keywords: protein, polysaccharide, ionic liquid, thermoplastic

Universiti Malaysia

**PENCIRIAN KOMPOSIT POLI ASID LAKTIK DIPERKUKUHKAN DENGAN
SELULOSA DAN KERATIN DIRAWAT DENGAN 1-BUTIL-3-
METILIMIDAZOLIUM KLORIDA**

ABSTRAK

Polimer biodegradasi seperti poli asid laktik telah menerima banyak perhatian pada tahun-tahun kebelakangan ini kerana pencemaran plastik yang memenuhi lautan, menyebabkan bahaya kepada biodiversiti laut. Disebabkan oleh kos tinggi dan sifat mekanikal yang rendah dalam polimer biodegradasi, selulosa kristal mikro dan keratin dari serat bulu ayam diperkenalkan sebagai pengukuhan ke dalam poli asid laktik untuk menentukan kesan pengisi-pengisi tersebut kepada sifat terma, mekanikal dan morfologi kepada komposit. Pelarutan pengisi dalam cecair ionik 1-butyl-3-metilimidazolium klorida telah dilaksanakan untuk menyiasat peningkatan penyebaran serat bulu ayam dan selulosa kristal mikro dalam matrik poli asid laktik. Filem komposit poli asid laktik telah disediakan melalui pengadun pengukur dan pengacuan mampatan dengan suhu 180 °C dengan 1 % berat pengisi dalam 5 komposisi serat bulu ayam kepada selulosa kristal mikro dan komposisi masing-masing adalah 100/0, 70/30, 50/50, 30/70 dan 0/100. Keamatan yang tinggi dari puncak penyerapan komposit di spektra spektroskopi intramerah transformasi Fourier mengesahkan bahawa campuran polimer tidak dipengaruhi oleh pemprosesan suhu tinggi dan cecair ionik. Oleh kerana nisbah serat bulu ayam/ selulosa kristal mikro meningkat dalam komposit tanpa cecair ionik, suhu peralihan kaca menurun. Suhu peralihan kaca merosot selanjutnya dengan tambahan cecair ionic dalam komposit kerana peningkatan rantai fleksibiliti dan pemendekkan panjang rantaian polimer. Hal ini bercanggah dengan kenaikan kekerasan Vickers dan kestabilan terma apabila komposisi serat bulu ayam meningkat dengan kehadiran cecair ionik. Penggabungan cecair ionik dalam komposit menghasilkan struktur berliang dalam

matrik poli asid laktik seperti yang dilihat dalam pengimbasan imej mikroskop elektron yang sepadan dengan pengurangan suhu peralihan kaca, suhu lebur dan kestabilan haba secara relatif berbanding dengan komposit tanpa cecair ionik. Selain daripada pemisahan fasa yang diperhatikan di pengimbasan mikroskop elektron, cecair ionik dapat meningkatkan keserasian komposit dengan mengurangkan suhu peralihan kaca yang berganda kepada tunggal dalam sampel 0/100 dan 100/0. Walaupun PLA-CFF₇₀MCC₃₀IL memperolehi sifat krystal yang tertinggi iaitu 46 % dalam kalorimetri pengimbasan berbeza, corak difraksi sinaran-X menunjukkan bahawa PLA-CFF₇₀MCC₃₀ selanjutnya mencapai 41 % indeks sifat krystal. Meskipun cecair ionik memberi kesan yang lebih ketara kepada komposit daripada komposisi pengisi, 70/30 adalah nisbah yang terbaik dalam mencapai keserasian polimer dan fleksibiliti rantaian polimer yang optimum.

Kata kunci: protein, polisakarida, cecair ioni, termoplastik

ACKNOWLEDGEMENTS

I sincerely thank my main supervisor, Associate Prof. Ir. Dr. Ching Yern Chee for her scientific mentorship with numerous fresh ideas and important comments during my research. The research would not be successful without her supportive funding as well as from the Head of University of Malaya Centre for Ionic Liquids, Prof. Dr. Mohd Ali Bin Hashim for the supplement of different kinds of valuable ionic liquids. I was fortunate to have my co-supervisor, Prof. Dr. Gan Seng Neon who had given vast and valuable opportunities for me to learn new experiences in my research related conference and student exchange. Especially, the inspiring research stories from his lifelong experience as a professor.

Special thanks to my laboratory seniors who guided me through the beginning stage of getting used to the laboratory and life in University of Malaya. They are Mok Chun Fah, Yee Yin Yin, Sampath Udeni Gunathilake and Goh Kar Yin who patiently taught me the laboratory instruments operation and providing technical feedback on my work. At the end, I could not be more grateful to my parents for devoting a big portion of their life to me and encouraging me to pursue higher degree education as well as the endless mental support from my loved one.

TABLE OF CONTENTS

Abstract	iii
Abstrak	v
Acknowledgements	vii
Table of Contents	viii
List of Figures	xi
List of Tables.....	xiii
List of Symbols and Abbreviations.....	xiv
CHAPTER 1: INTRODUCTION.....	1
1.1 Research Background	1
1.2 Problem Statement.....	5
1.3 Research Objectives.....	6
1.4 Scope of Study.....	7
1.5 Thesis Outline.....	8
CHAPTER 2: LITERATURE REVIEW.....	9
2.1 Poly(lactic acid) (PLA).....	9
2.1.1 Chemical Structure	9
2.1.2 Properties and Applications.....	10
2.2 Polymer Reinforcement in PLA Composite Films.....	13
2.2.1 Cellulose.....	13
2.2.2 Keratin	16
2.2.2.1 Keratin Protein from Feather.....	17
2.2.3 Cellulose-Keratin Composites.....	19
2.2.4 Other Types of Organic Fillers.....	22

2.2.4.1	Chitin	23
2.2.4.2	Starch.....	25
2.3	Green Chemistry for Polymer Composite	27
2.3.1	Type of Green Chemistry	27
2.3.2	Green Solvent – Ionic Liquids.....	28
2.3.3	Types and Properties of Ionic Liquids	29
2.3.4	The Use and Application of Ionic Liquids in Polymers.....	31
2.3.5	The Role of 1-Butyl-3-methylimidazolium chloride (BMIMCl) in Biopolymers	33
2.4	Processing Techniques.....	36
2.4.1	Dissolution of Polymers in BMIMCl.....	36
2.4.2	Fabrication Routes.....	38
2.4.2.1	Solvent Casting	38
2.4.2.2	Melt Compounding	41
2.5	Summary of Literature Review	44
 CHAPTER 3: MATERIALS AND METHODS		47
3.1	Introduction.....	47
3.2	Materials	47
3.3	Methodology.....	47
3.3.1	Physical Treatment of Chicken Feather Fibers (CFF).....	47
3.3.2	Preparation of Composite Films.....	48
3.3.2.1	Experimental Setup	48
3.3.2.2	Dissolution of Fillers in BMIMCl.....	48
3.3.2.3	Film Fabrication	49
3.4	Characterizations of PLA Composite Films	51
3.4.1	Torque Rheometer	51

3.4.2	Fourier Transform Infrared Spectroscopy (FTIR) Analysis.....	52
3.4.3	Thermogravimetric Analysis (TGA).....	52
3.4.4	Differential Scanning Calorimetry (DSC).....	52
3.4.5	X-ray Diffraction Analysis (XRD).....	53
3.4.6	Surface Morphology.....	53
3.4.7	Vickers Hardness Test.....	54
CHAPTER 4: RESULTS AND DISCUSSION		55
4.1	Processing Behavior and Torque Evaluation.....	55
4.2	FTIR Molecular Analysis	64
4.3	Thermogravimetric Analysis	69
4.4	DSC Thermal Properties.....	74
4.5	XRD Phase Identification.....	82
4.6	Scanning Electron Microscopy.....	87
4.7	Vickers Hardness Test.....	95
CHAPTER 5: CONCLUSIONS.....		99
5.1	Conclusions	99
5.2	Recommendations.....	100
References.....		101
List of Publications and Papers Presented		120

LIST OF FIGURES

Figure 1.1: Repeat unit structure of poly(lactic acid)	2
Figure 2.1: Structural formula of PLA formation from the precursor lactic acid	9
Figure 2.2: Chemical structures of PLA stereoisomers	10
Figure 2.3: Cellulose structure with intermolecular and intramolecular hydrogen bonds adapted from Wang et al. (2012)	14
Figure 2.4: Schematic diagram of different components of keratin protein adapted from Khosa and Ullah (2013)	16
Figure 2.5: Disulphide bond in thiol groups of amino acid cysteine	17
Figure 2.6: Schematic dynamic of cellulose-keratin crosslinking process adapted from Zhang et al. (2017b)	21
Figure 2.7: Types of cationic groups commonly used in ionic liquids	30
Figure 2.8: Chemical structure of 1-butyl-3-methylimidazolium chloride (BMIMCl) ..	33
Figure 2.9: Dissolution mechanism of cellulose in BMIMCl adapted from Feng and Chen (2008).....	35
Figure 2.10: Preparation methods for composites: (a) melt compounding and (b) film casting adapted from Li et al. (2010)	42
Figure 4.1: Cleaned chicken feathers <i>via</i> Soxhlet extraction (left) and crushed chicken feather fibers in powder (right)	56
Figure 4.2: Dissolution of CFF in BMIMCl at 110 °C; before (left) and after (right)....	57
Figure 4.3: Torque-time curves of PLA composite blends without BMIMCl.....	59
Figure 4.4: Torque-time curves of PLA composite blends with BMIMCl	60
Figure 4.5: Comparison plastogram of PLA composites with and without BMIMCl	62
Figure 4.6: FTIR spectra of lactic acid characteristic peaks in PLA and its composites	64
Figure 4.7: FTIR spectra of CFF and MCC characteristic peaks in PLA composites	66
Figure 4.8: Moisture absorption peaks of PLA and its composites in FTIR spectra	67
Figure 4.9: Infrared spectra of PLA characteristic peaks intensity	68

Figure 4.10: Thermal stability of PLA composite films and the raw materials in TGA.	71
Figure 4.11: TGA thermogram of BMIMCl as comparison factor in PLA composites .	73
Figure 4.12: Thermal degradation rate of PLA composites with and without BMIMCl	74
Figure 4.13: DSC thermal behavior of PLA and the composites.....	75
Figure 4.14: Glass transition temperature thermogram of PLA and the composites in DSC.....	76
Figure 4.15: DSC curves of T_g and T_c for PLA and its composites.....	77
Figure 4.16: Correlation plot of T_c versus χ of PLA blends.....	79
Figure 4.17: Melting temperature of PLA composites with and without BMIMCl	81
Figure 4.18: X-ray diffraction pattern of PLA and the composites	84
Figure 4.19: Comparison XRD pattern of PLA and MCC reinforced PLA composites	85
Figure 4.20: Interaction scatterplot between CI and DTG of PLA and its composites ..	87
Figure 4.21: SEM cross section images of PLA (a) and PLA-IL (b).....	88
Figure 4.22: SEM cross section images of PLA-CFF ₅₀ MCC ₅₀ (a) and PLA-CFF ₅₀ MCC ₅₀ IL (b).....	90
Figure 4.23: SEM cross section images of PLA-CFF ₁₀₀ (a) and PLA-CFF ₁₀₀ IL (b).....	91
Figure 4.24: SEM cross section images of PLA-MCC ₁₀₀ (a) and PLA-MCC ₁₀₀ IL (b)...	92
Figure 4.25: SEM cross section images of PLA-CFF ₅₀ MCC ₅₀ (a), PLA-CFF ₁₀₀ (b), and PLA-MCC ₁₀₀ (c) with lower resolutions.....	94
Figure 4.26: Vickers hardness test values of PLA blends with and without BMIMCl...	96

LIST OF TABLES

Table 2.1: Amylose and amylopectin composition in starch from different sources adapted from Muller et al. (2017)	26
Table 3.1: Composition of PLA blend composite films	51
Table 4.1: Thermal degradation temperatures and DTG data of PLA and its composites	70
Table 4.2: DSC data of neat PLA and its composite films	82
Table 4.3: XRD crystallinity index (CI) of PLA and composite films	86

Universiti Malaysia

LIST OF SYMBOLS AND ABBREVIATIONS

ΔC_p	:	Heat capacity
ΔH_f	:	Enthalpy of melting
3D	:	3 dimensions
ATR	:	Attenuated total reflectance
a.u.	:	Arbitrary unit
BMIMCl	:	1-butyl-3-methylimidazolium chloride
BMIMPF ₆	:	1-butyl-3-methylimidazolium hexafluorophosphate
CFF	:	Chicken feather fiber
CI	:	Crystallinity index
CNC	:	Crystalline nanocellulose
D-lactide	:	Dextro-lactide
DSC	:	Differential scanning calorimetry
DTG	:	Differential thermogravimetric
DTS	:	Diametral tensile strength
EC ₅₀	:	Half maximal effective concentration
FTIR	:	Fourier transform infrared spectroscopy
GT	:	Gauche-trans
HV	:	Vickers hardness
HPE	:	Hyperbranched polyphosphate ester
IL	:	Ionic liquid
L-lactide	:	Levo-lactide
MCC	:	Microcrystalline cellulose
PDLLA	:	Poly (D,L-lactic acid)
PLA	:	Poly(lactic acid)

PLLA	:	Poly(L-lactic acid)
POM	:	Polarizing microscope
Rpm	:	Revolution per minute
SEM	:	Scanning electron microscopy
SPLA	:	Starch-poly(lactic acid)
T_c	:	Crystallization temperature
T_{final}	:	Final temperature
T_g	:	Glass transition temperature
TGA	:	Thermogravimetric analysis
T_m	:	Melting temperature
T_{max}	:	Maximum temperature
T_{onset}	:	Onset temperature
TT	:	Trans-trans
VHN	:	Vickers hardness number
w/v	:	Weight per volume
Wt%	:	Weight percentage
XRD	:	X-ray diffraction
χ_c	:	Crystallinity percentage

CHAPTER 1: INTRODUCTION

1.1 Research Background

In the recent decades, plastics made from synthetic polymers have been widely used in storage, packaging and various other applications. However, plastic pollution has been a threat to global ecology due to plastic's resilience against degradation and its proliferation in industry (Webb et al., 2012). Polymer resins often require the incorporation of additive chemicals to improve performance. The additives such as lead and tributyl tin in polyvinyl chloride, PVC are potentially toxic to animals and humans (Thompson et al., 2009). Disposal of these synthetic plastics into the ocean impacted over 270 species of marine life, including turtles, fish, seabirds, and mammals due to the ingestion or entanglement in plastic debris that impaired their movement, starvation, or death (Sigler, 2014). On the other hand, degradable biopolymers such as poly(lactic acid) have been produced on an industrial scale to replace conventional oil-based plastics due to more environmentally aware consumers, increased price of crude oil and global warming (Petersson & Oksman, 2006; Thompson et al., 2009).

Poly(lactic acid) (PLA) is one of the highly versatile and biodegradable aliphatic polyesters (Figure 1.1) derived from 100 % renewable resources of corn and sugar beets (Drumright et al., 2000). PLA has long been researched as an alternative to petroleum based plastics that offers wide range of commercial and commodity applications due to its environmental friendliness and transparency properties. Indeed, compostable polymers provide added advantage of being disposable green products. However, pure PLA product has poor mechanical properties and barrier performance as compared to conventional thermoplastics (Duan et al., 2013). Besides, PLA has a very slow crystallization rate whereby high level of crystallinity could be achieved with multiple methods of processing such as plasticization, copolymerization, and melt blending

(Nagarajan et al., 2016) with different superior properties of polymers, additives or fillers.

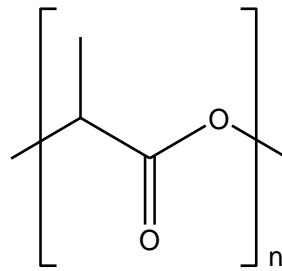


Figure 1.1: Repeat unit structure of poly(lactic acid)

In conjunction to the unsatisfactory characteristics of PLA, the composites with two or more discrete components combination consisting of matrix and reinforcement were produced (Kakar et al., 2015). There are various potential types and sources of reinforcement that could be applied to the polymer matrix, including organic materials from biomass feedstock. These organic wastes are regarded as better promising materials to replace synthetic polymers with a low cost while maintaining its polymer properties as well as to reduce global dependency on fossil fuel sources (Barone et al., 2005; Tran et al., 2016). Protein and polysaccharide are most common fillers as reinforcements in biopolymer due to their abundance and renewability such as keratin and cellulose.

Keratin protein is found abundantly in hair, wool and feathers, consisting approximately 90 % of protein fibers. Global meat manufacturers produce an estimated 15 million tons of chicken feather by-products annually and these feathers are disposed inefficiently in landfill, burned or processed to make a low-grade animal feedstock (Chinta et al., 2013) which cause environmental pollution. These chicken feather fiber (CFF) waste which comprises almost entirely keratin could be a valuable research material to be transformed into useful polymer composite filler. Keratin from CFF possesses the properties of being lightweight with lowest density value as compared to

most natural and synthetic fibers, having high thermal insulation and thermal stability, non-abrasive behavior and low energy dissipation (Subramani et al, 2014).

In the field of medical engineering, keratin is widely researched on wound care, tissue reconstruction, cell seeding and diffusion as well as drug delivery as topical or implantable biomaterial (Tran et al., 2016). For instance, feather keratin has been found to possess molecular sized and shaped adsorption pockets which are biochemically determined and have selective heavy metal ions affinity such as Cu^{2+} , Fe^{2+} , Cr^{6+} and Hg^{2+} to be useful in environmental applications of removing these harmful ions from solution (Chinta et al., 2013; Schmidt & Jayasundera, 2004). Despite some of the pros, pure keratin has a major drawback of having poor intrinsic mechanical characteristics (Kakar et al., 2015). Alternatively, Tran and co-workers (2016) suggested that cellulose could interact stronger with feather keratin, contributing to its mechanical strength.

Cellulose is the major constituent that builds up plants which could be obtained in low cost (Hina et al., 2015). The ordered structure of this semi-crystalline polymer consists of surface OH functional groups that could initiate the polymerization of lactic acid (Gupta & Katiyar, 2017). Thus, cellulose may provide its fibrous, tough and water insoluble characteristics to PLA (Niroomand et al., 2016) to enhance the thermal and mechanical properties of the composites. However, hydrophilic surface property of cellulose hampers its compatibility with hydrophobic of poly(lactic acid). Keratin protein consists of both hydrophobic and hydrophilic surface chemistry with the composition of 60 % and 40 % respectively makes it a promising biomaterial to be at least partially compatible with all polymers (Barone & Schmidt, 2005).

From the amphiphilic properties of keratin, CFF is able to act as a “bridge” for the blending and bonding in between the incompatible hydrophilic cellulose and hydrophobic poly(lactic acid). Recent work reported that CFF basically do not require

chemical modification and could be used as a whole in composite processing without separating the fiber from the quill to save time, energy and production costs (Carrillo et al., 2013). For better particle distribution, cleaned CFF could be grinded before melt blending with PLA. In spite of that, organic fillers such as microcrystalline cellulose (MCC) and CFF are often in powder or solid form which have much higher melting point than that PLA do not melt at melt blending temperature and cause less dispersible.

Different route for making biopolymer blends has been researched by dissolving the polymer (Pinkert et al., 2009). The dissolution is to form interwoven network between the MCC and CFF chains with PLA biopolymer strands. However, the basic building amino acids in keratin chains are interacted by highly cross-linked network structure with strong intramolecular and intermolecular bonds especially disulphide bonds (Na Ayutthaya, et al., 2015). Tightly packed keratin microfibrils result in CFF having high resistance to common proteolytic enzymes, biological degradation and insoluble in most organic solvents as well as weak alkali and acids (Kammiovirta et al., 2016; Sinkiewicz et al., 2017). Sinkiewicz and co-workers (2017) mentioned that extraction of keratin from CFF required to break these strong bonds with reducing substances such as 2-mercaptoethanol is harmful to the environment, high cost and not industrial viable.

To dissolve both MCC and CFF for PLA biopolymer blending, Tran and Mututuvvari (2015) found that ionic liquids (ILs) such as 1-butyl-3-methylimidazolium chloride (BMIMCl) could dissolve various polymers including keratin, cellulose and many more polysaccharides and proteins. As similar to the significance of biodegradable polymer, ILs are green solvent which are non-volatile, non-flammable and thermally stable organic molten salts (Huddleston et al., 2001). The literature from Pinkert et al., (2009) revealed that BMIMCl was not acutely toxic ($EC_{50} \approx 13 \mu\text{M}$) in the application on all higher organisms' nervous system such as marine algae, luminescent bacteria and

leukemia cell lines. Martins and his co-workers (2014) discovered the inference to the choice of ionic liquid used. Apart from the role of IL as a solvent, chloride ion of BMIMCl could produce homogenous mixture as plasticizing agent in polymeric blend of starch-poly-lactic acid (SPLA) besides producing a porous structure.

As far as different types of polymers being researched on ionic liquid dissolution, various works have been reported on only dissolved keratin (wool, hair, chicken feather) and cellulose in ionic liquid. These dissolved polymers have yet been used as a filler in poly(lactic acid) as reinforcement. The significance of this study are the implication of mixer and compression molding technique in IL dissolved fillers and transforming CFF waste materials into potentially useful biopolymer products. In order to study the effect of keratin (CFF) and cellulose (MCC) dissolved in BMIMCl as reinforcements in PLA, the composite films were fabricated and characterized to study their thermal, mechanical and morphological properties.

1.2 Problem Statement

The issues of plastic pollution have reached a crucial stage in harming the biodiversity in ocean due to high usage and discard of single-use packaging made from synthetic polymers. Although plastics recycling such as polyethylene terephthalate (PET) polymer has been implemented, recycling some items made of composites are still not possible (Thompson et al., 2009). Since then, degradable biopolymers have received much attention as an alternative to conventional oil-based plastics. However, production of biopolymers in industrial scale still remain challenging as they are more expensive than conventional polymers (Thompson et al., 2009). Biodegradable polymer such as poly(lactic acid) has glassy characteristics aside from being relatively high cost. Reinforcements in PLA may enhance the properties of the composites apart from being cost effective. In fact, CFF was revealed to be able to improve the mechanical and

thermal properties of PLA composites (Baba & Özmen, 2015). The biodegradation rate of cellulose (M_w 5,000-250,000), 25.00 ± 0.6 % is higher than that PLA (M_n 200,000), 0.97 ± 0.26 % as reported by Guo et al. (2012) and quoted by Webb et al. (2012) may contribute to their thermal stability. However, substantial research is still necessary to produce biodegradable polymers with comparable physical properties to conventional plastics (Webb et al., 2012). Apart from the keratin-cellulose reinforced PLA blends that were lack of extensive studies, deterioration of physical properties in composites were often caused by the dispersion of fillers. Therefore, dissolution of fillers in ionic liquid, BMIMCl were studied alongside with the use of mixer and compression molding. Compatibility between the polymers is also one of the factors affecting the performance of the composites. Characterization studies of the PLA composite films were obtained in term of thermal, mechanical and morphological properties.

1.3 Research Objectives

The main objectives of the study are shown below:

1. To investigate the interaction and compatibility between the different compositions of CFF and MCC with poly(lactic acid) in the composite films.
2. To examine the function and effect of 1-butyl-3-methylimidazolium chloride in the dissolution of CFF and MCC to the properties of poly(lactic acid) composite films.
3. To determine the effect of CFF/MCC composition and 1-butyl-3-methylimidazolium chloride in the thermal, mechanical and morphological properties of poly(lactic acid) composites.

1.4 Scope of Study

The overall scope of this research is to fabricate a thin film made of biopolymer composites which mainly composed of at least 94 wt% poly(lactic acid), while the rest of the components are comprised of fillers and ionic liquid. The fillers are of different surface properties such as cellulose and keratin which are hydrophilic and amphiphilic, respectively. Both are also different from the hydrophobic PLA. Therefore, interaction and compatibility between these biopolymers will be further investigated *via* observation during fabrication as well as characterization studies such as torque rheometer, Fourier transform infrared spectroscopy (FTIR) and X-ray diffraction (XRD).

Reason for the incorporation of ionic liquid is none other than the role of solvent in these biopolymers. Ionic liquid will be investigated based on its feasibility in dissolving the fillers to disperse the particles in PLA matrix. As ionic liquid is often used as a dissolving medium in solvent casting due to its high polarity, its possible application in the industrial melt compounding and compression molding method are still uncertain and rare to be found. Thus, the function and effect of ionic liquid to the entire polymer matrices will be examined.

1-butyl-3-methylimidazolium chloride is the focused ionic liquid in this study due to the lower viscosity and has less bulky side chains as compared to other ionic liquid. The fabrication is unique from the aspect of merging the dissolved fillers in ionic liquid with subsequent feeding into the measuring mixers and finished with a hot press. As some biopolymers were reported to be heat sensitive, thermal, mechanical and morphological properties will be studied by the characterization of differential scanning calorimeter (DSC), thermogravimetric analysis (TGA), Vickers hardness test and scanning electron microscope (SEM).

1.5 Thesis Outline

This thesis is organized in 5 chapters as follows:

Chapter 1 introduces briefly on the PLA background and the advantages of PLA composites reinforced with cellulose and keratin. The research problem statement, objectives and scope of study are also included.

Chapter 2 consists of comprehensive past literature on PLA, polymer reinforcement, ionic liquid and processing techniques in term of properties, mechanism and related applications.

Chapter 3 is the detailed materials used and methodology from the processing of raw materials to the preparation and fabrication of PLA composites. Instruments used in the characterization of composite films are also discussed.

Chapter 4 describes the results obtained from characterization studies. The results are compared and contrast to answer the research objectives and problem statement. Statistical values from past work are also discussed to evaluate and support the data.

Chapter 5 is the concluding statements of the findings from results and discussion in chapter 4 and whether they achieve the research objectives and solve the problem statement. Future recommendation is also mentioned for the improvement of this field of study.

CHAPTER 2: LITERATURE REVIEW

2.1 Poly(lactic acid) (PLA)

2.1.1 Chemical Structure

Lactic acid is well-known to be outsourced from renewable organic materials. Ring formation of lactic acid dimer produces the monomer lactides. Lactide has been an important intermediate in the industrial production of copolymer poly(lactic acid), PLA. The high molar mass PLA structure consisting of repeating ester group is synthesized *via* step-growth polymerization or ring-opening polymerization (Inkinen et al., 2011). The chemical structure transformation of lactic acid to its polymer with repeating unit is as illustrated in Figure 2.1.

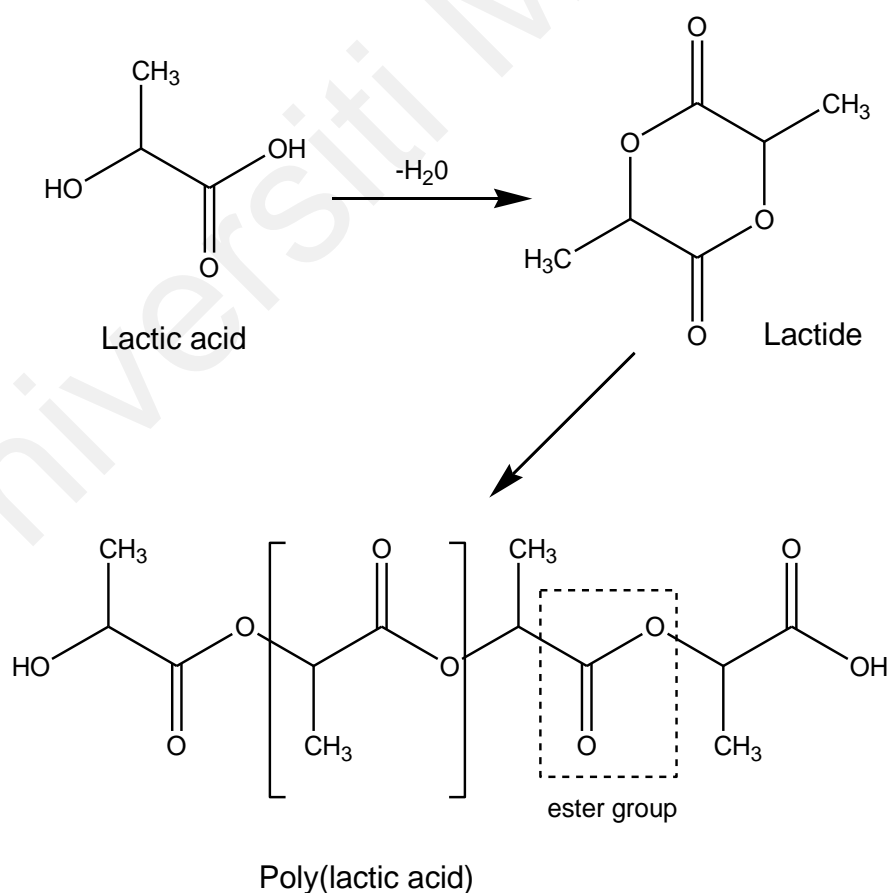


Figure 2.1: Structural formula of PLA formation from the precursor lactic acid

Due to the chiral nature of lactic acid, lactides exist in three forms of stereoisomers namely, L-lactide, D-lactide, and meso-lactide as depicted in Figure 2.2 (Drumright et al., 2000). The stereochemical composition of these lactides affects the properties of the resulting polymer such as enthalpy of melting and rate of crystallization and Garlotta (2001) reported the difference in the melting point of the isomers with 52 °C for L-lactide which is lower than both D- and meso-lactide of 97 °C. Duan et al. (2013) specified that optically pure PLA will have higher crystallinity because of their greater chain symmetry. On the other hand, the commercial PLA grade used in this research comprises of poly(L-lactic acid) (PLLA) and poly(D,L-lactic acid) (PDLLA) which are produced from L-lactides and D,L-lactides, respectively as described by Martin and Averous (2001).

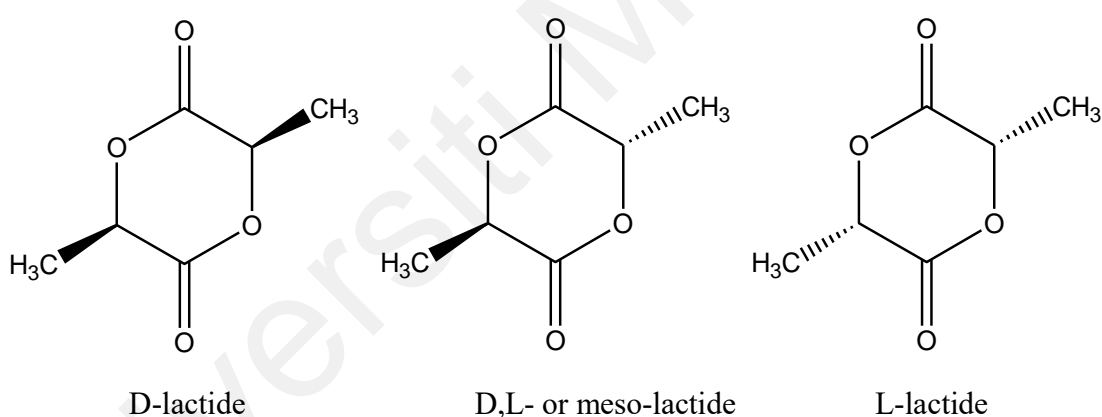


Figure 2.2: Chemical structures of PLA stereoisomers

2.1.2 Properties and Applications

PLA is a glassy polymer with less than 10 % of elongation at break (Xiao et al., 2012) and its thermal stability is similar as poly(vinyl chloride) but relatively lesser than that polystyrene, polypropylene, polyethylene and poly(ethylene terephthalate) (Auras et al., 2004). Considerable attempts have been done to improve the PLA properties to

compete with other biopolymers in term of low cost and flexibility such as modifying PLA with biocompatible plasticizers (Martin & Averous, 2001). Plasticizers are generally used to increase the ductility and flexibility of polymers in plastic manufacturing industry such as soft film packaging and gaskets molding (Tee et al., 2014). Hence, different types of plasticizers with the properties of low molecular weight, high boiling point, low volatility as well as different polarity and functional group have been explored to lower the glass transition temperature (T_g) of PLA (Xiao et al., 2012).

Glass transition temperature is one of the most prominent parameters in determining PLA chain mobility to predict the polymer behavior. Pillin et al. (2006) mentioned that lactide monomer is a good candidate in plasticizing PLA but with a drawback of its migration to films surface over time and causing film stiffening. The authors successfully lowered the glass transition, melting and crystallization temperatures of poly(lactic acid) by using poly(ethylene glycol) as plasticizer and the miscibility was confirmed *via* the calculation of Flory-Huggins relation.

Crystallization temperature and crystallinity are correlated in affecting mechanical properties and morphology of PLA. During isothermal crystallization of PLA by Day et al. (2006), the rate was greatly enhanced by nano clay particles approximately 15 to 20 times faster than that for the neat PLA. Crystallization rate increment enables formation of more uniform and perfect crystals, thus, increase in crystallinity. Polymer crystallinity is one of the most important properties which is often emphasized in food packaging (Setiawan, 2015). As PLA is a semi-crystalline polymer, level of crystalline component in relationship to its amorphous component is crucial in influencing polymer brittleness, stiffness or modulus, optical clarity, creep or cold flow, barrier resistance and long term stability.

As for the degradation properties, PLA is broken down by hydrolysis upon the exposure to moisture for a period of few months. Auras and co-workers (2004) explained that the degradation occurs in two stages; non-enzymatic chain scission of the ester groups which reduces polymer molecular weight as well as microbial action that lead to low molecular weight PLA diffuses out of the bulk polymer to produce carbon dioxide, water and humus. Researchers have made use of these PLA properties in biomedical field such as drug delivery system. The system works when the water infiltrated into the device and initiates the degradation of the ester bonds of the biodegradable polyesters after the polymeric drug release (Alsaheb et al., 2015). Due to the high volatile combustible byproducts of PLA, Chen et al. (2012) successfully lessen the gas released at thermal degradation of TGA-FTIR analysis from hyperbranched polyphosphate ester (HPE) catalyzed PLA.

Apart from drug delivery, Manavitehrani et al. (2016) prospected that the application of PLA in regenerative medicine and tissue engineering requires modification to obtain more hydrophilic and cell-interactive polymers. Subsequently, Gonzalez et al. (2016) concerned the drawback of PLA as biosensor substrate due to its hydrophobicity. Therefore, the authors fabricated biotin surface functionalized hydrophilic PLA nanofibers to interact and immobilize biological molecules as most biological systems are in aqueous. The results from water stability test showed that the PLA nanofibers were stable up to 24 hours.

Likewise, application of PLA in textile industry utilizes enzyme in order to promote hydrophilicity of PLA fabric. Lee and Yeo (2016) hydrolyzed the ester bonds of poly(lactic acid) with proteolytic enzyme, *B. licheniformis* alcalase and the results concluded that the enzymatic hydrolysis increased the moisture regain of the PLA fabric with 1.36 % as compared to untreated PLA fabric, 0.72 %. Enzymatic reaction requires

additional step in considering parameters and factors such as effectiveness of enzymatic reaction activator, pH, enzyme concentration as well as temperature that may lead to degradation of the polymer. Hendrick and Frey (2014) suggested a simpler and quicker feasible method to increase hydrophilicity by incorporating hydrophilic polymer in PLA such as the abundantly available biopolymer cellulose.

2.2 Polymer Reinforcement in PLA Composite Films

2.2.1 Cellulose

Glucose, a hexose 6-carbon sugar is the monomer that forms cellulose with two anhydroglucopyranose rings that linked *via* β -1,4-glycosidic linkage to form the dimer, β -1,4-cellobiose (Shanks, 2014). Cellulose, a major structural material of plants, has a planar structure with strong intermolecular and intramolecular hydrogen bonding (Figure 2.3) that forms a high molar mass biopolymer (540 000 to 1 800 000 g/mol) resulted from large number of hydroxyl groups (Hina et al., 2015). With a mean particle size of less than 10 μ m, microcrystalline cellulose is a white, odorless, tasteless, relatively free flowing crystalline powder which is insoluble in water, organic solvents, dilute alkalis and acids (Tuason et al., 2014). Although cellulose is an OH rich polymer, the strong hydrogen bonding and the length of its long chain structure are a relevant factor in prohibiting its interaction with solvent molecules. Olsson (2014) suggested that solvent with a high capacity for hydrogen bonding is necessary to break these bonds.

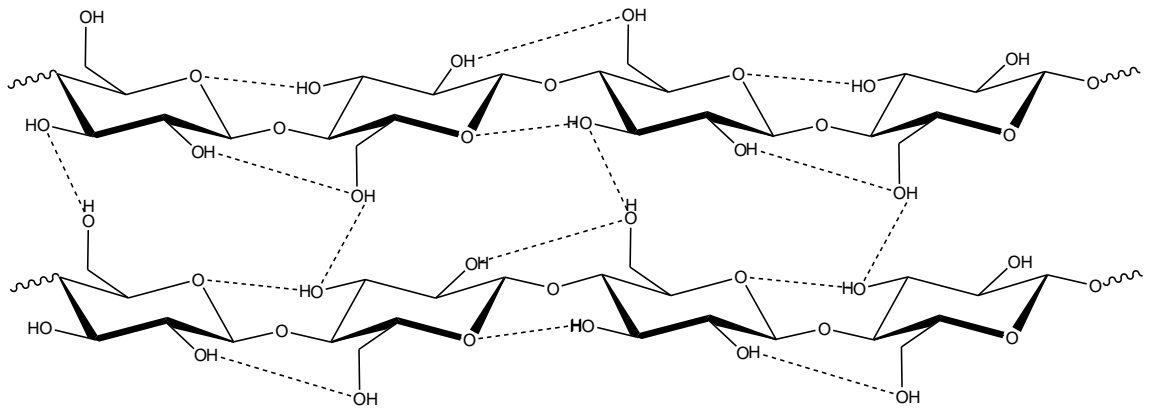


Figure 2.3: Cellulose structure with intermolecular and intramolecular hydrogen bonds adapted from Wang et al. (2012)

MCC has the advantageous ability to increase the crystallinity of PLA as reported in the work of Murphy and Collins (2016) in which the PLA/cellulose composites were being fabricated *via* fusion deposition modeling 3D printer. The increase in the crystallinity is affected by the ability of nanocellulose to act as nucleating agent and promote crystallization (Sullivan et al. 2015). The inference corresponded to the cryo-fracture surface scanning electron microscope (SEM) images that appeared to have more brittle fracture upon addition of crystalline nanocellulose.

The nucleating effect was seen in the addition of 5 wt% MCC in PLA matrix that did not change the crystalline structure of PLA but increased the intensity of crystallinity at 9.38° and 28.30° in XRD (Li et al., 2016). MCC was able to improve the rigidity and strength of poly(lactic acid) by restricting the movement of polymer chains. For example, addition of 30 wt% of cellulose fiber increased the stiffness of PLA from 3.3 to 5.4 GPa (Huda et al., 2006). On the contrary, elongation at break decreased from 194 % to 70 % and below when the cellulose content increased (Liu et al., 2010).

Reinforcement of cellulose nanoparticles in PLA composites was reported to have increased thermal stability as compared to neat PLA due to the fiber and matrix interaction (Ketabchi et al., 2016). However, reducing particle size in nano or micron

results in the likelihood of the particles to agglomerate upon drying which may be due to the bonding between smaller size particles (Tuason et al., 2014). The effect of size reduction was in agreement to Halász and Csóka (2013) where the aggregation displays poor compatibility with hydrophobic polymeric matrices. The authors also mentioned that its strong sensitivity to water and moisture as well as the polar surface cause non-uniform dispersion of cellulose in apolar polymers. SEM morphological studies of Mathew et al. (2005) also reported MCC aggregation and the blending resulted many holes in the PLA matrix, indicating that there is no adhesion or interaction between the PLA and MCC.

Consequently, multiple steps of modification on the surface properties have been done over the past decades while others reported swelling of MCC to allow PLA chain penetration into the cellulose compact particles. For instance, swollen MCC reinforced PLA composite achieved 12 % of elongation at break due to the better dispersion of swollen MCC in chloroform during solvent casting (Petersson & Oksman, 2006). However, this method only limited to small scale process mainly for laboratories. In contrast, addition of plasticizer tributyl citrate in nanocellulose reinforced PLA composites further improved the elongation at break to 205 % as compared to pure PLA for the making of plastic packaging materials (El-Hadi, 2017) .

A recent study of Gu and Catchmark (2013) explored on the use of amphiphilic whole milk casein as dispersant in cellulose nanowhisker reinforced PLA composites. The observation from Calcofluor staining demonstrated a better dispersion of cellulose in PLA matrix than that without the dispersant. Enhancement in mechanical properties was also significant with 40 % higher Young's modulus. Although it is almost impossible to impose great compatibility with only MCC in PLA as suggested by

Hendrick and Frey (2014), the idea of incorporating amphiphilic polymer such as CFF may result in greater compatibility in between hydrophobic PLA and hydrophilic MCC.

2.2.2 Keratin

Keratin is one of the most abundant proteins found in the bodies of mammals, birds and reptiles as hair, hooves, wools, nails, horns and feathers that provide strength to the body (Sharma & Gupta, 2016). These microcrystalline keratins exist in two forms; fiber and quill/rachis in which resulted in α -helix fibers and β -sheet films which were confirmed with the evidence of infrared spectroscopy and X-ray crystallography techniques (Schmidt & Jayasundera, 2004) as illustrated in Figure 2.4.

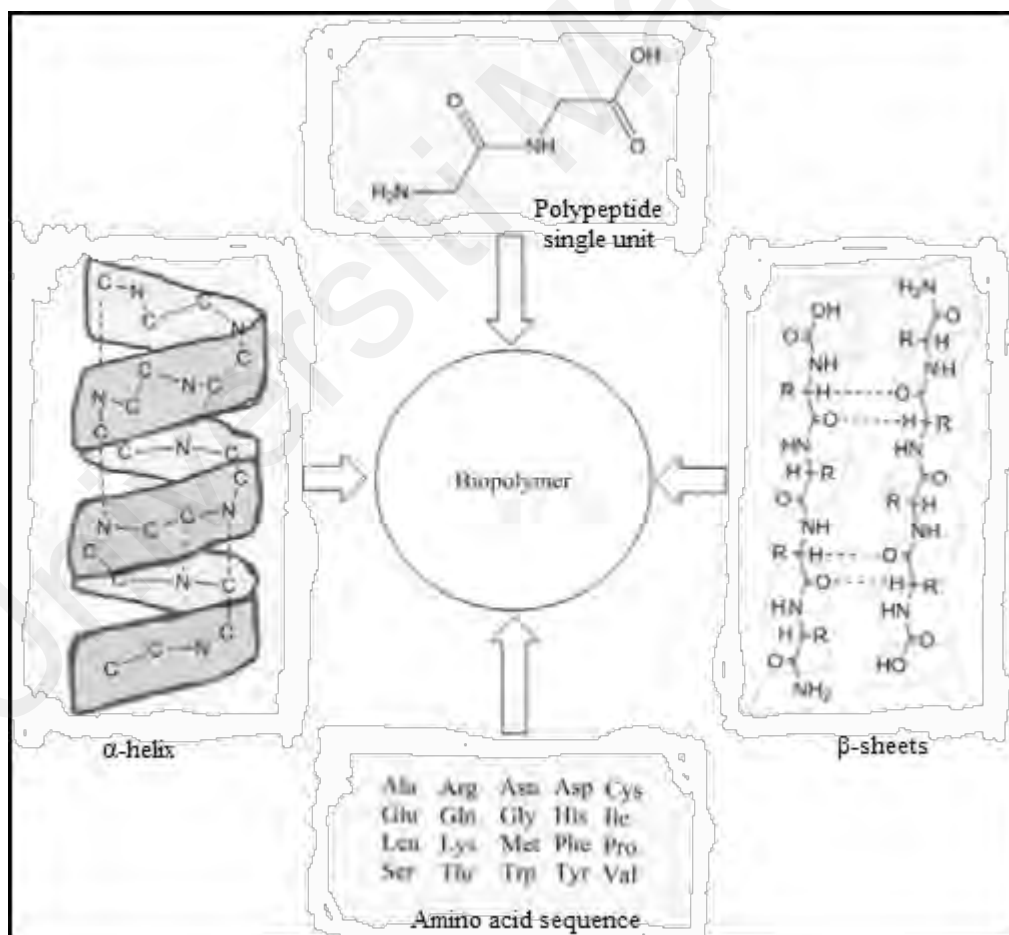


Figure 2.4: Schematic diagram of different components of keratin protein adapted from Khosa and Ullah (2013)

2.2.2.1 Keratin Protein from Feather

Feather keratin has 41 % α -helix, 38 % β -sheet and 21 % disordered protein structures (Barone & Schmidt, 2005). While raw poultry feathers consist of about 91 % keratin, 1.3 % fat, and 7.9 % water, protein in the keratin has both hydrophilic and hydrophobic amino acids and 39 of the 95 amino acids are hydrophilic (Chinta et al., 2013). Of all hydrophilic groups on peptide backbone namely serine, threonine and aspartate that offer covalent bonding within the polymer, serine is the most abundant amino acid whereby the hydroxyl group causes the moisture absorption from the air of about averagely 7 % (Barone & Schmidt, 2005; Chinta et al., 2013). Apart from covalent bond, cysteine (Figure 2.5) is a sulfur containing amino acid responsible for the strong disulphide bond and cross-linking in the keratin structure.

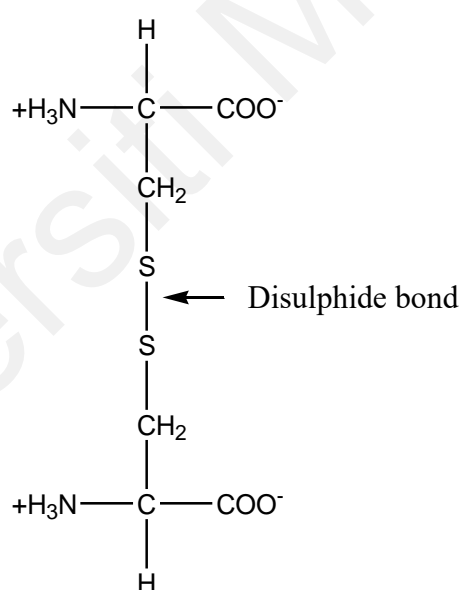


Figure 2.5: Disulphide bond in thiol groups of amino acid cysteine

Several efforts of extracting keratin from CFF have been made by breaking the strong covalent and disulfide bonds including the use of strong reducing agent sodium metabisulphite *via* sulphitolysis method in which produced inconsistent molecular weight of keratin depending on the amount of reducing agent used (Na Ayutthaya & Wootthikanokkhan, 2013). The inconsistency may hinder the final product and

properties of polymer blend. A simpler alkaline pre-treatment were performed with 5 % w/v NaOH solution before blending and grounding. Although alkali treatment increases the surface area of the fibres available for contact to the PLA matrix, the drawback of the treatment is the enhancement of chicken feather roughness and removes hydrophilic components located on the fibre surface (Aranberri et al., 2017).

Alkaline treatment is not a suitable method because CFF was initially being reinforced for the amphiphilic properties to improve the compatibility of hydrophobic PLA and hydrophilic MCC. In fact, the processing method of CFF was rarely reported extensively in past literature. Barone et al. (2005) was so far the first to report detailed processing method CFF without separating the quill by grinding on Retsch PM 400 ball mill at 200 rpm for 30 min to obtain CFF powder with the size of less than 75 μm . In 2013, Spiridon and co-workers practiced similar methodology as Barone et al. (2005) with continuous grinding and sieving to obtain uniform length of fibers between 30 μm to 70 μm as confirmed by laser diffraction.

Over the years, scientists have explored the potential usage of chicken feather fiber due to its fine size of 5 μm thickness. Keratin was found to have nucleating effect as similar to cellulose. Aranberri et al. (2017) discovered the DSC crystallinity of PLA with 60 wt% of CFF increased from 30.5 % to 36.0 %. In addition, low crystallinity of PLA/chitosan experienced crystallinity increment with only 2 wt% keratin reinforcement (Tanase & Spiridon, 2014). Subsequently, biological assessment using these biopolymer composites onto human osteosarcoma cell line showed good viability/proliferation outcome which could be a potential substitute materials for bone tissue engineering.

Apart from crystallinity enhancement, incorporation of keratin shifted the neat PLA thermal degradation to higher temperature (Spiridon et al., 2013). The reason to that is

due to the tendency of keratin to form char protective layer on material surface that delay the heat transfer to the composite. As keratin was known for the “bridging effect” between hydrophobic and hydrophilic polymers, the network formed has been observed in SEM fracture surface images of CFF reinforced PLA composites (Lam et al., 2009). The authors believed the bridging could prevent crack propagation and enable effective stress transfer between the matrix and the fibers.

CFF reinforced PLA from the work of Cheng et al. (2009) showed enhancement from 3.6 in PLA to 4.2 GPa stiffness with 5 % CFF as well as increase in thermal stability. As stiffness increases with increasing CFF content, polymer loses elasticity at the same time. No doubt that elongation at break decreased up to 12 % as compared to neat PLA when 25 wt% of CFF was added, contributing more inflexibility (Cañavate et al., 2015). Lam et al. (2009) and Zhao et al. (2008) also reported similar reduction in tensile strength as 2-10 wt% of CFF was added in PLA composites. Considering each keratin and cellulose contributes tremendous properties enhancement to poly(lactic acid) in the past literature, a few investigations were also reported in the merging of only cellulose and keratin.

2.2.3 Cellulose-Keratin Composites

One of the first few literature on cellulose-keratin composites was reported in 2013. Chinta et al. (2013) suggested a solution to excessive agricultural feather waste problem by fabricating the composite filter paper with only 49 % wood pulp and 51 % feather fiber that able to trap more spores, dust and dander which also used in air filter. Incorporation of cellulose with high degree of polymerization in brittle keratin may modify its properties for more applications in medical development. Liebeck et al. (2017) believed the hybridization of these keratin and cellulose bio-wastes into reusable composites could give idea to designing new hybrid biopolymers with combined

properties of proteins and polysaccharides. For instance, the existence of polypeptides among cellulose chains may provide sites enhancing a specific 'breathing motion', a fluctuation in the three-dimensional structure like proteins do.

In fact, the complex polypeptide structure and properties are highly affected by the source of keratin and polymer molecular bonding. Tran and Mututuvvari (2016) developed cellulose and/or chitosan reinforced wool keratin composites to study the protein structure after fabrication. Based on the Partial Least Squares Regression (PLSR) Analysis of the FTIR amide bands, the secondary structure of the keratin from composites have relatively lower α -helix, higher β -turn and random form than keratin in native wool. This is due to the incorporation of cellulose and/or chitosan that seem to hinder the reformation of the α -helix. In results, mechanical strength and thermal stability were enhanced where cellulose-keratin composites showed better tensile strength and higher decomposition temperatures with increasing cellulose composition as compared to chitosan-keratin composites.

Although keratin and cellulose may be good source of reinforcements in composites, solubilizing these highly cross-linked polymers for better homogenous composite is a challenging stage. Liebeck et al. (2017) introduced a method of dissolving goose feathers using superheated deionized water as solvent to produce aqueous keratin hydrolysate solutions. This method requires tuning of temperature and heat treatment duration to obtain optimum yield of keratin before undergoes homogenization with methyl cellulose in an ethanol–water solution. The oligopeptides in the composite films acted as plasticizer with improved elongation at break but decreased Young's modulus and offset yield strength with increasing hydrolysate fraction.

On the other hand, chemically cross-linked cellulose-keratin using glutaraldehyde was reported on wool and cellulose pulp. CHO group of glutaraldehyde is able to react

with the α -amino groups of amino acids, the N-terminal amino groups of some peptides and the sulfhydryl group of cysteine (Ma et al., 2016) as well as the hydroxyl of cellulose (Zhang et al., 2017b) as illustrated in Figure 2.6 below. Ma et al. (2016) reported cellulose-keratin composite with 54 % increment in elongation at break as compared to pure cellulose film. Glutaraldehyde was able to improve the thermal stability of cellulose-keratin which corresponded to the work of Zhang et al. (2017b) where the crystallinity of the cross-linked cellulose and human hair keratin film increased. However, hair keratin increases the thermal degradation rate.

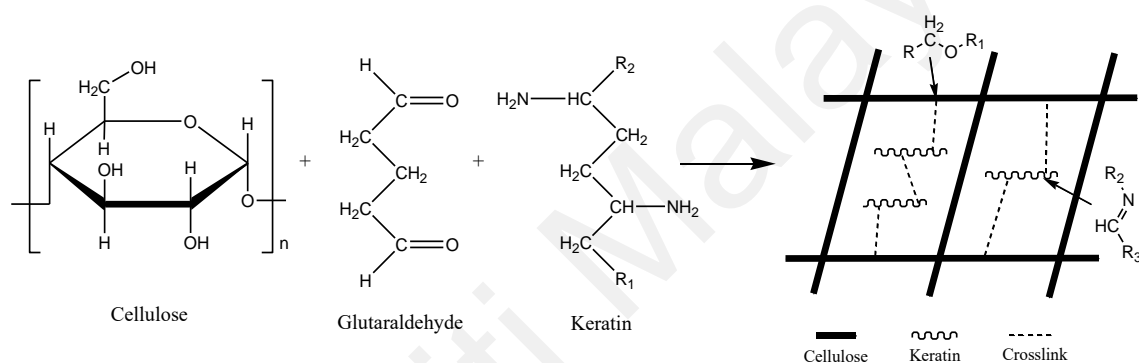


Figure 2.6: Schematic dynamic of cellulose-keratin crosslinking process adapted from Zhang et al. (2017b)

The increasing thermal degradation rate properties allow modified waste protein such as cattle hair keratin incorporated as coating in cellulosic–elastomeric material containing cotton and carboxylated styrene–butadiene latex to increase the susceptibility of the coated fabric to undergo bio-decomposition (Tshela Ntumba & Prochoń, 2016). Apart from resulting in better tensile strength and increased glass transition temperature, this material could potentially be applied as a fertilizer in agriculture. Rosewald et al. (2014) reported similar enhancement in tensile strength at least 4 times when cellulose fraction was increased from 25 % to 75 % in cellulose-keratin composites.

Aside from mechanical properties, cellulose-keratin composites were reported to have numerous investigations in microbiological and medical applications. For instance,

cytometry through immunophenotyped macrophages results confirm that presence of keratin and/or chitosan in cellulose composites effectively serve as an anti-inflammatory agents. Meanwhile, cellulose/keratin-catechin composite hydrogel exhibited good adhesiveness and hemadsorption, providing a rapid blood coagulation (Sun et al., 2018). This is because keratin could accelerate thrombin activation and promote the platelet aggregation, whereas catechin is a natural polyphenols derived from green tea known for its anti-oxidative, anticancer and anti-inflammatory properties.

Tran and colleagues (2016) reported the test of antibacterial properties in cellulose-keratin composites which was found to be majorly affected by the type of keratin. In the earlier work of Tran and Mututuvvari (2015), the cellulose-keratin composite was tested on drug delivery and the kinetic of drug release could be controlled by adjusting the concentration of keratin. From the results of past literature, CFF could be a compatibiliser in polymer matrices based on its properties enhancement in both cellulose and PLA composites. However, possible agglomeration of cellulose may lead to deterioration of mechanical properties (Ketabchi et al., 2016). Facile dissolving medium for cellulose and keratin could be implemented to provide better filler dispersion.

2.2.4 Other Types of Organic Fillers

Organic fillers may come from many sources and they are often referred as natural fibers. Apart from cellulose and keratin, agricultural waste has been used to replace expensive polymers for composite fabrication. However, not all natural fibers portray similar or better properties as compared to synthetic or inorganic fillers in order to be implemented in various applications. For instance, there are hemp hurds, alfalfa and grape stem (Battezzore et al., 2018). These cheaper alternatives were incorporated at about 10–50 wt% in PLA by melt blending. Results showed that the composites had

increased in rigidity but decreased in tensile strength and elongation at break. Thus, these fillers are not as suitable for the glassy PLA in the composites fabrication.

In contrast, a lignocellulosic filler, paddy straw was reported to have improvement in modulus of elasticity in PLA composites as the wt% of filler increased (Yaacab et al., 2016). The drawbacks of the composites are poor tensile strength and elongation at break. All in all, natural fibers have the advantage of simple production method by direct melt processing without preliminary chemical treatment such as the use of ground chestnut shell by Barczewski et al. (2017). The chestnut shell was grounded as powder without hydrolytic degradation of the polyester matrix. In comparison to neat polymer, natural filler in composites has the tendency to increase water absorption, hence influences their biodegradation process.

2.2.4.1 Chitin

In the recent years, one of the most widely investigated organic fillers in biopolymer was chitin. In contrast to agricultural waste materials, chitin is found abundantly in many crustacean sources such as crabs, shrimp shells and lobsters (Mohd Asri et al., 2014). Apart from that, the β -(1 \rightarrow 4)-*N*-acetyl-D-glucosamine that made up this crystalline high molecular weight linear polysaccharide is also found in cell walls of fungi, yeast and green algae (Nasrin et al., 2017; Salaberria et al., 2017). These sources such as lobsters and squid pens in the α -crystalline and β -chitin, respectively, are naturally synthesized over one billion tons per annum (Mohd Asri et al., 2014; Broers et al., 2018).

The reason for its high demand is the biodegradable, non-toxic and hydrophobic properties provided that chitin is the second most abundant natural polymers after cellulose (Mohd Asri et al., 2014; Broers et al., 2018). Chitin has been reported to have

the ability to heal wounds with the inert property in the gastrointestinal tract of mammals (Nasrin et al., 2017). In the laminated chitin-PLA composites by Broers et al. (2018), the composites showed optimum thermal stability with low water absorption capacity and antimicrobial activity which is suitable for bone implantation. As the concentration of chitin increased, the tensile strength, UV-blocking and heat tolerance improved with constant processing temperature of extruder and hot press.

On the other hand, a derivative of chitin, chitosan can be formed by acid treatment *via* partial deacetylation, unveiling the amino moieties (Broers et al., 2018). Chitosan also has barrier properties improvement in polymer matrix which is useful for retaining food shelf life in the food packaging (Broers et al., 2018). Generally, extraction of chitin from prawn shell required treatment with sodium hydroxide, sodium chlorite and glacial acetic acid to complete the deproteinisation and bleaching steps (Nasrin et al., 2017). However, these treatments discard large amount of chemical waste as compared to keratin extraction or processing of keratin fiber. As a result, their industrial applications are not widely commercialized.

Subsequently, Mohd Asri et al. (2014) utilized lactic acid fermentation as environmental friendly and cheaper production cost approach to purify chitin from crustacean waste in order to produce fermented chitin nanowhiskers. The results of the chitin-PLA composites showed improvement of Young's modulus and tensile strength with increasing chitin composition at 2 phr. As the chitin reached 4 phr, elongation at break decreased sharply and instant agglomeration occurred. Likewise, Hishammuddin and Zakaria (2016) also reported similar results in tensile strength and elongation at break but an increasing elastic modulus with respect to increasing chitin concentration. Poor filler dispersion was also observed from the surface morphology study *via* atomic force microscopy, indicating poor polymers interfacial compatibility.

Aggregation occurred due to strong hydrogen bonds formed upon drying of chitin powder. To enable uniform dispersion, Li et al. (2017) fabricated chitin-PLA composites with premixing of chitin water slurry with PLA followed by freeze-drying before the polymer blends were extruded. Improvement in mechanical properties of tensile, flexural and impact strength as well as viscosity and shear stress were obtained from poplar chitin reinforced composite. Another solution to incompatibility includes surface functionalization by acylation. Salaberria et al. (2017) introduced hydrophobic functional group in chitin with acetic anhydride and dodecanoyl chloride acid under heterogeneous conditions. Hydrophobicity was enhanced together with the improved antifungal activity for active food packaging application.

Although many approach has been done to solve the compatibility of PLA with chitin including the addition of glycerol triacetate plasticizer up to 20 wt% (Herrera et al., 2016), incorporation of too many additives may cause the composites to be non-environmental friendly. This is due to the use of toxic chemicals and putting extra cost in obtaining the product with low impurities such as the extraction of chitin.

2.2.4.2 Starch

Alongside with cellulose and chitin, starch is also one of the biopolymers that is found abundantly. Native starch could be easily retrieved and commercially available from wheat, corn and potato as compared to chitin extraction. In fact, starch falls under the same polysaccharide classification linked by glycosidic bonds as similar to chitin, except that it is found in plant instead (Muller et al., 2017). Starch comprises of 2 distinct polymers, the relatively linear amylose and branched amylopectin (Ke et al., 2003). Different composition of these types of starch would affect the properties of polymer blends. The examples of starch from different sources with amylose and amylopectin content are summarized in Table 2.1.

Table 2.1: Amylose and amylopectin composition in starch from different sources adapted from Muller et al. (2017)

Type of starch	Amylose (%)	Amylopectin (%)
Wheat	30	70
Corn	28	72
Potato	20	80
Rice	20-30	80-70
Cassava	16	84

Starch is highly hydrophilic in nature that exhibits high water solubility with poor water vapour barrier capacity (Muller et al., 2017). Therefore, starch and PLA often encounter phase separation due to their surface properties which are thermodynamically immiscible. In addition, starch/PLA blends are intrinsically brittle and eventually results in poor mechanical properties (Koh et al., 2018). Koh et al. (2018) suggested toughening strategies that have been actively conducted by researchers over the years including additive plasticization, mixture softening, elastomer toughening and interphase compatibilisation.

One of the most common enhancement methods used in starch/PLA blends is the addition of plasticizer. Glycerol was incorporated in PLA composites up to 17 wt% and developed poor elongation at break and tensile strength other than exhibiting higher biodegradation kinetic as compared to cellulose/PLA blends (Masmoudi et al., 2016). On the other hand, Shirai et al. (2016) successfully improved the elongation at break, tensile strength and Young's modulus by using diisodecyl adipate, an adipate ester as plasticizer. The authors explained that it was due the high molecular weight of diisodecyl adipate that contributed to the properties enhancement. Similar increase in

tensile and impact strength were also obtained from the epoxy palm oil plasticized starch-PLA composites (Ali et al., 2016).

Nonetheless, water sensitivity of starch in the composites has been as issue of over swelling due to the absorption of water. Ke et al. (2003) discovered that increasing amylose content up to 70 % had reduce the swelling of corn starch as compared to blends with waxy corn starch. The PLA matrix phase became continuous as amylose ratio increased. In conjunction with the addition of maleic anhydride compatibiliser, Zhang and Sun (2004) incorporated an initiator, 2,5-bis(*tert*-butylperoxy)-2,5 dimethylhexane to induce the maleic acid interaction with PLA free radicals. As a result, starch/PLA blend with 55/45 ratio recorded the highest tensile strength and elongation of 52.4 MPa and 4.1 %, respectively. However, as more steps are introduced to strengthen the properties of composites, the more chemicals are used and the more complex the methodologies become.

2.3 Green Chemistry for Polymer Composite

2.3.1 Type of Green Chemistry

The pioneer of green chemistry, Anastas and Warner (1998) defined green chemistry as the design of chemical products and processes that lessen or remove the use or generation of hazardous substances. In other words, it is also known as sustainable chemistry. To make a greener chemical, process, or product, 12 principles of green chemistry were created by Anastas and Warner (1998):

1. Waste prevention
2. Atom economy or efficiency
3. Less hazardous chemical syntheses
4. Safer products by design

5. Safer solvents and auxiliaries
6. Energy efficiency by design
7. Use of renewable feedstock
8. Derivatives reduction
9. Catalysis
10. Design for degradation
11. Real time analysis for pollution prevention
12. Inherently safer chemistry

Sustainable chemistry is the practice of sustainability in the concept of production and use of chemicals and chemical products as well as the application of chemistry and chemical products to enable sustainable development (Welton, 2015). Related examples include biodegradable plastics from natural polymers and modern paints with reduced toxic chemicals (Helmenstine, 2017). To fulfill the green chemistry criteria, solvent classes have been suggested. They include water, supercritical fluids, gas expanded liquids, ionic liquids, liquid polymers and solvents derived from biomass (Welton, 2015). This is because solvents are important factor in green industrial process and would be required to replace the conventional solvents that result in the emission of volatile organic compounds (Plechko & Seddon, 2007).

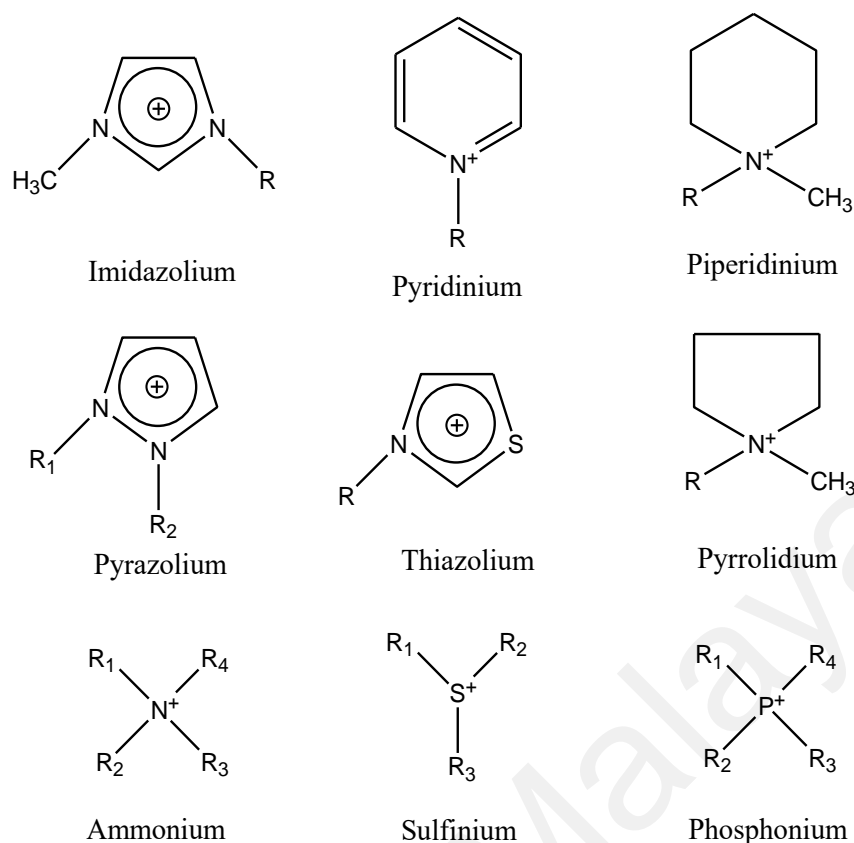
2.3.2 Green Solvent – Ionic Liquids

In applied chemistry, room-temperature ionic liquids (ILs) have received much attention as novel and green technology (Nishikawa et al., 2007) due to significant environmental benefits. Ionic liquids are poorly coordinated cations and anions molten salts that melt below the boiling point of water, 100 °C (Shamsuri & Daik, 2015). Ionic liquids portray many interesting properties such as low vapor pressure that makes them non-volatile (Zhang et al., 2005), besides being very stable, polar, non-flammable, high

thermal stability of more than 250 °C, soluble in organic solvents and water (Shamsuri & Daik, 2015). Most importantly, IL is able to dissolve and solvate many organic and inorganic materials such as polymers.

2.3.3 Types and Properties of Ionic Liquids

Ionic liquids has been a popular choice in the dissolution properties of various polymers. Apart from ionic and covalent interactions between the ions, there are also relatively weaker interactions such as hydrogen bonding and π -stacking, which are not commonly found in organic solvents (Handy, 2011). The diversity in the availability of cationic and anionic enables IL to be implemented in dissolution and various applications. The chemical structures of typical cation found in ILs are illustrated in Figure 2.7.



$R_{1,2,3,4} = \text{CH}_3(\text{CH}_2)_n$, $n = 1, 3, 5, 7, 9$, aryl, etc

Figure 2.7: Types of cationic groups commonly used in ionic liquids

Adequate selection of cation and anion constituents would result in different physical and chemical properties in ILs. Anions also play an important role in affecting the viscosity and melting point of the salts. For instance, strong basicity anions such as formate, acetate, or phosphate are more suitable for cellulose dissolution under mild condition provided with preferred cation candidates such as imidazolium, pyridinium and pyrrolidinium (Gupta & Jiang, 2015). Anions could range from simple halides, small inorganic ions to large and bulky ones. Meanwhile, some anions are not suitable in the application with carbohydrate and carbohydrate-related polymer. For example, tetrafluoroborate, BF_4^- hexafluorophosphate, PF_6^- would undergo rapid hydrolysis with free hydroxylic cations and cause difficulties for their use with either aqueous solvents (Handy, 2011).

2.3.4 The Use and Application of Ionic Liquids in Polymers

Among the ILs, not all types are studied extensively or widely available for applications. For instance, alkylpyridinium ILs have high melting points which are not favorable as solvent (Farran et al., 2015). Instead of acting as a solvent, it is the only heterocyclic aromatic cation which has great potential in aiding organic synthesis (Handy, 2011). Subsequently, Peng et al. (2013) reported the effectiveness of sulfonic acid-functionalized imidazolium and pyridinium based ILs in copolymerization of L-lactic acid and ϵ -caprolactones. The average molecular weights of copolymers of both 1-(butyl-4'-sulfonic acid)-3-methylimidazolium hydrosulfate and 1-(butyl-4'-sulfonic acid)pyridinium hydrosulfate with similar anion were 35.6 and 35.9 kDa, respectively.

Pyridinium and pyrrolidinium ILs have good biodegradable property which is possible for biopolymer utilization (Handy, 2011). Therefore, acidic ILs range from pyrrolidinium bisulfate, pyrrolidinium chloride to morpholinium bisulfate were studied for catalytic activity in ring-opening polymerization of ϵ -caprolactones in toluene with an initiator of benzyl alcohol (Mecerreyes, 2015). Intramolecular interaction between the ILs and polymer resulted in decrease in inherent viscosity. Pyrrolidinium and piperidinium salts were able to achieve high extraction efficiency in aqueous two-phase systems as additives. Aqueous two-phase systems composed of polyethylene glycol and ILs are an alternative technique for the extraction, separation and/or purification of diverse biomolecules (Almeida et al., 2014). Although 1-butyl-1-methylpyrrolidinium chloride did not show the best phase separation among ILs, the performance was still better as compared to 1-butyl-1-methylpiperidinium chloride IL due to the low affinity to water.

Another type of IL is the thiazolium group where thiazoles are commonly known for the nutrition of thiamine (Vitamin B1) in the form of substituted thiazolium salt (Handy,

2011). From the literature of Grygiel et al. (2014), 4-methylthiazolium salts were polymerized via free radical polymerization and anion exchange reactions. The poly(ionic liquid) was able to achieve anion-dependent tunable solubility in water and organic solvents. On the other hand, phosphonium salts are also implemented in polymer inclusion membranes as ion carrier. The membranes were made up of cellulose triacetate based membranes and ILs to facilitate transport of valuable and toxic metal ions such as cadmium (II) and copper (II) ions from aqueous chloride solutions (Pospiech, 2015). Results from the use of trihexyl(tetradecyl)phosphonium chloride and trihexyl(tetradecyl)phosphonium bis(2,4,4-trimethylpentyl)phosphinate showed fast and efficient extraction of cadmium (II) at over 99 %.

Pyrazolium and imidazolium cation groups' structures are almost similar but with the difference on the position of nitrogen. However, both types of ILs portrayed quite a different properties as investigated by Chiappe et al. (2013). Results from Chiappe et al. (2013) showed that 1,2-dialkylpyrazolium-based ILs had higher solvatochromic effect as compared to 1,3-dialkylimidazolium salts which was probably due to the greater hydrogen bond donor ability from closely positioned nitrogen atoms. However, the hydrogen bond donor ability is strongly affected by the length of alkyl chains. Apart from this superiority, olyferrocenylsilane polymer which is composed of ferrocene molecules bridged by silicon atoms is insoluble in imidazolium-based ILs. Matsuura and Furuta (2015) discovered that secondary amine in pyrazolium acted as an oxidant for ferrocene, allowing olyferrocenylsilane to be dissolved.

As a comparison with various types of cations in ILs, imidazolium salts were the most established and extensively researched in every aspects such as toxicity and its impacts in applications. One of its profound studies is the use of 1-ethyl-3-methylimidazolium acetate and 1-ethyl-3-methyl imidazolium diethyl phosphate as an

extracting agent of agarose from microalgae (Rhodophyta) originated from western coastal regions of India (Trivedi & Kumar, 2015). The dissolution under heating and microwave irradiation resulted in high extraction of good quality agarose up to 39 % as compared to conventional method.

2.3.5 The Role of 1-Butyl-3-methylimidazolium chloride (BMIMCl) in Biopolymers

Of all ionic liquids, 1-butyl-3-methylimidazolium chloride (BMIMCl) (Figure 2.8) that exist in solid state at ambient temperature has considerably low melting point of 41 °C (Huddleston et al., 2001) with reducing viscosity as temperature increases. According to El-Hadi (2002), BMIMCl is considered a perfect plasticizer because of the mobile and small size of the molecules with low glass transition temperature. Thus, 20 wt% of ionic liquid loading resulted in lowering of glass transition temperature in PLA by 28 °C (Peng et al., 2017). Meanwhile, viscosity of IL is inversely proportional to shear rate. As smaller cation in BMIMCl showed higher extractive ability than the other ionic liquids due to lower intermolecular van der Waals interactions, BMIMCl is naturally less viscous than other IL (Dharaskar et al., 2013c; Wasewar, 2013).

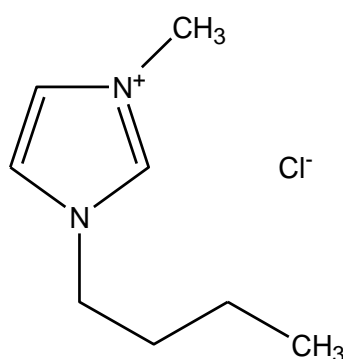


Figure 2.8: Chemical structure of 1-butyl-3-methylimidazolium chloride (BMIMCl)

Despite of the BMIMCl small size and low melting point, most imidazolium salts have high thermal stability. Thermogravimetric analysis of Dharaskar et al. (2013b)

described the thermal decomposition stages of BMIMCl which begun at 270 °C and stayed constant at 370.6 °C with more than 10 % of residue. The thermal behavior studies of BMIMCl by Nishikawa et al. (2007) using super sensitive and high-resolution DSC showed that BMIMCl had long-ranged pre-melting phenomenon and a complex freezing behavior. This phenomenon was caused by the gauche-trans (GT) and trans-trans (TT) conformational change of the butyl group linking with the phase transitions. Another study of BMIMCl on long-term isothermal TGA exhibited long-term thermal stability up to 160 °C as the decomposition temperature fell in the range of 150-200 °C (Kamavaram & Reddy, 2008).

There are several reasons for the choice of BMIMCl selection as Holm and Lassi (2011) mentioned that dissolution and functional modification strength largely depends on their polar characteristics to form hydrogen bonds with the polymers. The polarity of IL is caused by the electronegativity and small size of anions while chloride is one of the most electronegative ions. Interaction strength between IL and cellulose was also being reported by Elhi et al. (2016) where IL chloride anion showed the strongest. The dissolution mechanism behind the strong interaction between cellulose and ionic liquid was explained by Feng and Chen (2008) which involves the formation of electron donor-electron acceptor complexes.

Figure 2.9 illustrates the oxygen atom of cellulose as electron pair donor whereas the hydrogen atom acts as electron acceptor. Dissociation of ionic liquid into [BMIM]⁺ and [Cl]⁻ ions results in their penetration between cellulose chains (Han et al., 2013). Free chloride anion and [BMIM]⁺ cation attack the hydroxyl proton and oxygen atom respectively to cause the hydrogen bonds opening between the cellulose molecular chains. Thus, dissolution occurs due to the swelling of cellulose. The ease of the hydrogen bonds formed between hydrogen atoms of hydroxyls and the aromatic protons

in the imidazolium cation was due to the relatively small anions which was less steric hindrance (Zhang et al., 2017a).

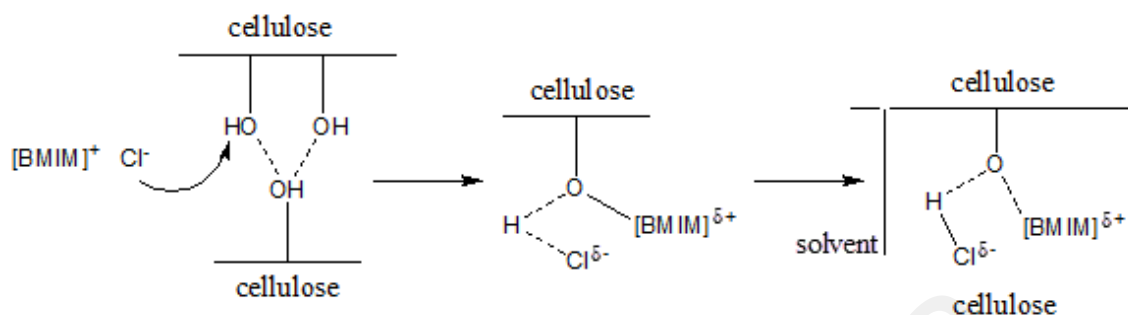


Figure 2.9: Dissolution mechanism of cellulose in BMIMCl adapted from Feng and Chen (2008)

Apart from the efficiency of BMIMCl dissolution mechanism, the compatibility of ionic liquids with polymers is crucial in order to avoid phase separation. The miscibility could be further enhanced with the addition of materials with amphiphilic character (Shamsuri & Daik, 2015). Herein, source of protein keratin from CFF is best suited for the mentioned criteria as Wang et al. (2014) explained that the imidazole ring in BMIMCl can dissolve keratin by weakening the intermolecular hydrogen bonding within the protein structure. Cl^- anion also reacts with the strong S-S bonds as well as weaken the hydroxyl bonds, intramolecular and intermolecular hydrogen bonds.

Good compatibility between IL and polymers allow the amount of polymer dissolved in IL to be maximized, besides showing significant improvement in the polymer blend mechanical and chemical properties. For example, keratin-cellulose blend films of Hameed and Guo (2010) exhibited an increase in thermal stability as well as tensile strength and elongation at break as the cellulose content increases which was due to the disruption of polymer hydrogen bonding by BMIMCl.

BMIMCl is able to alter the morphology of polymers apart from chemical bonding disruption. In the work of Yin et al. (2016), the authors enhanced the porosity PLA

scaffolds with ionic liquid for the medical application of bone repair. The PLA porosity was found to have increased by 60 % for the flow of nutrients and metabolic waste as well as cell adhesion in order to promote cell proliferation and growth. Porosity of polymer was determined by gravimetric method while Li et al. (2004) reported other alternative method by using pycnometer.

In consequence to the porosity effect, ionic liquid is widely investigated in glassy poly(lactic acid) in order to enhance its flexibility. According to (Park, 2008), reduction in the size of ionic liquid molecular structure creates more free space and volume for polymer to reduce its molecules entanglement. For instance, thermogravimetric results by Zhang et al. (2008) reported that the thermal stability of PLLA was better with 1-butyl-3-methylimidazolium pentafluorophosphate (BMIMPF₆) than the conventional plasticizer, poly(ethylene glycol). The improvement of polymer chain mobility was also confirmed *via* polarizing microscope (POM) and transition temperature reduction to as low as 40 °C with the increasing content of BMIMPF₆ from 2 wt% to 10 wt%.

2.4 Processing Techniques

2.4.1 Dissolution of Polymers in BMIMCI

Cellulose derivatives have been a common topic of research to enable the dissolution of high degree polymerized cellulose in most organic solvents *via* chemical modification of the OH functional group (Olsson, 2014). From the extraction of cellulose out of natural resources to its application in environmental friendliness context, the use of organic solvent is certainly not ecologically safe and often encounters toxicity issues. The dissolution of fillers in IL has the purpose of promoting dispersion in producing homogenous composites besides eliminating the use of conventional organic solvent in polymer blending.

Generally, the dissolution of polymers in BMIMCl requires comparative studies of the methods, different sources of keratin and cellulose as well as the parameters to fully optimize the amount and effectiveness of IL dissolution. From the studies of Swatloski et al. (2002), pulp cellulose dissolution BMIMCl showed second highest solubility up to 10 wt% upon heated at 100 °C while microwave heating dissolved up to 25 wt% while producing clear viscous solution. Although microwave heating is often reported to achieve the highest solubility, conventional heating method is still more commonly practiced with appreciable solubility as compared to room temperature dissolution.

Meanwhile, high efficiency of imidazolium-based BMIMCl in deep desulphurization of liquid fuels proved that BMIMCl is an ideal solvent in dissolving sulphur containing keratin polymer (Dharaskar et al., 2013a). Idris et al. (2013) also discovered that temperature has a strong effect on the solubility of keratin from turkey feather. It was observed that 130 °C was the optimum temperature in maintaining high solubility up to 50 wt% while minimizing the potential of any protein degradation or decomposition of the ionic liquid whereas Avicel 398 cellulose attained 20 wt% solubility in BMIMCl heated to 100 °C (Pinkert et al., 2009).

Another study involving 8 wt% of human hair keratin in BMIMCl was conducted with the similar condition as keratin, 130 °C for 10 minutes (Wang et al., 2014). The observation from polarizing microscope showed that the human hair samples were completely dissolved due to swelling from amorphous to crystalline to obtain clear and viscous mixture. This morphological study with respect to the condition of the dissolution is important to identify the optimum parameters for the filler dissolution without affecting the integrity of the polymers. At lower temperature, homogenous cellulose solution with optical microscopy investigation was obtained with only 75 minutes of dissolution (Peng et al., 2011).

BMIMCl is hygroscopic in nature and absorbs moisture instantly under room condition despite the ability to dissolve most polymers. Consequently, several works have also been reported on the use of inert atmosphere to conduct the composite synthesis. For instance, Tran and Mututuvvari (2015) dissolved the cellulose-chitosan-keratin composites in nitrogen atmosphere. The dissolution of keratin was first dissolved at 120 °C and reduced to 90 °C for cellulose and chitosan. The temperature difference for both difference types of polymer is necessary due to the stronger disulfide and hydrogen bonds in the keratin protein structure aside from the prevention of excessive heating that induces cellulose pyrolysis (Swatloski et al., 2002).

The effect of moisture to the dissolution process is equally significant as reported in the work of Olsson (2014) who explained that more water will cause the decrease in the solubility of the polymers. This is because the dilution of water that decreases the overall viscosity of IL may increase the mobility of dissolved fillers and lead to aggregation. However, high processing temperature may also eliminate the side effect of water content to the dissolved fillers by having more permanent bonding between the BMIMCl and polymers.

2.4.2 Fabrication Routes

2.4.2.1 Solvent Casting

Solvent casting is also known for solution intercalation or solvent blending with the advantage of polymers able to be dissolved and dispersed in the same solvent (Gao, 2012). As PLA is soluble in chloroform, most PLA composites utilize chloroform in solvent casting up to 1 hour sealed stirring to prevent the evaporation of the volatile solvent (Jiang et al., 2014). Apart from that, other solvents were also practiced in the dissolution of PLA such as methylene chloride and 50:50 of methylene chloride and acetonitrile (Byun et al., 2012). This method is a conventional way and important for

fabrication of polymers with low or no polarity that favors the preparation of thin membranes. Polymer and organic fillers could avoid thermal degradation due to the absence of elevated temperatures (Marras et al., 2010).

Solution casting remains as a popular choice in laboratory processing method for decades due to the best dispersion of cellulose nanofibers in PLA (Thakur & Thakur, 2017), besides enhanced the properties of composite films. Studies from Fortunati et al. (2012) showed that PLA composites processed by solvent casting had improved elongation at break which was probably due to the residual solvent that acted as plasticizer. The solvent casted PLA composites also had high ductile behavior at low nanocellulose content which is a desired property for flexible packaging applications.

Apart from that, Rhim et al. (2006) also reported similar results as Fortunati et al. (2012) in PLA films. From the TGA data, more than 10 % of chloroform that was retained in the films. Hence, the ductility of the sample film increased dramatically as compared to thermally dry compressed films, but with the deterioration of tensile strength and thermal stability. DSC analysis of Marras et al. (2010) recorded lower crystallization temperature of solution casted poly(L-lactic acid) nanocomposites as compared to melt compounding method. Therefore, film fabrication method is important in determining the desired properties of the composites.

In some nanocomposite thin films, the film casting method utilizes spin coating of the nanoparticle-polymer solution (Li et al., 2010). During the coating process, the solvent which acts as a dispersant evaporates in the ambient temperature or by subsequent oven treatment to result in the formation of homogenous films. Solvent is one of the main factor that affect the crystallization properties of composites. For instance, solvent casted PLA dissolved in equal ratio of methylene chloride and acetonitrile showed highest thermal expansion stability and crystallinity as compared to

other tested solvents, but with the sacrifice of oxygen permeability properties (Byun et al., 2012).

However, not all polymer/filler system possess favorable thermodynamics for composite formation (Gao, 2012). The challenging parts in solving the unfavorable thermodynamics are breaking the agglomerates of primary nanoparticles and conserving the dispersed/intercalated/exfoliated structure after processing. Gao (2012) proposed an interfacial compatibilisers which is solvent miscible such as maleic anhydride grafted polymers could limit the loss of microstructure. Meanwhile, surface modification was introduced to improve the polymer matrix compatibility between cellulose and PLA as well as the fiber dispersion in the matrix to prevent the irreversible agglomeration of cellulose/PLA upon drying (Thakur & Thakur, 2017).

In contrast, when more fillers were incorporated in the composites such as keratin polymer with strong disulphide groups, solubilisation of polymers in the solvent becomes a limitation. For example, composites of PLA with poly(ethylene glycol) resulted in amorphous blend with different miscibility as confirmed *via* XRD and SEM characterizations (Jiang et al., 2014). In comparison with melt-compounded samples, the results showed better compatibility. On top of that, use of organic solvents in solvent casting is environmentally unfriendly and economically unadvisable from the industrial point of view (Marras et al., 2010). Laboratory analysis of Young (2008) reported high toxicity of chloroform aside from having severe inflammation with acute exposure.

Fabrication *via* solvent casting is limited to the surface area of glass plates other than having the disadvantage of time consuming. This is because the conventional drying in solvent casting through the evaporation of solvent requires at least 24 hours (Fortunati

et al., 2012). This method is considered inefficient from the factor of time with respect to the yield of product.

Ultimately, the product of solvent casting is not uniform or known to be not reproducible in a consistent parameter despite this method results in a thinner films of at least 200 μm (Fortunati et al., 2012) as compared to compression molding. Jiang et al. (2014) reported that the solvent casted PLA film appeared to have inconsistent white and semi-transparent patches, which indicated that the film is not well mixed. Since the conventional solvent casting method portrayed disadvantages in composite fabrication, alternative routes may have to be considered from the aspect of simplified procedure and future economic purpose.

2.4.2.2 Melt Compounding

Melt compounding is normally referred to the process of melting the polymer pellets at their melting temperature to obtain homogenous blending. It includes the employment of injection molding, twin-screw extruder or measuring mixers together with the film fabrication *via* hot press/compression molding. As compared to the conventional laboratory solvent casting method, melt compounding provides bigger scale of production in polymer manufacturing industries. The differences of these two preparation methods are as illustrated in Figure 2.10 below.

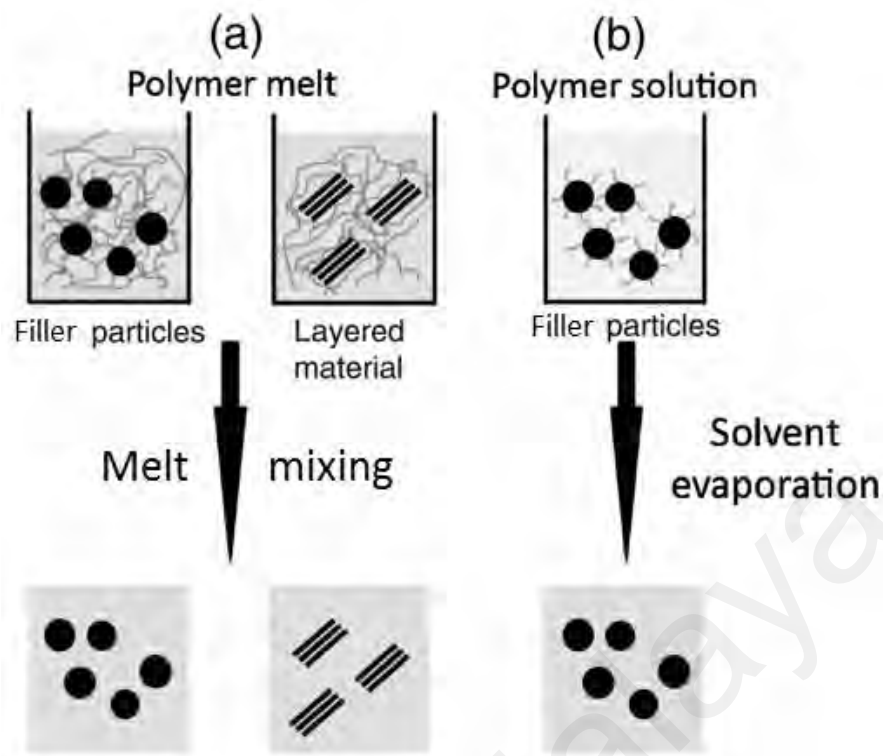


Figure 2.10: Preparation methods for composites: (a) melt compounding and (b) film casting adapted from Li et al. (2010)

According to Yin et al. (2016), a combination of polymer with innocuous materials in melt processing and compression molding are a set straightforward, convenient and efficient way to devise its application in tissue engineering scaffolds apart from pursuing solvent-free route. To further avoid the effect of moisture, some PLA resins were dried under vacuum overnight prior to melt compounding (Hassan et al., 2013; Nanthananon et al., 2015).

The use of these melt processing equipment require attention in considering the parameters such as rotor speed, duration and temperature that may affect the properties of the final product. According to the work of Auras et al. (2004), increase in temperature lowers the shear viscosity for both amorphous and semi-crystalline PLA although it was reported that semi-crystalline PLA has higher shear viscosity than amorphous PLA. For instance, Cañavate et al. (2015) reported optimum parameters for CFF reinforced PLA composite to be 170–180 °C for 5 min with the mixing speed of 50

rpm. The processing specification provided promising mechanical test results including Young's modulus, tensile strength and elongation.

Sufficient processing duration is also important in the study of the composites homogeneity. For instance, increase in the rotation speed up to 100 rpm that elevates the mechanical energy of the melt blending could enhance the exfoliation and dispersion of filler particles in melted matrix of PLA (Darie et al., 2014). Tawakkal et al. (2010) further explained that good distribution of polymer within its matrix is indicated by the stabilization zone monitored *via* mixing torque curve. The torque rheometer curves generated from the Brabender Plastograph mixer during melt processing could provide useful information such as the final stock temperature, torque shear rate and time needed for homogenous blend of the polymers in minimizing sample degradation and mechanical wear (Tee et al., 2014).

Apart from melt mixing, compression molding/hot press has similar effect to the film fabricated. Garkhail et al. (1999) reported that compression molding produces composites with better mechanical properties as compared to injection molded composites such as increase in impact resistance, fiber length and toughness. However, Sullivan et al. (2015) found that the later method of melt spinning has more advantageous than that compression molding in their crystalline nanocellulose-poly(lactic acid) (CNC/PLA) composites. The authors explained that melt spinning minimized the size of CNC agglomerates.

Subsequently, cooling process is necessary for every high temperature molded composites. Sullivan et al. (2015) practiced ambient air cooling to below polymer glass transition temperature in order to minimize plastic deformation and thermal residual stresses. Lower cooling rate was presumed to increase portion of the melt crystallization, hence, degree of crystallinity also increases (Běhálek et al., 2013). This

is because increasing cooling rate resulted in insufficient time for defective crystal of melted polymer to undergo perfection during heating (Setiawan, 2015). On the other hand, Herrera et al. (2015) investigated on the effect of slow and fast cooling to the composites by cooling in air (20 min) and inside the metal plates (5 min), respectively. It was found that fast cooled films showed the highest elongation at break of 300 % with the most transparent appearance.

As the main drawback of PLA is its stiffness and lack of elasticity, addition of plasticizers in PLA is regularly conducted and BMIMCl has the potential of acting as plasticizing agent in PLA. In melt processing, melt viscosity plays an important role in affecting the final polymer blend produced. Auras et al. (2004) added that the amount of plasticizer directly influences the PLA processing stock temperature and shear rate. The plasticizing effect in the work of Pillin et al. (2006) only resulted enhancement in PLA mechanical properties from 10 % up to 30 % w/w whereas any higher plasticizer content showed poor tensile properties.

Cellulose nanofibers which was reported by Jawaid and Swain (2018) to have high surface area has the tendency to aggregate when dried. The authors recommended mixing the blends in a suitable medium prior to further processing such as extruder or melt compounding. In this case, ionic liquid which has high polarity and low melting point could be a suitable medium for this PLA composite fabrication route. Hence, results comparison from plenty of previous works showed that melt compounding method is more favorably considered as compared to solvent casting.

2.5 Summary of Literature Review

Poly(lactic acid) is well known for its renewability and biodegradability for packaging applications to replace the synthetic polymers. However, its glassy and low

ductility properties hinders such applications. Hence, PLA composites are produced with incorporation of plasticizers, functional groups and organic fillers to enhance its chemical and mechanical properties. Reinforcement of organic materials seems a promising method to improve the PLA properties while reducing cost.

Organic fillers are available from agricultural waste or plant source such as cellulose, keratin, starch and chitin which are long chains of polysaccharides or proteins. Among these biopolymers, cellulose has a remarkable high crystallinity properties that may contribute to the thermal stability of the PLA composites. Since the hydrophilic cellulose may have immiscible effect towards hydrophobic PLA. Introducing keratin, an amphiphilic protein would act as a bridge in between cellulose and the PLA matrices. In comparison with the sources of organic fillers, implementing cellulose and keratin fibers are the most environmental friendly with least chemical usage in extraction and with simple preparation.

While examining between solvent casting and melt compounding method, dispersion has always been an issue in polymer composites especially the agglomeration of cellulose. Ionic liquid has superior green solvent properties in term of stability and polymer dissolution ability than that organic solvent. There are different types of ionic liquids ranging from imidazolium, pyridinium, piperidinium, pyrazolium, thiazolium, pyrrolidinium, ammonium, sulfonium to phosphonium based ILs. From the aspect of toxicity, applications in biopolymer and thermal stability, imidazolium salts were more extensively studied for their properties, especially BMIMCl where the mechanism of dissolution was also widely investigated.

In most solvent casting, organic solvents are utilized in film fabrication to allow the evaporation of solution. Since ionic liquid is responsible for the dissolution of polymers, melt compounding would be a better option as its large scale of production would

commercialize industrial application. This overall method provides a set of straightforward and convenient way of fabrication PLA composites.

Universiti Malaya

CHAPTER 3: MATERIALS AND METHODS

3.1 Introduction

This chapter describes the materials and comprehensive methodology of physical treatment of CFF and preparation of composite films. All experimental setup and equipment for characterization were conducted in laboratory condition under room temperature.

3.2 Materials

Poly(lactic acid) (2003D Ingeo™, melt flow index (MFI) 6 g/10 min at 210 °C/ 2.16 kg, relative viscosity 4.0, peak melting temperature 145-160 °C, glass transition temperature 55-60 °C) was purchased from NatureWorks LLC, USA. The chicken feathers were collected from local wet market. 1-Butyl-3-methyl-imidazolium chloride (BMIMCl, purity ≥99.0 % (HPLC), melting point 67-71 °C, molecular weight 174.67 g/mol), n-Hexane (ACS, Reag. Ph Eur) and dichloromethane (ACS, ISO, Reag. Ph Eur) were purchased from Merck KGaA, Darmstadt, Germany. Microcrystalline cellulose (MCC) powder, 20 μm (Cotton linters, particle size distribution: d50 18-22 μm, pH 5.5-7.0) was obtained from Sigma-Aldrich Co., MO, USA. All of the chemical reagents were used without further purification.

3.3 Methodology

3.3.1 Physical Treatment of Chicken Feather Fibers (CFF)

The chicken feathers were washed with clean water for several times and dried completely in oven to ensure no contamination of water during extraction. Chicken feathers were inserted into extraction thimble approximately 70 % full to prevent overflowing of feathers in the Soxhlet extractor. A 500 mL mixture of 1:1 ratio of

dichloromethane and hexane were prepared for Soxhlet extraction at the temperature of approximately 80-100 °C for 7-9 hours to remove the fatty acids and dirt from the feathers. The clear and colorless organic solvents mixture turned yellow and slightly cloudy after 7-9 hours, indicating the presence of fats and dirt from feathers. The feathers were rinsed with hexane and dried in oven before being stored in sealed plastic bags. The chicken feathers were cut into smaller sizes before further crushed into powder with centrifugal ball mill (S 100, Retsch GmbH) for about 2 hours at 400 rpm speed to obtain non-uniform particle size of brown CFF powder. The chicken feather fibers powder with the size of below 250 μm was collected with vibratory sieve shaker (AS 200, Retsch GmbH). The CFF powder was kept in 45 % humidity drying cabinet for further use.

3.3.2 Preparation of Composite Films

3.3.2.1 Experimental Setup

The Plastograph EC Plus with measuring mixer W 50 EHT (Model 835205.002, Brabender GmbH & Co KG, Duisburg, Germany) for melt-blending was preheated at 180 °C for approximately 15 minutes until the stock temperature stabilized and reached close to 180°C. The heating parameter was set to 60 rpm speed, 50 Nm of measuring range with 3 zones of mixers. Likewise, the hot press machine (GT-7014-A30C, GoTech, Taiwan) was preheated at 180 °C on both sides of heating plate until the temperature stabilized.

3.3.2.2 Dissolution of Fillers in BMIMCl

The dissolved fillers in BMIMCl was first prepared by melting BMIMCl (2.0 g, 5 wt% of total polymer weight) at 100 °C to remove water vapour. 20 wt% of fillers (total weight of 0.4 g depending on the CFF and MCC composition) were prepared.

Subsequently, the temperature was raised to 110 °C and slowly dissolved CFF a little at a time and then reduced to 90 °C for MCC. The mixture was stirred with magnetic stirrer until the mixture thickened to form a gel-like solution. The mixture was continuously stirred with hand stirring to ensure all fillers were completely dissolved. The mixture was let to cool down at room temperature for approximately 2-3 hours to form a gel or paste before melt-blending.

3.3.2.3 Film Fabrication

The preparation of the films were divided into 3 parts; neat PLA, PLA composites, and composites with added BMIMCl. The composition of composite films is as summarized in Table 3.1.

The neat poly(lactic acid) was prepared as a constant variable by melt-blending. PLA pellets (40 g) were first loaded in the measuring mixer at 180 °C for 8 minutes as accordance to the blending torque upon reaching constant value with the rotor speed of 60 rpm until the transparent PLA was well blended. Subsequently, blended PLA was preheated at 180 °C in between the heating plates for 10 minutes in the hot press machine. Upon compression at 180 °C, the bubbles trapped in the film was released by repeatedly compressed and released for 6 times. The PLA was compressed at 180 °C for 5 minutes under the pressure of 30 tons per square inch (tsi) followed by 3 minutes rapid cooling to room temperature to form neat PLA film with 1 mm thickness (180 mm x 180 mm dimension).

The fabrication steps for PLA composites without BMIMCl with the CFF/MCC ratios of 100/0, 70/30, 50/50, 30/70 and 0/100 were almost similar to the neat PLA. 99 wt% of PLA pellets (39.6 g) were loaded in the measuring mixer at 180 °C until the pellets were fully melted followed by the addition of 1 wt% of fillers (0.4 g) a little at a

time. The composites were melt-blended for 8 minutes at 60 rpm until the blending torque reached a constant value. Then, the composite blend was preheated in between the heating plates for 10 minutes in the hot press machine. Upon compression, the bubbles trapped in the film was released by repeatedly compressed and released for 6 times. The composite was compressed at 180 °C for 3 minutes under the pressure of 30 tsi followed by 3 minutes rapid cooling to room temperature to form 1 mm thickness film.

PLA composites with BMIMCl and CFF/MCC compositions of 100/0, 70/30, 50/50, 30/70 and 0/100 respectively, required the dissolution of fillers prior to melt-blending. As soon as the translucent gel-like mixture of dissolved fillers in BMIMCl was formed, it was premixed with PLA pellets (39.6 g) before loading onto the 180 °C measuring mixer for 6-8 minutes. Meanwhile, PLA-IL required only premixing with 2.0 g of BMIMCl before melt-mixing. Subsequently, the mixture of dissolved fillers in BMIMCl was melt-blending with PLA for 5-7 minutes at 60 rpm depending on blending torque upon reaching constant value. The composite blend was preheated in between the heating plates for 4 minutes in the hot press machine. Upon compression, the bubbles trapped in the film was released by repeatedly compressed and released for 6 times. The composite was compressed at 180 °C for 2 minutes under the pressure of 30 tsi followed by 3 minutes rapid cooling to room temperature to form 1 mm thickness film. All samples were stored individually in 45 % humidity drying cabinet for at least 1 to 2 weeks before characterization studies to observe the stability of the composite films.

Table 3.1: Composition of PLA blend composite films

Sample	CFF/MCC ratio	Composition (wt%)		
		PLA	Filler(s)	BMIMCl
PLA	-	100	-	-
PLA-CFF ₁₀₀	100/0	99	1	-
PLA-CFF ₇₀ MCC ₃₀	70/30	99	1	-
PLA-CFF ₅₀ MCC ₅₀	50/50	99	1	-
PLA-CFF ₃₀ MCC ₇₀	30/70	99	1	-
PLA-MCC ₁₀₀	0/100	99	1	-
PLA-IL	-	95	-	5
PLA-CFF ₁₀₀ IL	100/0	94	1	5
PLA-CFF ₇₀ MCC ₃₀ IL	70/30	94	1	5
PLA-CFF ₅₀ MCC ₅₀ IL	50/50	94	1	5
PLA-CFF ₃₀ MCC ₇₀ IL	30/70	94	1	5
PLA-MCC ₁₀₀ IL	0/100	94	1	5

3.4 Characterizations of PLA Composite Films

3.4.1 Torque Rheometer

The change in torque (Nm) as a function of time (s) of CFF-MCC reinforced PLA blends with different compositions were analyzed in a Brabender torque rheometer with roller blades (Mixer W 50 EHT, Plastograph® drive, WinMix software, Version 4.2.16). The torque curve generated by the plastograph illustrated the fusion behavior of PLA composites such as viscosity, fusion time, gelation speed and mechanical energy input.

3.4.2 Fourier Transform Infrared Spectroscopy (FTIR) Analysis

The chemical structures of the raw materials, CFF, MCC, BMIMCl as well as PLA composite films were determined *via* FTIR Spectrum 400 (Perkin Elmer, USA) using diamond attenuated total reflectance (ATR) surface characterization technique on the composite films. The transmission spectra were obtained in a scan range of 4000-450 cm^{-1} , scan rate of 32 units scan and a 4 cm^{-1} resolution.

3.4.3 Thermogravimetric Analysis (TGA)

The thermal stability of the raw materials, CFF, MCC, and sample films were examined using TA Instruments Q500 (Switzerland) from room temperature to 500 °C at the rate of 5 °C/min under nitrogen atmosphere with the standard operating sample film mass of 5-10 mg. The results were plotted as percentage of sample weight loss against temperature to identify the onset and peak of sample degradation temperature as well as the percentage of residue up to 500 °C.

3.4.4 Differential Scanning Calorimetry (DSC)

DSC experiments were carried out using Mettler Toledo DSC 1 (Switzerland) instrument. The measurements were performed on the neat PLA and PLA composites films with the sample weight of 5-10 mg each under nitrogen gas atmosphere at the rate of 10 °C/min from -60 °C to 220°C. The data collected was plotted as heat flow against temperature. The crystallinity of the samples (χ_c) were calculated by the following equation:

$$\chi_c = \frac{\Delta H_f}{\Delta H_f^0 W} \times 100 \%$$

where ΔH_f is the apparent specific melt enthalpy of the sample, ΔH_f^0 is the melt enthalpy of PLA (93 Jg^{-1}) and W is the weight fraction of PLA over the total sample weight (Martins et al., 2014; Yeh et al., 2008).

3.4.5 X-ray Diffraction Analysis (XRD)

Rigaku (Japan) X-ray diffractometer (operated at 40 kV and 40 mA) was performed on the film surface of PLA composite with and without BMIMCl at a wavelength of 1.54 \AA with Cu K α radiation. The intensity was collected over a 2θ range of 5° to 90° , at a scan rate of $0.026^\circ/\text{s}$. XRD non-destructively records the diffracted X-rays pattern made by the PLA composite film crystals (Dutrow & Clark, 2019). The degree of crystallinity was calculated using the equation below:

$$\chi_c = A_c / (A_c + A_a)$$

where A_c and A_a are the crystalline and amorphous areas on the X-ray diffractogram respectively (Yee et al., 2016).

3.4.6 Surface Morphology

Scanning electron microscope (SEM) (Phenom ProX, Netherlands) was used to study the morphology of the film cross section at an activation voltage of 5 kV at room temperature. The composite films of PLA, PLA-IL, composites with CFF/MCC ratio of 0/100, 50/50 and 100/0 for both with and without IL were fixed by a mutual conductive square metal plate on aluminum stubs and coated with thin layers of gold using sputter coater to avoid charging effect. The cross section images were captured at lower and higher resolution with the magnification of 430x ($200 \mu\text{m}$) and 1100x ($50 \mu\text{m}$) respectively.

3.4.7 Vickers Hardness Test

The hardness testing was conducted on all PLA composites using Vickers hardness tester (Mitutoyo Corp., Kawasaki, Japan) with the diamond pyramid indenter of 136° top angle (Djellali et al., 2013). Indentation load of 2 kgf was applied for a holding time of 10 s. The width of the sample film indentation observed from optical microscope with 10x magnification was measured and calculated from the hardness, HV equation below:

$$HV = 1.8544 \frac{P}{d^2}$$

where P is the indentation load (kgf) and d is the arithmetic mean of the pyramidal diagonal lengths $(D1+D2)/2$ (mm²) (Orozco et al., 2009; Torres, 2010).

CHAPTER 4: RESULTS AND DISCUSSION

4.1 Processing Behavior and Torque Evaluation

The film fabrication of glassy poly(lactic acid) involved both protein and polysaccharide reinforcements, chicken feather fibers and microcrystalline cellulose respectively. Among the raw materials used, chicken feather was collected from wet market and underwent colour sorting with naked eye and obtained only one batch processing to prevent the possible difference in their chemical properties. Some chicken feathers obtained had variation in colour such as light brown, dark brown, red, grey, black, or a mixture of a few colours mentioned. The colour of the chicken feathers were sorted by the similar tone of the brown colour and the feathers with a mixture of more than one colour were eliminated. Apart from the consideration of its shelf life, the chemical structures may also affect its overall properties to the composite films. Grinding of chicken feather was rather uncommon as compared to keratin extraction. Chicken feathers are separated by 2 distinct types of protein with different properties, α -helix and β -sheet. As the feather fibers are mainly α -helix while the inner quill is β -sheet structure, the ordered structure of β -sheet inner quill possesses stronger mechanical properties. To be consistent with the state appearance of readily MCC for the ease of composite fabrication, the CF grinding *via* centrifugal ball mill was repeatedly crushed and sieved to obtain optimum size distribution of particles as illustrated in Figure 4.1.



Figure 4.1: Cleaned chicken feathers *via* Soxhlet extraction (left) and crushed chicken feather fibers in powder (right)

From the past literature, biopolymers reinforcement such as keratin and cellulose were often incorporated at least 10 wt% up to 60 wt% for PLA properties enhancement and cost reduction (Huda et al., 2006; Lam et al., 2009; Aranberri et al., 2017). However, Cheng et al. (2009) reported increasing keratin concentration worsened the mechanical properties significantly such as tensile strength and elongation. Despite 2 wt% and 5 wt% CFF loading slightly improved the mechanical properties, CFF was indeed brittle. Besides, PLA composites of Aranberri et al. (2017) with 60 wt% CFF degraded at lower temperature than that 50 wt % CFF. Therefore, fabrication of CFF-MCC reinforced PLA in this work maintained as low as 1 wt% to observe the impact of fillers to the PLA matrices and properties.

Reinforcement of powdered CFF alongside with MCC resulted PLA composites to be slight brown in colour with reduced transparency as compared to neat PLA. In contrast, PLA composites with fillers dissolved in ionic liquid had darker brown appearance with higher transparency. This is because the powders remained in solid in high temperature processing with poly(lactic acid) while BMIMCl completely dissolved the fillers into highly viscous liquid as shown in Figure 4.2 before being more

homogeneously blended with PLA. The observation concurred with Zhang et al. (2017a) who mentioned that strong interface interactions of hydrogen bonding between the hydroxyl groups of fillers would create better fillers dispersion. Hence, reduction in CFF particle size and the use of BMIMCl were able to enhance the fillers dispersion in PLA.



Figure 4.2: Dissolution of CFF in BMIMCl at 110 °C; before (left) and after (right)

The use of BMIMCl was considerably step sensitive as several work were reported to dissolve the fillers separately before blending (Kammiovirta et al., 2016). However, it was found that one pot dissolution was more efficient than mixing them separately as similar to the method used by Kuzmina et al. (2012) in dissolving chitosan and cellulose. Another significant result observed was the dissolved fillers which was less viscous in higher temperature needed to be cooled down to viscous paste for slow crystallization. Turner et al. (2004) practiced similar additional step to cellulose dissolution to cool the polymer matrix to room temperature. The consequence of skipping this step and direct melt blending with PLA will create phase separation with non-uniform dispersion of fillers.

Filler dispersion and homogenous blending were also aided by the Brabender measuring mixer which uses heat to dry melt and blend the polymer without using organic solvent to dissolve it. This method is well known for being quick, easy and environmental friendly. However, the mixing mode of blending duration, rotor speed and temperature are crucial in obtaining effective composite preparation. From the observation, increasing melt blending time darkened the composites. Duration of blending was differed based on stabilized torque and viscosity of the polymers to prevent further decomposition of dissolved fillers under high temperature. Although increasing the rotating speed could be a way to achieve shorter blending time, only 60 rpm was implemented as accordance to similar previous work (Lim et al., 2015). According to Figovsky and Beilin (2014), polymer shear stresses elevate with increasing blade speed and this condition will fail to provide sufficient time for the polymer relaxation to develop. Hence, affecting its flow properties where the composites are pulled away from mixer walls and prevent agitation. When 80 rpm was applied, segregation occurred.

Torque does not only represent the viscosity of the polymer blends as a function of time but also explains the condition of the composites *via* 3 torque stages. As represented in Figure 4.3, the first stage was the beginning of PLA or its composites melting affected by heat transfer processes until upon the maximum torque (García et al., 2017). An abrupt decrease of torque values in second stage was the fillers diffusion that hinder the free rotation of twin rotating blades. The final stage showed the constant value of torque recovered to the steady-state where the polymers are completed mixed homogeneously. The torque curve is also a measure of fusion time, gelation speed, and the mechanical energy input of the composites.

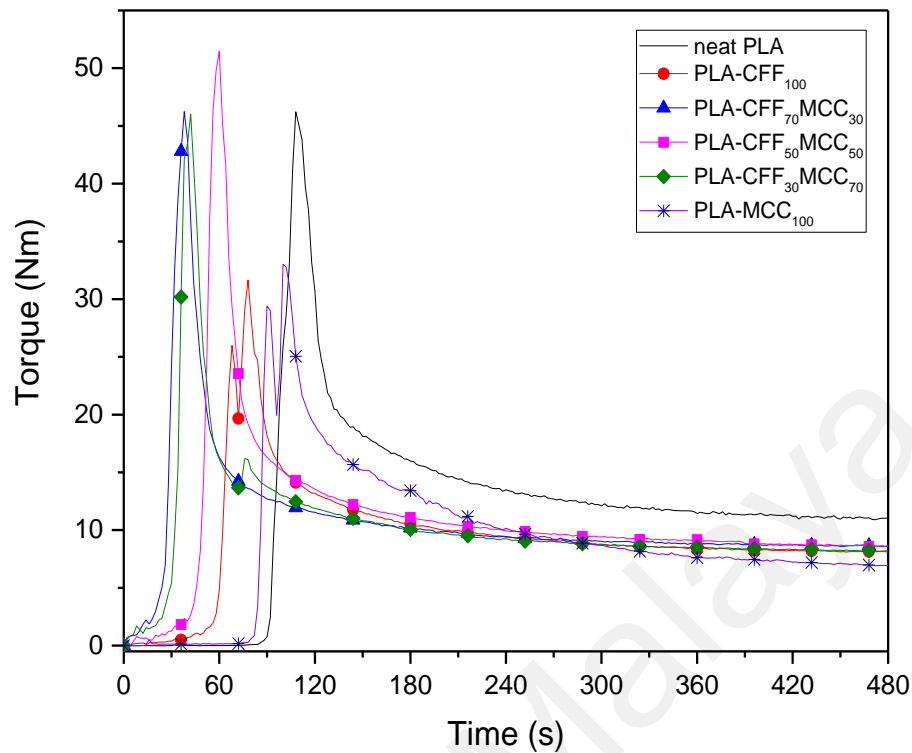


Figure 4.3: Torque-time curves of PLA composite blends without BMIMCl

Maximum torque value is considerably significant in comparing composite viscosity and resistance to rheometer blades (Garcia et al., 2016). For instance, PLA composite without BMIMCl with CFF to MCC of 50/50 showed highest maximum torque, 51 Nm comparatively more than neat PLA, 46 Nm. Nevertheless, maximum torque of PLA-MCC₁₀₀IL (Figure 4.4) was the highest of 13 Nm among composites with BMIMCl while the rest remained about the same as PLA-IL, 10 Nm. Tawakkal et al. (2010) explained that higher maximum torque indicates higher mechanical shear forces are applied to flow the cold resins. On the other hand, Yeh et al. (2008) suggested that maximum torque is proportional to melt viscosity which successively implies stronger PLA and fillers interaction with increasing maximum torque. The reason for PLA-CFF₁₀₀ and PLA-MCC₁₀₀ (Figure 4.3) remained the lowest may be due to the lack of interaction between PLA with CFF and MCC individually. The results indicated stronger interaction between PLA with both CFF and MCC.

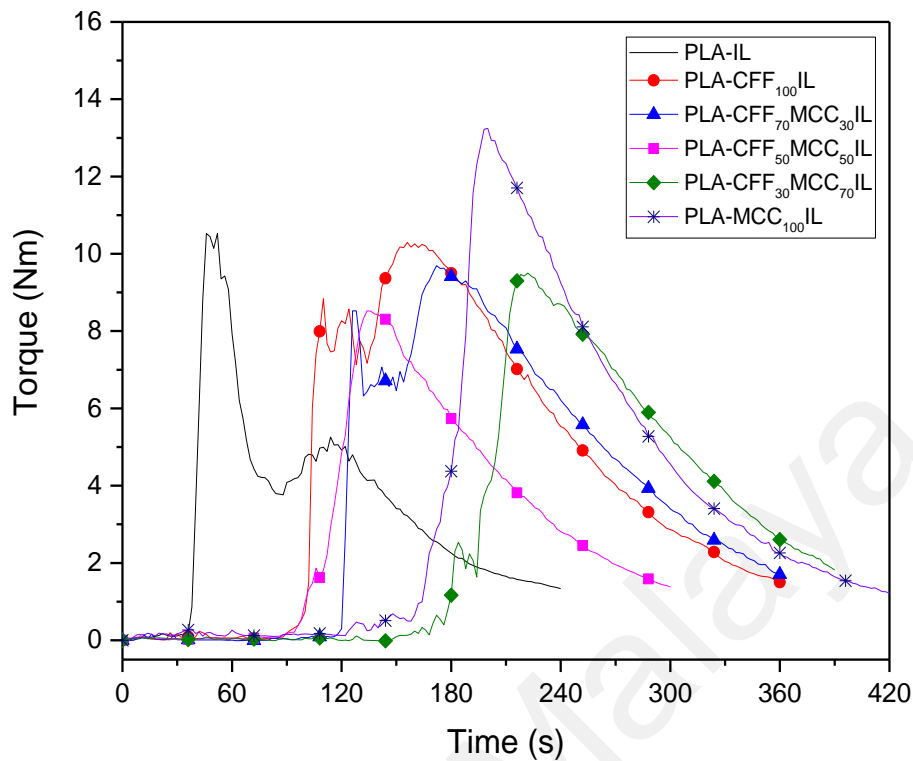


Figure 4.4: Torque-time curves of PLA composite blends with BMIMCl

The lack of interaction between PLA with CFF and MCC individually may also be the cause of the only 2 maximum torques in PLA-CFF₁₀₀ and PLA-MCC₁₀₀ as compared to the rest of the composites. The incompatibility may have resulted the detection of separate maximum viscosity of both CFF or MCC and PLA. In addition to the intensity of maximum torque, the plastogram in Figure 4.4 showed larger gap of time from 1 to more than 3 minutes for the composites with BMIMCl to reach maximum torque as compared to composites without BMIMCl. PLA-CFF₃₀MCC₇₀IL was recorded at 3.7 min with the longest time followed by PLA-MCC₁₀₀IL. The delay of time may be close related to the most composition of MCC dissolved in BMIMCl that affected its melt viscosity and shear rates. MCC and BMIMCl may also have higher heat capacity that slow down the heat transfer process during the mixing (García et al., 2017).

Since viscosity is closely related to the height of maximum torque, viscosity of the composites is proportional to their molecular weight. Similarly, Galimova et al. (2015) reported increasing maximum torque indicated higher degree of vulcanization in natural rubber. In other words, PLA-CFF₅₀MCC₅₀ (Figure 4.3) showed highest cross-linking density between the fillers and PLA matrices among the PLA composites without BMIMCl. The cross-linked network resulted in the maximum torque 5 Nm higher than other compositions composites and neat PLA. The composites of 70/30 and 30/70 ratio of CFF to MCC remained similar molecular weight as neat PLA. The torque-time curve also implied that individual reinforcement of CFF and MCC had poor cross-linking with PLA matrices as seen in PLA-CFF₁₀₀ and PLA-MCC₁₀₀.

In general, presence of BMIMCl decreased the viscosity of PLA composites with less than 14 Nm. The occurrence was due to the ionic liquid that deformed the polymer chains causing their frictional resistance to subside or diminish (Răpă et al., 2015; Răpă et al., 2017). Thus, increasing the polymer chain mobility. Likewise, Gao et al. (2015) explained that as viscosity and molecular weight of polymer decreased, molecular entanglement reduced, causing the ease of the molecular chain motion. As the torque of PLA composites with BMIMCl decreased to critically low values in the second stage, beginning of polymer thermal degradation was observed due to the darkening colour with increasing time. As a result, the melt blending time was adjusted based on their optimum viscosity or torque value of about 2 Nm.

As a comparison of selected PLA composites with the presence of BMIMCl variable in Figure 4.5, both sets of PLA composites showed similar trend of decreasing torque and increasing time to reach maximum torque with the addition of ionic liquid. This may be due to BMIMCl that promoted the thermal degradation of composites and decreased the melt viscosity. In contrast, BMIMCl enhanced the compatibility of

previously mentioned PLA-CFF₁₀₀ and PLA-MCC₁₀₀ with 2 maximum torques to single value in PLA-CFF₁₀₀IL and PLA-MCC₁₀₀IL. The ionic liquid also stabilized and lowered the mechanical shear forces of PLA composites with BMIMCl with less intense maximum torque fluctuation such in non BMIMCl added composites. In brief, considerably lower melt viscosity demonstrates better processibility during mixing and shear rate conditions (Menon, 1999). The viscosity of composites without BMIMCl of CFF to MCC arranged in a group of ascending order as; 100/0, 0/100 < 70/30, 30/70, neat PLA < 50/50 while PLA composites with BMIMCl remained almost constant except for relatively higher viscosity of PLA-MCC₁₀₀IL.

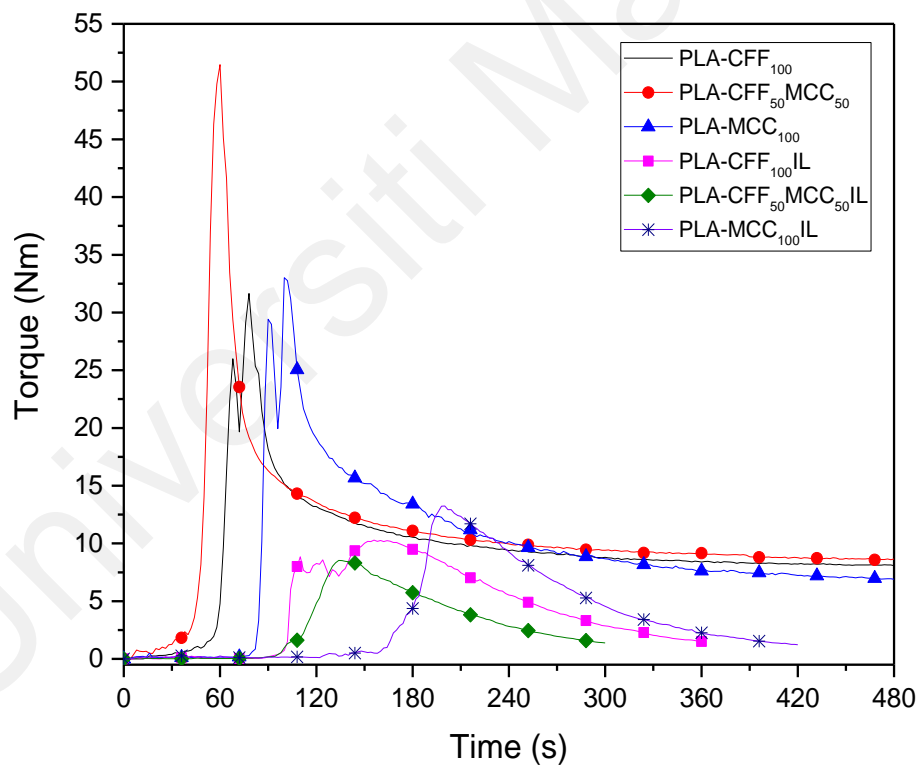


Figure 4.5: Comparison plastogram of PLA composites with and without BMIMCl

For the final step of sample film fabrication, the optimization of compression molding also play an important role in preheating, compressing and cooling in order to obtain good finishing. Sample being hot pressed without sufficient time of preheating

will cause trapped bubbles and cracks. As similar to Herrera et al. (2015), the composites were cooled in the metal plates to allow crystallization. The compression molding has the advantage of producing smooth surface film on both sides with similar surface morphology in which was further studied *via* SEM in Section 4.6. Addition of BMIMCl reduced the viscosity and softening point of the PLA blends. Therefore, the compression time of PLA composites with BMIMCl were reduced and optimized to avoid the overheating and leaking of PLA blends from the metal mold.

The film compression molding fabrication *via* 3 minutes quick cooling from 180 °C to room temperature may be one of the factors that worsen the composite films crystallinity as discussed in XRD data (Section 4.5). Setiawan (2015) revealed that increasing hot press cooling rate reduced polymer crystallinity, increasing their amorphous. Un-annealed PLA of Tabi et al. (2010) was amorphous and subsequent annealing at 80 °C showed intense crystalline peak at 16.3° in XRD pattern. Fast cooling of compression molding could be a disadvantage to the biopolymer fabrication that require high crystallinity.

Stability of polymer films is important in accessing their composite shelf-life and possible applications. Incorporation of BMIMCl significantly influenced the bonding between the polymer matrices that resulted in film swelling upon storage for a period of time. According to Nijenhuis et al. (1996), swelling of polymer blends are due to the increased hydrophilicity. In the case of ionic liquid added PLA composites, hygroscopic nature of BMIMCl may have contributed to the absorption of moisture. On the other hand, PLA composite films without BMIMCl remained stable with no swelling observed.

4.2 FTIR Molecular Analysis

Infrared spectra of ATR technique was used to study the effect of fillers and ionic liquid to the chemical properties of PLA composites *via* comparison with the raw materials. The absorption peaks of lactic acid were distinctive in the spectra of PLA composites illustrated in Figure 4.6, especially the carbonyl and methyl functional groups. The C=O of ester group of PLA was observed as an intense peak in 1747 cm^{-1} (Yeh et al., 2008; Tawakkal et al., 2010). The absorption bands of 1181 cm^{-1} , 1127 cm^{-1} , 1081 cm^{-1} and 1044 cm^{-1} were attributed to the CH_3 rocking as reported by Martins et al. (2014). Regardless the presence of BMIMCl, the intensity of these characteristic bands were unaffected.

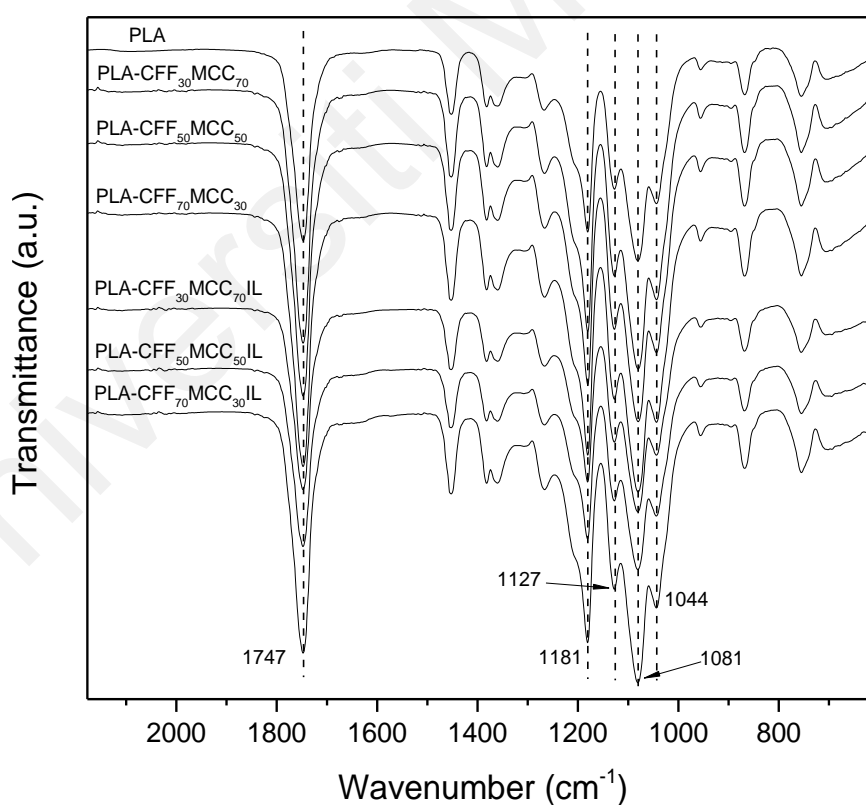


Figure 4.6: FTIR spectra of lactic acid characteristic peaks in PLA and its composites

Aside from PLA characteristic peaks, the composites reinforcement of keratin from CFF should also have a stretching vibration of C=O bond of the Amide I in between 1700-1600 cm^{-1} (Gallagher, 1997; Wu et al., 2015; Wang et al., 2017) and MCC with a -C-O- stretching of the carboxyl group within the range of Amide I at 1646 cm^{-1} reported by Zhang et al. (2013). However, these absorption bands found in individual MCC and CFF at 1642 cm^{-1} and 1627 cm^{-1} respectively in Figure 4.7 are rather weak relatively to that neat poly(lactic acid). In agreement to Na Ayutthaya et al. (2015), fillers with less than 10 % are hardly detectable from the ATR surface characterization. In fact, most of the prominent peaks of CFF and MCC overlapped with PLA broad and intense peaks among the region of 1500 cm^{-1} to 1000 cm^{-1} and Doncea et al. (2010) defined this characteristic region of cellulose in between 1400-1000 cm^{-1} as “fingerprint region”.

Nevertheless, an additional peak (1676 cm^{-1}) was found on PLA composites which was close to the C=C stretching of BMIMCl, 1674 cm^{-1} (Dharaskar et al., 2013a). The weak vibration which was not visible in neat PLA spectrum was present in the represented composites of PLA-CFF₁₀₀IL and the intensity increased steadily in PLA-MCC₁₀₀IL and PLA-IL. This suggests that the signal may be attributed to the interaction of BMIMCl with MCC (1642 cm^{-1}) that resulted in the slight shift to a higher wavenumber. The effect of CFF at 1627 cm^{-1} to the weak absorption was less significant as seen in PLA-CFF₁₀₀IL.

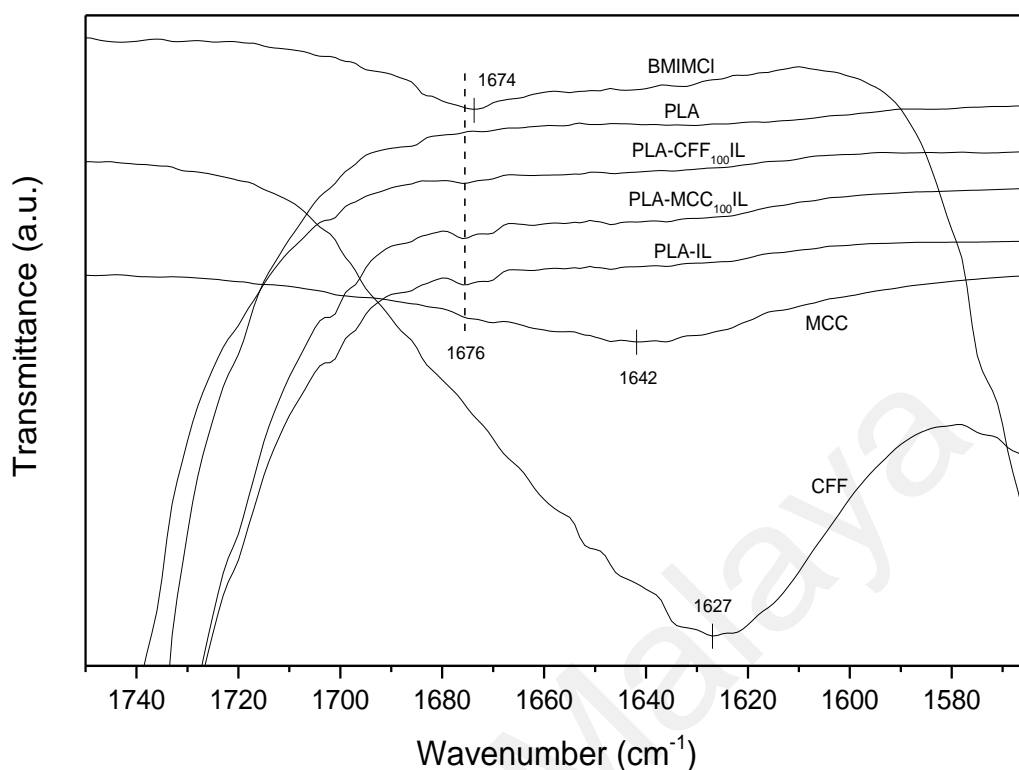


Figure 4.7: FTIR spectra of CFF and MCC characteristic peaks in PLA composites

Poly(lactic acid) is known to be hydrophobic in nature with no broad OH peak above 3200 cm^{-1} as shown in Figure 4.8. Although both MCC and CFF consist of hydrophilic surface properties due to the OH group in cellulose structure and side chains of amino acids, PLA composites without ionic liquid with the ratio of 30/70, 50/50 and 70/30 showed no sign of moisture absorption band. High temperature melt blending and hot press may have been the reason for the escape of moisture trapped on the surface of fillers and altered the surface properties of these components.

However, the wide OH absorption band intensified with increasing CFF composition in the PLA composites with BMIMCl. The interaction of hygroscopic BMIMCl with CFF that absorbed moisture into the composite films could be the possible reason to this observation. This is as similar to the increase in water absorption with higher CFF content in PLA composites by Cañavate et al. (2015). While Dharaskar et al. (2013a)

claimed that the broad peak in the range 3330–3450 cm^{-1} was due to quaternary amine salt formation with chlorine in BMIMCl, the argument was not confirmed due to the overlapping of these two broad absorption bands. Singh and Kumar (2011) also mentioned that the presence of moisture content in the composites indicates the weakening of the hydrogen bonds between BMIMCl and CFF that created free hydroxyl group to interact with water

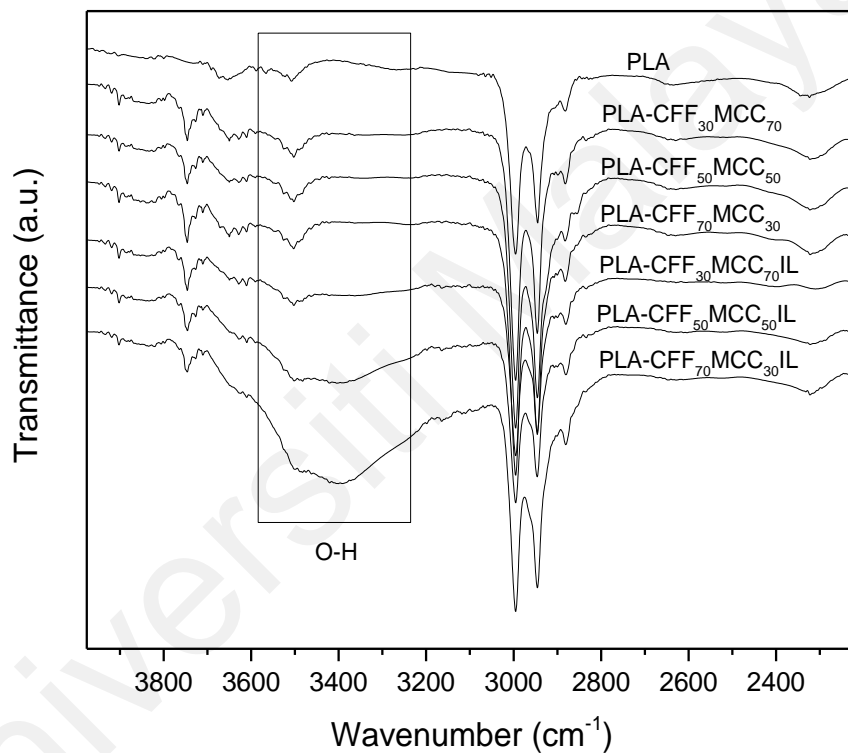


Figure 4.8: Moisture absorption peaks of PLA and its composites in FTIR spectra

Spiridon et al. (2013) mentioned that the absorption bands at 867 cm^{-1} and 754 cm^{-1} were attributed to the amorphous and crystalline phases of PLA, respectively. The intensity of these peaks were weak and broad in neat PLA (Figure 4.9). As CFF and MCC were incorporated in the composites, the intensity of crystalline phase decreased while the intensity of amorphous phase at 867 cm^{-1} was kept constant. The degree of crystalline phase increased with increasing MCC ratio, indicating MCC is a promising

nucleating agent. In comparison with similar fillers composition in composites with BMIMCl, the crystalline intensity was higher than that neat PLA and the composites without IL. Apart from the absorption bands of composites were narrower, PLA-CFF₇₀MCC₃₀IL had the highest crystalline intensity. Although the difference in the crystalline phase intensity was small, the results were comparable with the DSC thermogram in Section 4.4.

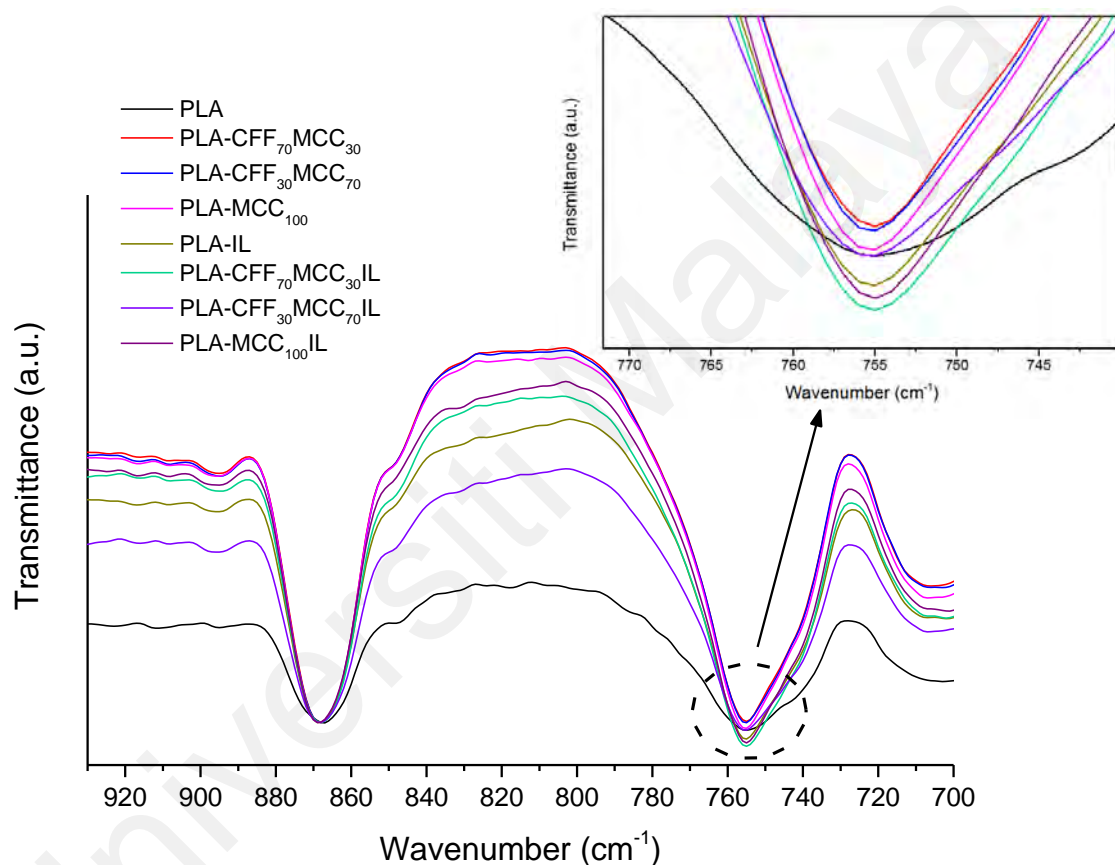


Figure 4.9: Infrared spectra of PLA characteristic peaks intensity

Other than the intensity of characteristic peak that was mentioned earlier, the PLA composites spectra were almost similar to that neat PLA with no missing of prominent peak which clearly defined that the dissolved fillers in PLA were unsusceptible to chemical degradation. Besides, no new absorption peak was found in the composites spectra as compared to the raw materials because there was no chemical reaction between ionic liquid with cellulose and keratin during dissolution. BMIMCl was proven to be a good solvent in disaggregating and disentangling the polymer chains under

heating and shearing, thus enhancing the chain mobility and polymer processibility (Wu et al., 2015). This suggests that fabrication of CFF and MCC dissolved in BMIMCl as reinforcements in poly(lactic acid) are feasible using high temperature melt processing and compression molding.

4.3 Thermogravimetric Analysis

The thermal properties of PLA and its composites were evaluated from thermal stability and thermal degradation of thermogravimetric analysis (TGA). The thermogram showed that neat PLA and the composites experienced single stage of degradation up to 400 °C with single polymer differential thermogravimetric (DTG) value as listed in Table 4.1. Generally, neat PLA has a constant range of thermal degradation in which it begins to degrade at 300 °C and the thermal decomposition completes at 400 °C (Auras et al., 2004). The thermal decomposition temperature range of the composites were based on the onset temperature of poly(lactic acid), $T_{\text{onset}} = 323$ °C which was also recorded to be having the highest thermal stability of all.

Neat PLA experienced maximum mass loss at 354 °C and reinforcement of keratin and cellulose accelerated the T_{max} by at least 6 °C. In the process of thermal decomposition, PLA experienced loss of ester group *via* inter- or intra-molecular transesterification to form oligomers or cyclic oligomers (Li et al., 2009; Teoh et al., 2016). PLA decomposition yielded significant amount of volatilized products such as aldehyde containing compounds, carbon monoxide, aliphatic esters and carbon dioxide (Chen et al., 2012). The volatile products were verified by Chen et al. (2012) *via* integrated TGA-FTIR analysis where fragments of major carbonyl containing compounds group exhibited at 1764 cm^{-1} were detected at around the T_{max} .

Table 4.1: Thermal degradation temperatures and DTG data of PLA and its composites

Sample	T_{onset} (°C)	T_{final} (°C)	$T_{\text{max/DTG}}$ (°C)	Residue (%)
PLA	323	375	354	1.28
PLA-CFF ₁₀₀	326	356	348	3.03
PLA-CFF ₇₀ MCC ₃₀	313	362	342	2.96
PLA-CFF ₅₀ MCC ₅₀	309	363	345	2.45
PLA-CFF ₃₀ MCC ₇₀	315	353	345	2.82
PLA-MCC ₁₀₀	315	368	343	1.83
PLA-IL	202	270	252	5.08
PLA-CFF ₁₀₀ IL	224	282	259	2.51
PLA-CFF ₇₀ MCC ₃₀ IL	209	273	258	1.55
PLA-CFF ₅₀ MCC ₅₀ IL	209	263	255	0.90
PLA-CFF ₃₀ MCC ₇₀ IL	211	262	251	1.72
PLA-MCC ₁₀₀ IL	220	286	265	3.51

According to Chen et al. (2012), the intensity temperature of aldehyde containing compounds from aliphatic esters reached maximum at 371 °C, close to the end of thermal decomposition. Certainly, the intensity of C=O at 1747 cm⁻¹ from the FTIR spectra in Figure 4.6 remained high even after the reduction of wt% in PLA after reinforcements and BMIMCl addition. Therefore, the thermal degradation of PLA ended at 375 °C, leaving less than 2 % residues. PLA composites without IL left behind relatively more residue than neat PLA upon complete thermal decomposition as CFF composition increases. Aranberri et al. (2017) claimed that the inorganic residue of CFF reinforced PLA composites remained above 400 °C belonged to CFF.

Although the thermal stability of PLA composites without BMIMCl represented by PLA-CFF₅₀MCC₅₀ (Figure 4.10) remained higher than the raw CFF and MCC with the respective T_{onset} of 262 °C and 308 °C, the composites decomposed at lower temperature but close to neat PLA. As a comparison with the similar ratio of 50/50, PLA composites with the presence of BMIMCl were listed the least thermally stable. The decline of the composite stability was caused by the reinforcements where Pang et al. (2013) also reported cellulose having only moderate thermal stability and rapid chemical decomposition of 315-400 °C. The onset temperature of CFF was lower than MCC, yet remained a weight of 21.80 % at 500°C while most samples residues were 5 % or less. It was suspected that the crushed quill and fiber have different thermal properties and the remaining weight residue may have much higher thermal decomposition above 500 °C.

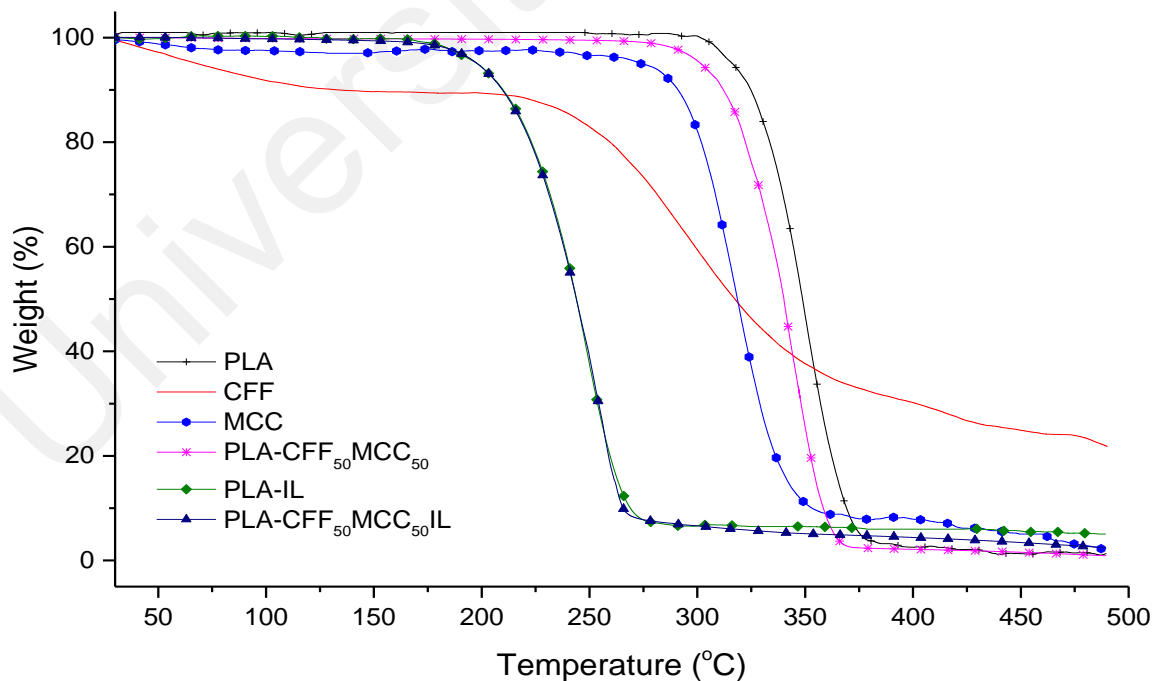


Figure 4.10: Thermal stability of PLA composite films and the raw materials in TGA

Raw CFF and MCC underwent two-stage decomposition due to the presence of moisture. Water has a boiling point of 100 °C and the curve of 10.10 % weight loss was observed in CFF, almost 5 times more than the moisture content of MCC 1.95 %. High moisture content in CFF was due to the evaporation of absorbed water from the hydrophilic groups of the keratin (Aranberri et al., 2017). However, no sign of weight loss was observed in PLA composites without BMIMCl around 100 °C corresponded to the moisture FTIR spectra in Figure 4.8. Likewise, composites with ionic liquid had similar results which may be due to the water weight loss that was too minimal to be seen in TGA thermogram. Due to the high temperature processing, permanent intermolecular bonding between polymers was expected to be formed upon cooling to room temperature which then hampered the nature ability of the hydrophilic surface of the fillers to absorb moisture.

A trend resembled to the torque results was observed in the thermal stability of composites with BMIMCl where ionic liquid did not only lower the viscosity, but also the thermal stability of composites. The thermogram of Figure 4.11 which illustrated only the thermal decomposition range of the composites showed that BMIMCl lowered the degradation temperature of the PLA composites by 100 °C as compared to those without ionic liquid. The occurrence was a result of ionic liquid ability to reduce molecular weight of polymer on solution processing with heat (Ren et al., 2017).

Similar ratio of composites with the variable of ionic liquid were not comparable as there was no definite orientation found in their thermal stability. As CFF composition increased in PLA composites with the absence of BMIMCl, the thermal stability decreased. In contrary, BMIMCl added composites encountered descend of thermal stability with increasing MCC composition. In other words, BMIMCl had more thermal degradation effect on MCC as compared to CFF which resulted PLA-CFF₃₀MCC₇₀IL

with the lowest onset temperature of 209 °C. Despite the influence of ionic liquid on CFF-MCC reinforced composites, the thermal stability of PLA-MCC₁₀₀IL remained the highest among the different compositions. It could be deduced that the influence of BMIMCl did not only affect the fillers individually but as a composition. Nonetheless, the difference of thermal stability between the ratios was almost negligible.

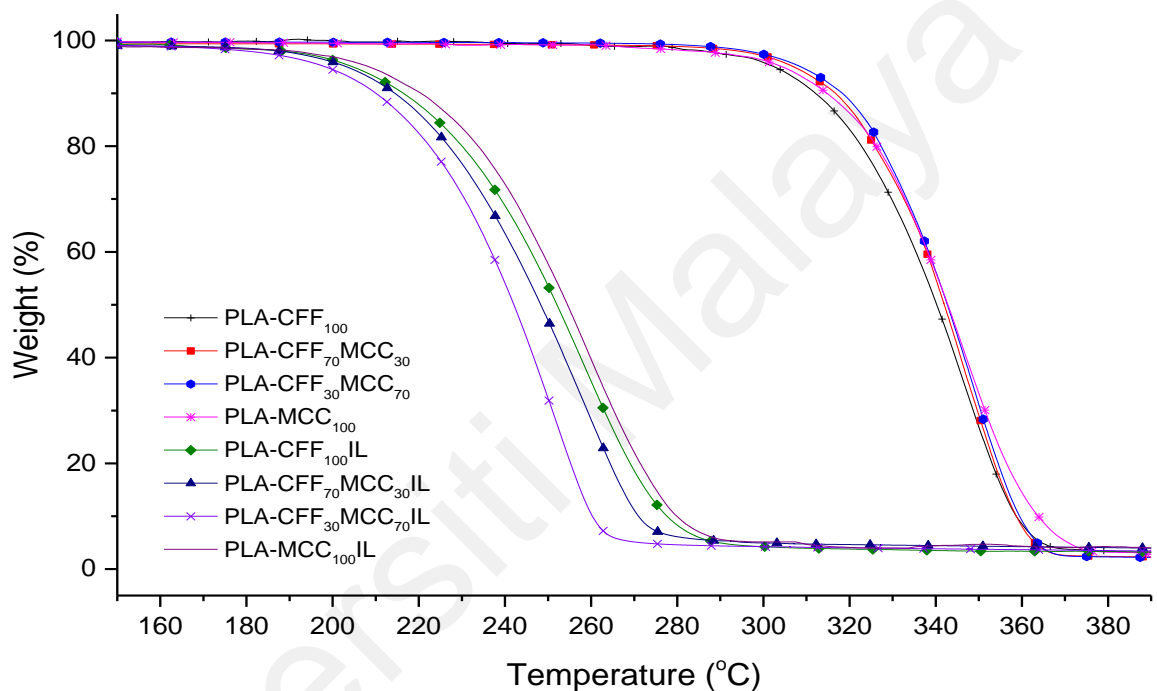


Figure 4.11: TGA thermogram of BMIMCl as comparison factor in PLA composites

In contrast, a distinct difference of degradation temperature range was found in BMIMCl added and non-added PLA composites. As two sets of similar compositions thermograms was compared in Figure 4.12, composites with IL experienced reduction in the rate of thermal degradation. This may be due to the higher thermal stability of BMIMCl. In the TGA analysis of Dharaskar et al. (2013a), BMIMCl began to decompose at 240 °C and the reaction completed at around 317°C with a weight loss of 81 % with no further decomposition. The data indicates high residual content of BMIMCl of about 19 %. Although BMIMCl has lower T_{onset} , its bulky molecular

structure is relatively more stable with increasing temperature. Although PLA produces carbonyl compounds and aliphatic hydrocarbons in the process of decarboxylation of the main chain upon high temperature (Chen et al., 2012), BMIMCl was able to broaden the thermal decomposition temperature range of PLA composites.

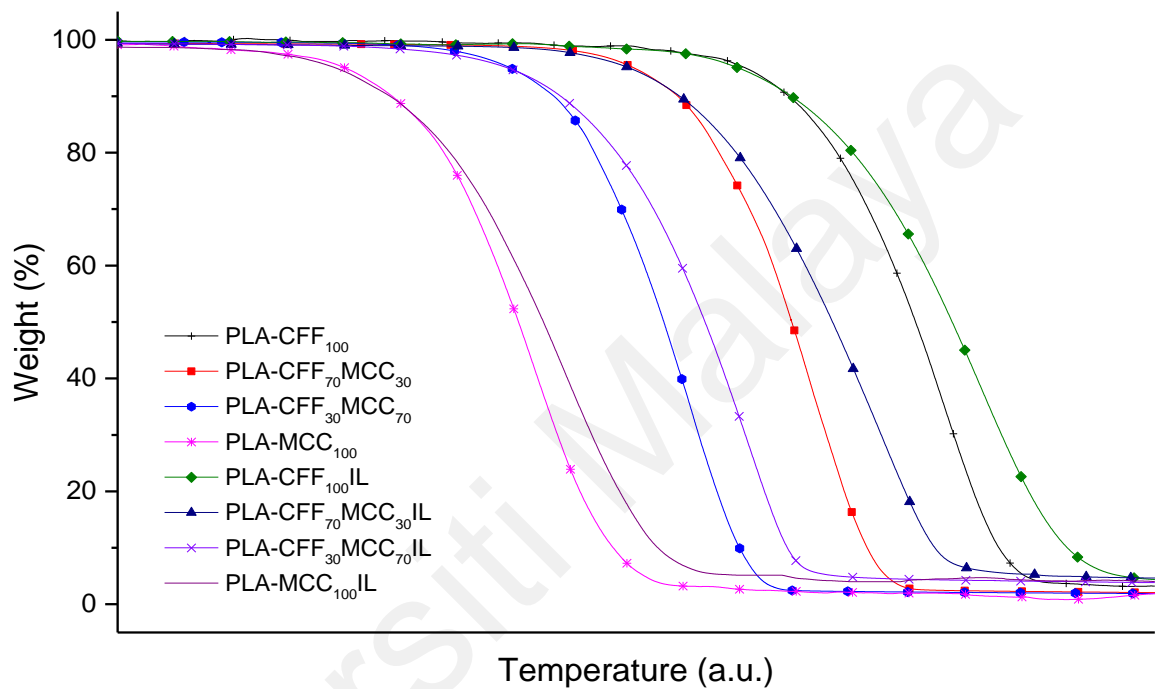


Figure 4.12: Thermal degradation rate of PLA composites with and without BMIMCl

4.4 DSC Thermal Properties

While TGA examines the change of mass in a sample, the DSC measures on the heat change where both also specialize on the thermal behavior of PLA and its composites. In general, poly(lactic acid) underwent a change of heat which began from 60 °C of glass transition temperature (T_g) to crystallization (T_c) and melting (T_m) temperatures that ended at 154 °C as represented in Figure 4.13. From the selected thermogram in Figure 4.13, addition of BMIMCl as well as reinforcement of CFF and MCC shifted all

T_g , T_c and T_m to lower temperature. Apart from that, the broad T_c and T_m peaks of PLA intensified and sharpened gradually as compared to its composites.

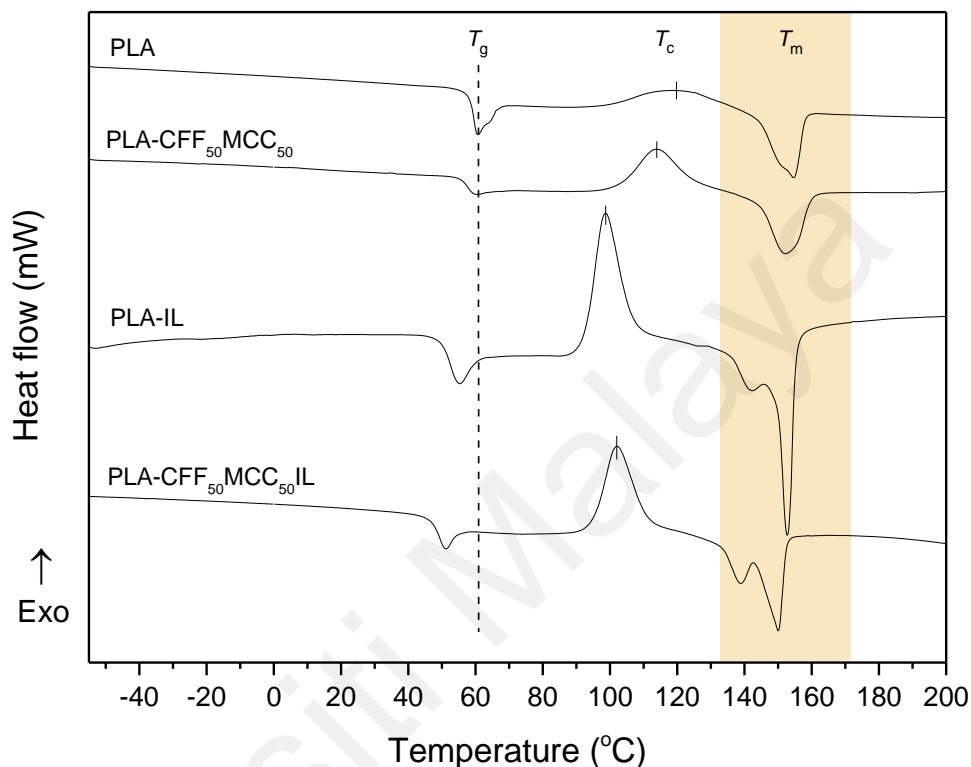


Figure 4.13: DSC thermal behavior of PLA and the composites

In contrast, the T_g shifted to higher temperature when 1 wt% of individual CFF and MCC was added to the PLA blend as PLA-CFF₁₀₀ and PLA-MCC₁₀₀ (Figure 4.14). As the ratio of CFF to MCC increased, the glass transition temperature decreased. This is because greater composition of MCC/CFF in the PLA composites promoted the film stiffness. The T_g of the composites was further reduced with the incorporation of BMIMCl. Wu et al. (2015) justified that the occurrence was caused by strong intermolecular hydrogen bond interaction between MCC and CFF with BMIMCl that impaired their crystalline regions. Thus, enhancing the polymer chain flexibility where Gajria et al. (1996) suggested it as plasticizing effect of ionic liquid.

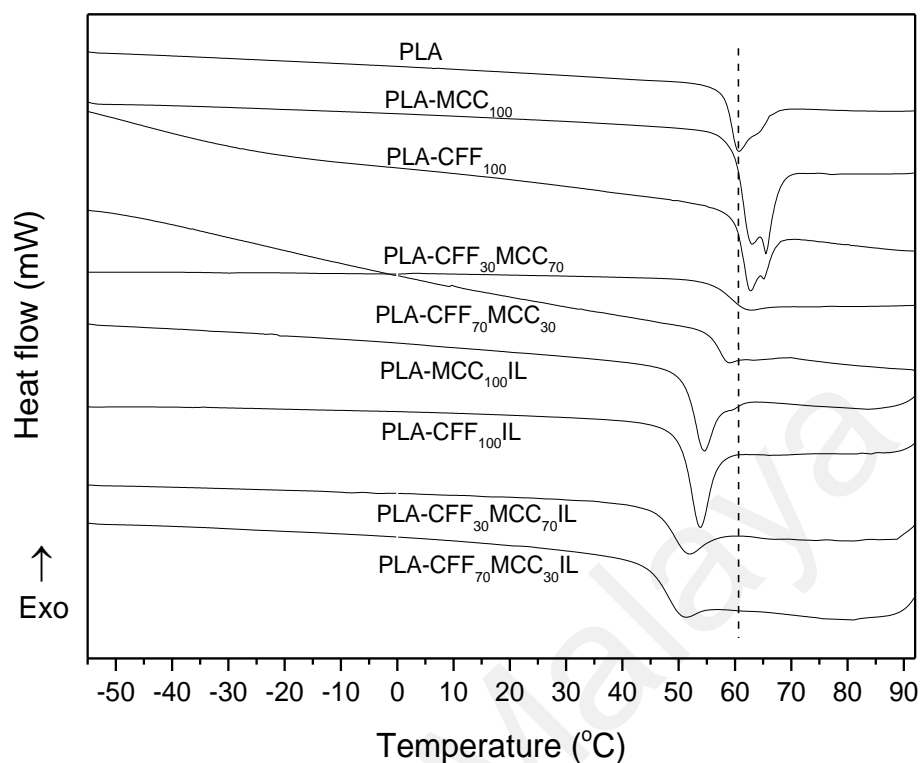


Figure 4.14: Glass transition temperature thermogram of PLA and the composites in DSC

The addition of BMIMCl also impacted the miscibility of PLA-MCC₁₀₀ and PLA-CFF₁₀₀ films. According to Yeh et al. (2008), single T_g affirmed the compatibility of the polymer blends such as neat PLA and the rest of the composites except PLA-MCC₁₀₀ and PLA-CFF₁₀₀. Similar results of 2 maximum torque were also observed in the plastogram in Figure 4.3. Subsequent dissolution of fillers in BMIMCl enhanced the miscibility between hydrophilic and hydrophobic fillers with PLA in the composites with single T_g in PLA-MCC₁₀₀IL and PLA-CFF₁₀₀IL. As these observations were only seen in the use of CFF and MCC individually in PLA blends, separate use of these fillers would cause phase separation (Jouannin et al., 2014).

In conjunction to the compatibility of BMIMCl with poly(lactic acid), the sample DSC measurement was done from freezing -60 °C onwards to clarify the presence of

BMIMCl glass transition temperature (-50 °C, 220-225 K) (Yamamuro et al., 2006; Sippel et al., 2016). The absence of the peak indicated that BMIMCl is an efficient plasticizer for PLA (Park, 2008). Although CFF and MCC reinforcement reduced the crystallization temperature of PLA composites as compared to neat PLA, BMIMCl further decreased the T_c more significantly as shown in the represented 70/30 composition sample in Figure 4.15. As a result, decrease in T_c raised the degree of crystallinity of PLA composites in agreement to Hassan et al. (2013) who mentioned that crystallinity of blends increased due to the slow movement of PLA chain when T_g decreased.

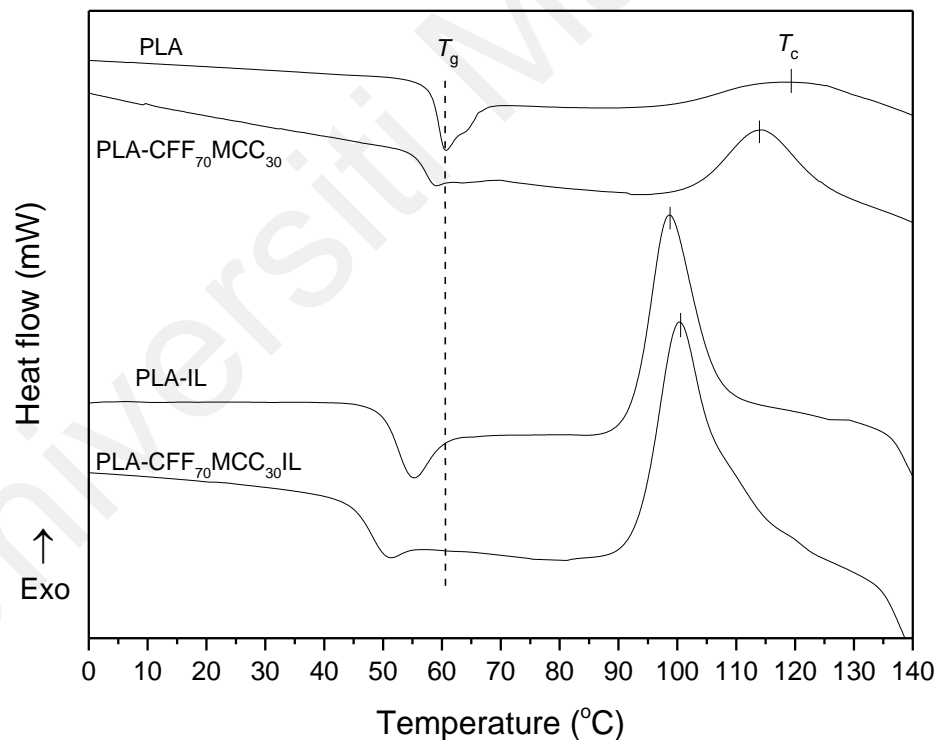


Figure 4.15: DSC curves of T_g and T_c for PLA and its composites

The area under the exothermic T_c peak is the cold crystallization or crystallinity, χ_c of the samples. Despite neat PLA obtained the highest T_c , its crystallinity was the lowest with only 17 %. In fact, neat PLA fabricated *via* mixer and compression molding by

Tanase and Spiridon (2014) also reported with only 20 % crystallinity. These crystallinity and crystallization temperature of composites were opposed to the highest thermal stability of neat PLA in TGA.

Reduction of T_c in the composites were correlated to the increment of χ_c as illustrated in the scatterplot in Figure 4.16 except for PLA-IL and PLA-CFF₁₀₀. The crystallinity of these 2 samples were low regardless of their crystallization temperature. BMIMCl decreased the T_c of the PLA composites by at least 10 °C as compared to the composites with the same compositions without ionic liquid. Concisely, CFF and MCC reinforcements promoted the degree of crystallinity of the polymer blends. Inclusion of BMIMCl contributed much higher χ_c to the composites especially the 70/30 composition with the lowest T_c . The highest crystallinity recorded in PLA-CFF₇₀MCC₃₀IL corresponded to the intensity of absorption bands comparison from FTIR spectra (Figure 4.9).

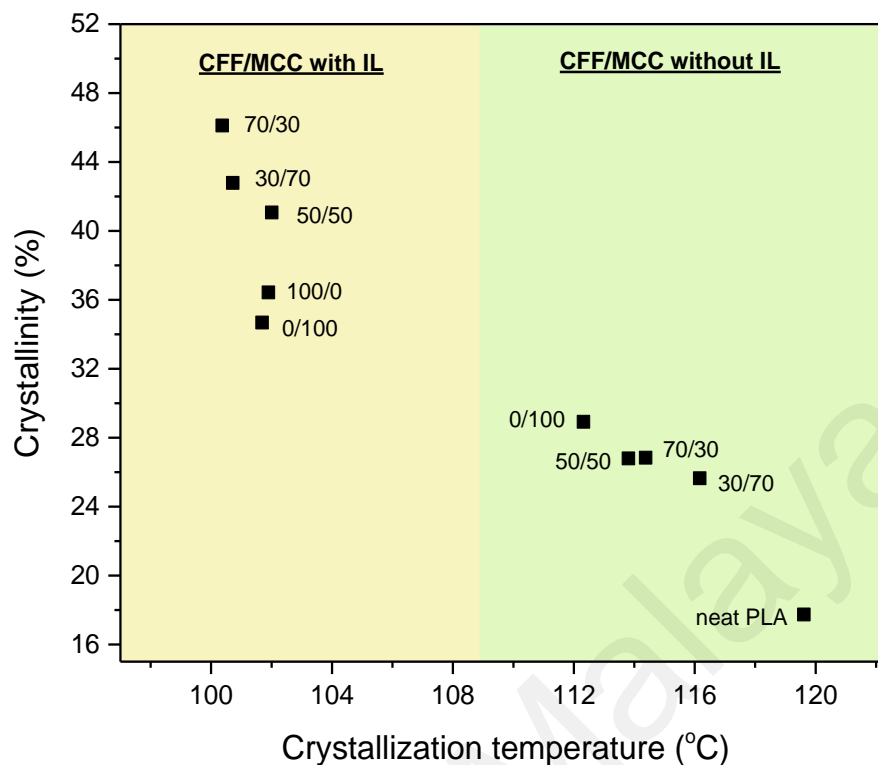


Figure 4.16: Correlation plot of T_c versus χ_c of PLA blends

Poly(lactic acid) begins melting at the temperature of about 140 °C and Tang et al. (2012) stated that the polymer exhibits slow melt-crystallization behavior. Based on the T_m in Figure 4.17, PLA-CFF₁₀₀ and PLA-MCC₁₀₀ exhibited weak and broad double melting curve at 149°C and 153°C. According to Tang et al. (2012) as mentioned in the work of Nanthananon et al. (2015), the double T_m was due to the melt-recrystallization mechanism of poly(lactic acid) where different crystals are formed during cold crystallization stage and recrystallization stage. The mechanism models explain that the small and imperfect crystals are undergoing successive change into more stable crystal. As melting and recrystallization are competing during the heating process, recrystallization is suppressed by higher heating rates, forming 2 different intensities of melting temperature peaks.

Inclusion of BMIMCl in the composites induced the double T_m peaks to be more intense and distinctive. Duan et al. (2013) defined the weaker lower temperature melting peak of PLA composites is the disordered crystalline form whereas the higher intense T_m corresponds to its ordered crystalline form. Precisely, the less thermally stable β crystal referred to the peaks of 139-141 °C and 149-153 °C were of more stable α crystal (Tabi et al., 2010; Suwannakas et al., 2016). The penetration of ionic liquid could have intensified the degree of disorder upon heating and blending (Gajria et al., 1996; Li et al., 2014). Apart from that possibility, quick cooling may had also resulted in two crystal phases. As supported from (Tabi et al., 2010), PLA composites transformed from double to single melting peaks after prolonged annealing.

Further decline of melting temperature in the BMIMCl added composites affirmed the decrease in their TGA thermal decomposition temperatures. Melting point of BMIMCl obtained from DSC in the work of Dharaskar et al. (2013a) recorded relatively low melting point of the ionic liquid, 65 °C could also contribute to the reduction in the T_m of composites. Conversion of broad single T_m in PLA-CFF₅₀MCC₅₀ to intense sharp double T_m in PLA-CFF₅₀MCC₅₀IL showed that IL that was only accounted for 5 wt% in the PLA composites was able to alter the polymer crystal forms. Despite BMIMCl had broadened the range of PLA composites melting temperatures to 139-154 °C, decomposition of the polymer blends occurred well above the T_m at 202-323 °C. The results indicate that the processing temperature were suitable and did not degrade the polymers.

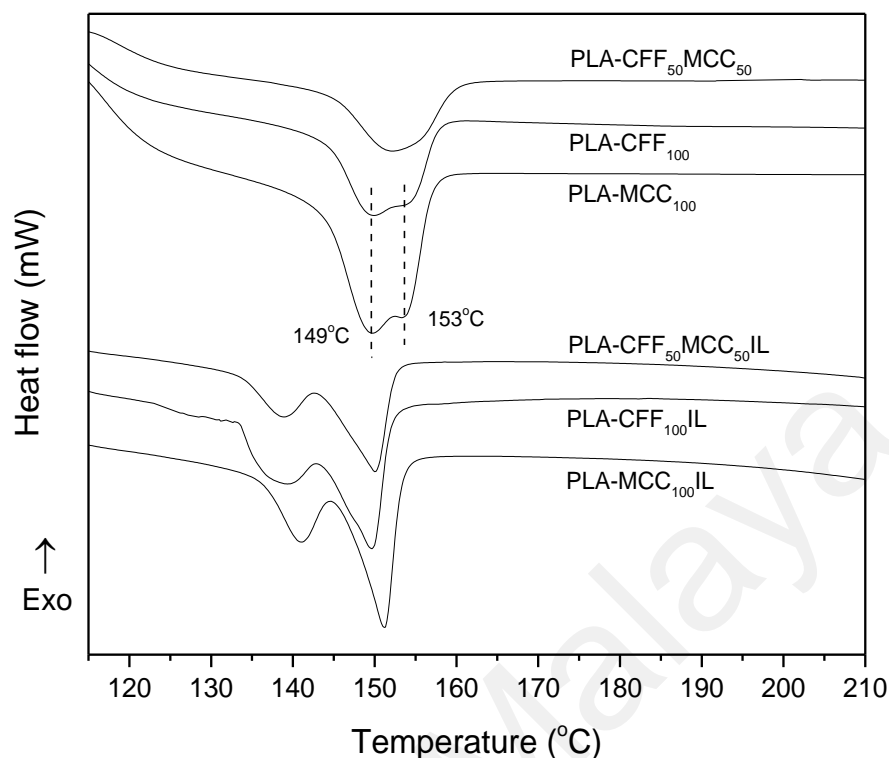


Figure 4.17: Melting temperature of PLA composites with and without BMIMCl

The three phases of transition behavior in DSC thermogram of PLA and the composites are interrelated. For instance, the only double T_m in PLA-CFF₁₀₀ and PLA-MCC₁₀₀ corresponded to their double T_g which was caused by the lack of interaction between individual fillers and PLA. Increase in the intensity of T_g in 100/0 and 0/100 compositions (Figure 4.14) lead to the increase of heat capacity (ΔC_p) (El-Hadi, 2002). Hence, degree of crystallinity decreased. This occurrence was observed in the χ_c of PLA-CFF₁₀₀IL and PLA-MCC₁₀₀IL which were significantly lower than other PLA composites with BMIMCl as calculated in Table 4.2.

Table 4.2: DSC data of neat PLA and its composite films

Sample	Glass transition temperature (°C)		Melting temperature (°C)		Cold crystallization		
	T_{g1}	T_{g2}	T_{m1}	T_{m2}	T_c (°C)	ΔH_f (Jg ⁻¹)	χ_c (%)
PLA	60.58		154.48		119.61	16.49	17.73
PLA-CFF ₁₀₀	62.53 ^a	65.20	149.54 ^a	153.00	110.26	21.20	23.03
PLA-CFF ₇₀ MCC ₃₀	58.70		151.17		114.38	24.70	26.83
PLA-CFF ₅₀ MCC ₅₀	59.77		151.99		113.81	24.67	26.79
PLA-CFF ₃₀ MCC ₇₀	61.94		150.60		116.17	23.61	25.64
PLA-MCC ₁₀₀	63.00	65.34 ^a	149.50 ^a	153.30	112.32	26.63	28.92
PLA-IL	55.09		139.20	149.34 ^a	98.77	22.32	25.26
PLA-CFF ₁₀₀ IL	53.72		139.00	149.39 ^a	101.90	31.94	36.43
PLA-CFF ₇₀ MCC ₃₀ IL	50.38		143.17	153.58 ^a	100.37	40.31	46.11
PLA-CFF ₅₀ MCC ₅₀ IL	51.08		139.00	149.76 ^a	102.01	35.90	41.07
PLA-CFF ₃₀ MCC ₇₀ IL	51.41		140.17	151.19 ^a	100.72	37.40	42.78
PLA-MCC ₁₀₀ IL	54.39		141.00	150.84 ^a	101.69	30.41	34.68

^a Tmin value.

4.5 XRD Phase Identification

Other than DSC, XRD was also performed to obtain the crystallinity index (CI) of neat PLA and the composites. Based on the XRD pattern in Figure 4.18, neat PLA was unusually found to have amorphous scattering at $2\theta = 15^\circ$. The results were in opposition to the cold crystallization, χ_c in DSC. The differences in crystallinity were predictable as surface analysis of X-ray diffraction was not comparable with the process

of heat change in DSC. Besides, commercial solvent casted neat PLA from the work of Yee et al. (2016) was semi crystalline with a sharp diffraction peak at $2\theta = 16^\circ$. Similarly, Lu et al. (2016) also claimed that the two PLA diffraction peak (31, 14) were referred to $2\theta = 16.4^\circ$ and 22.6° respectively.

A few evidences reported otherwise in which crystalline phase of commercial neat PLA transformed into amorphous after thermal treatment (Calleja & Fakirov, 2000; Kaczmarek et al., 2013). Lu et al. (2016) further explained that the high temperature of processing method may have led to the different degrees of molecule deformation. Not to mention that cellulose fibers that underwent electrospinning process were almost entirely amorphous (Isik et al, 2014). This is because PLA chains did not have sufficient time to reorganize into crystalline lamella due to the rapid cooling of the fibers during spinning or compression molding (Collins et al. 1973; Demirel et al., 2011; Halász & Csóka, 2013, Sullivan et al., 2015).

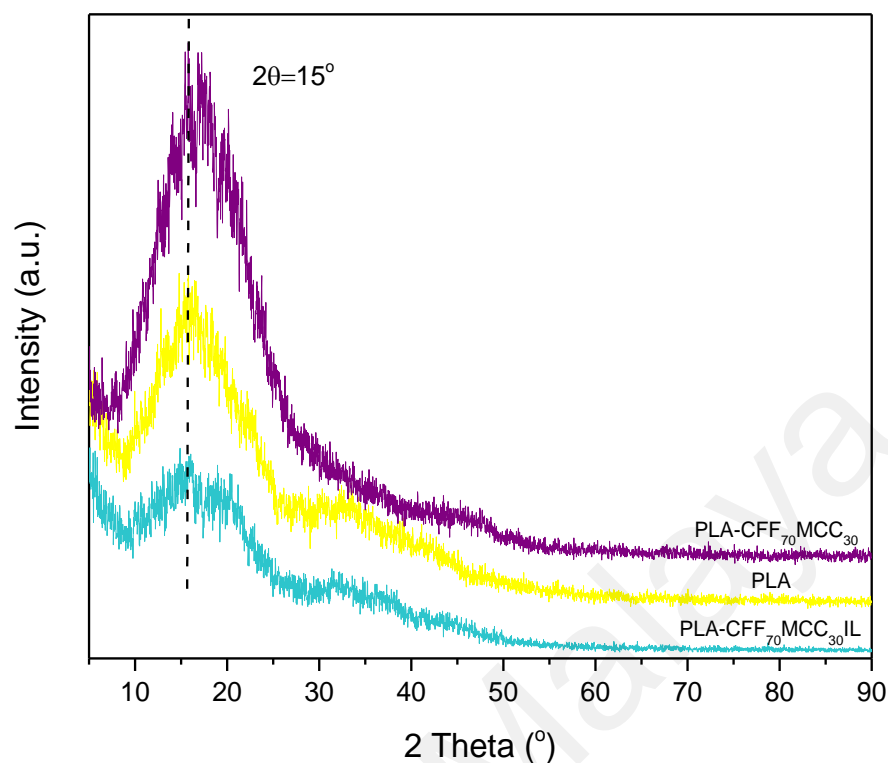


Figure 4.18: X-ray diffraction pattern of PLA and the composites

The XRD crystallinity index revealed contradicting trend from DSC thermogram. Although PLA-CFF₇₀MCC₃₀IL (Figure 4.18) was the optimum composition in obtaining highest χ_c (46 %), PLA-CFF₇₀MCC₃₀ was in turn to achieve the highest CI of 41 %. Yet, CI value of PLA-CFF₇₀MCC₃₀IL was the least (17 %). As a comparison of similar compositions with the presence factor of BMIMCl, the CI of most compositions were reduced by the ionic liquid except poly(lactic acid) and MCC reinforced PLA. Figure 4.19 shows that neat PLA underwent an increment from 26 % to 30 % in PLA-IL. Likewise, 21 % of PLA-MCC₁₀₀ had a slight rise to 23 % in PLA-MCC₁₀₀IL.

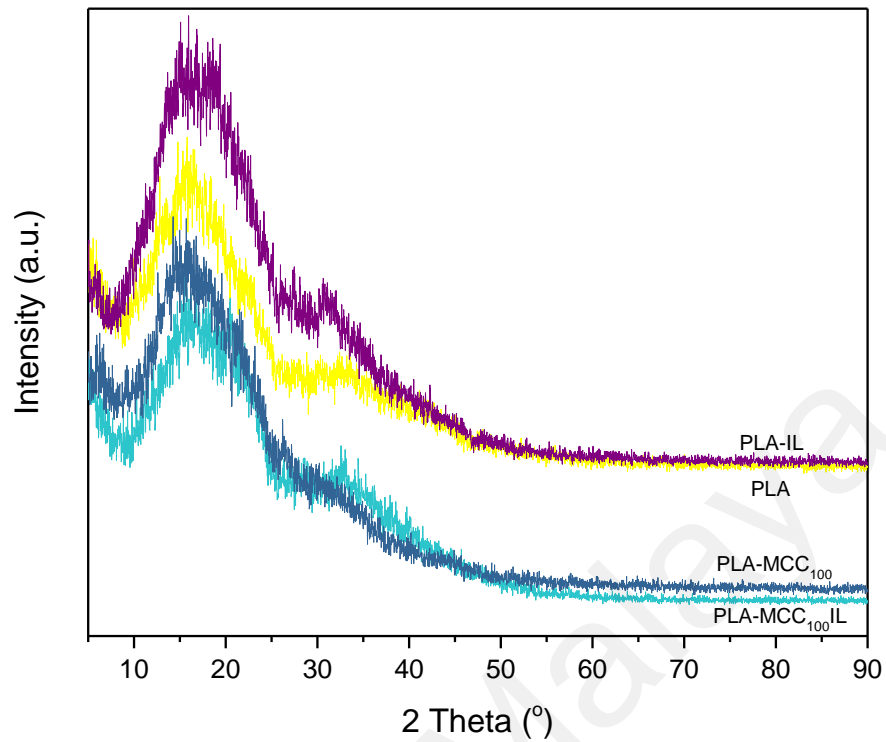


Figure 4.19: Comparison XRD pattern of PLA and MCC reinforced PLA composites

As the CI of composites decreased, the broad peaks at around 32° increased in intensity. Similar neat PLA that was melt blended and hot pressed by Spiridon et al. (2013) confirmed its amorphous structure. Although Liu et al. (2010) claimed that $2\theta = 18.6^\circ$ represented the amorphous part of cellulose, the PLA diffraction peak was too broad to distinguish the cellulose peak due to overlapping. Despite low crystallinity index of PLA composites as compared to the past literature, the CI as calculated and listed in Table 4.3 increased when keratin and cellulose were reinforced.

Table 4.3: XRD crystallinity index (CI) of PLA and composite films

Sample	CI (%)
PLA	26.82
PLA-CFF ₁₀₀	29.14
PLA-CFF ₇₀ MCC ₃₀	41.04
PLA-CFF ₃₀ MCC ₇₀	36.91
PLA-MCC ₁₀₀	21.94
PLA-IL	30.62
PLA-CFF ₁₀₀ IL	28.95
PLA-CFF ₇₀ MCC ₃₀ IL	17.46
PLA-CFF ₃₀ MCC ₇₀ IL	21.07
PLA-MCC ₁₀₀ IL	23.17

Correlation analysis between CI and DTG values in Figure 4.14 illustrates the thermal stability (DTG value) of the composites without IL somewhat declined with increasing crystallinity excluding neat PLA. Regardless of the CFF/MCC composition relationship to the CI and thermal stability, the results were corresponded to the speculation of increasing χ_c in DSC. However, inclusion of BMIMCl fluctuated the thermal stability of the composites as the CI increased. Concisely, the effect of ionic liquid to the reduction of CI was not as significant as the thermal properties from TGA and DSC measurements.

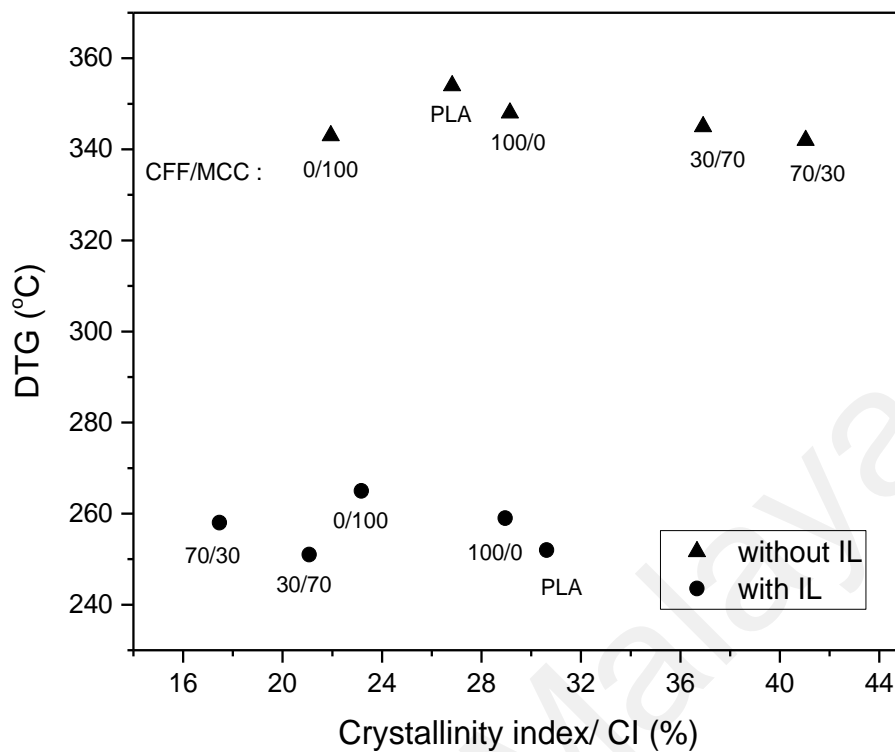


Figure 4.20: Interaction scatterplot between CI and DTG of PLA and its composites

4.6 Scanning Electron Microscopy

Cross section visual analysis of the neat PLA and the composites with and without the addition of BMIMCl portrayed distinct morphological changes. The cross section image of neat PLA (Figure 4.21a) consisted clusters of non-uniform lumps with a smooth surface. When BMIMCl was incorporated, the irregular shapes disappeared, remaining uniform porous structure in PLA-IL (Figure 4.21b) of 3.17 μm mean size. The porous structure in poly(lactic acid) was similar to the work of Martins et al. (2014) due to the plasticizing effect of ionic liquid. This may be the explanation to the decrease in glass transition temperature as chain flexibility was enhanced.

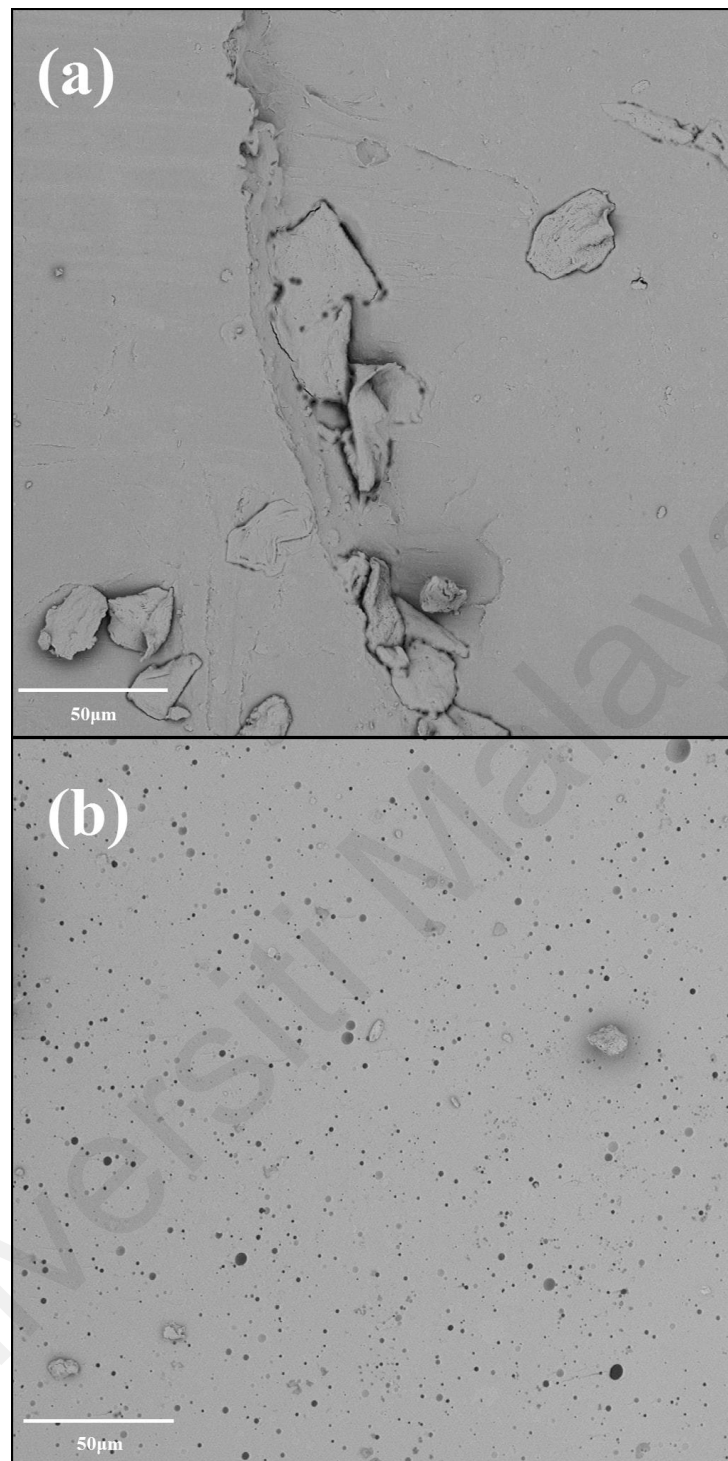


Figure 4.21: SEM cross section images of PLA (a) and PLA-IL (b)

As the pores became more abundant in the composite matrices, melting temperature and thermal stability declined. DTG of PLA-CFF₅₀MCC₅₀IL (255 °C) was lower than that PLA-CFF₁₀₀IL and PLA-MCC₁₀₀IL with the thermal decomposition temperature of 259 °C and 265 °C respectively. The comparison justified the porous structure in PLA-CFF₅₀MCC₅₀IL as shown in Figure 4.22b appeared to be more compact and visible. The porosity was likely due to the greater interaction of the 50/50 composition fillers with ionic liquid. Meanwhile, the pores seen in PLA-CFF₁₀₀IL were more apparent and larger in size than that PLA-MCC₁₀₀IL as exhibited in Figures 4.23 & 4.24. Kock (2006) and Tran et al. (2016) claimed that it was due to the porous keratin that contributed to the increased porosity.

Although the fillers absorption bands were barely detected in FTIR spectra, MCC particles were visible in PLA-MCC₁₀₀ (Figure 4.24a) with the average particle size of 4.48 μm . Irregular shape of CFF was also observed in PLA-CFF₅₀MCC₅₀ with a diameter of 21.7 μm , 4.8 times larger than MCC. Successive dissolution of CFF and MCC in BMIMCl produced almost similar of fracture surfaces among PLA composites which were smooth, clear and consistently compacted with pores. The filler particles were no longer visible in which Mathew et al. (2005) mentioned that the great difficulty to identify the fillers from the PLA matrix was due to good adhesion between matrix and filler that resulted the fillers to be coated with the PLA polymer.

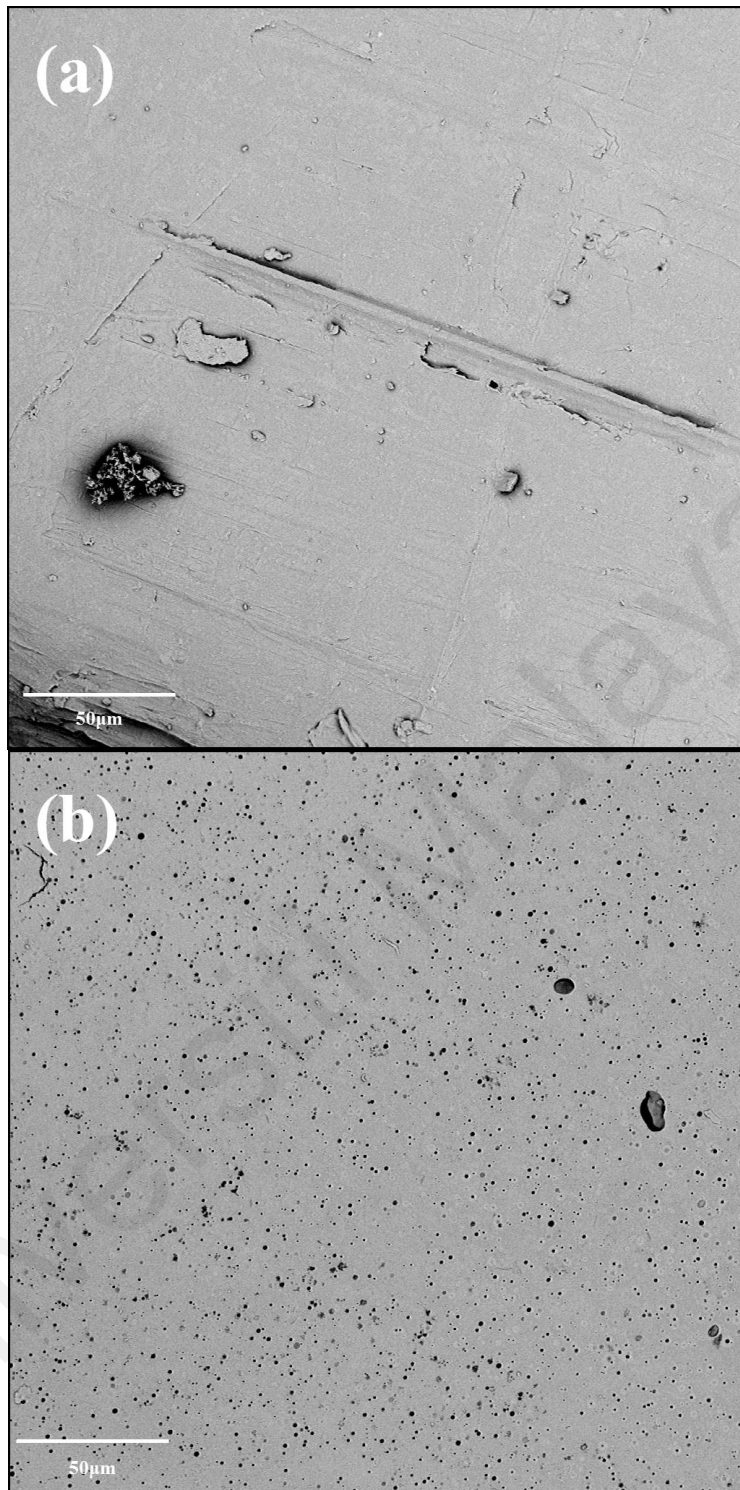


Figure 4.22: SEM cross section images of PLA-CFF₅₀MCC₅₀ (a) and PLA-CFF₅₀MCC₅₀IL (b)

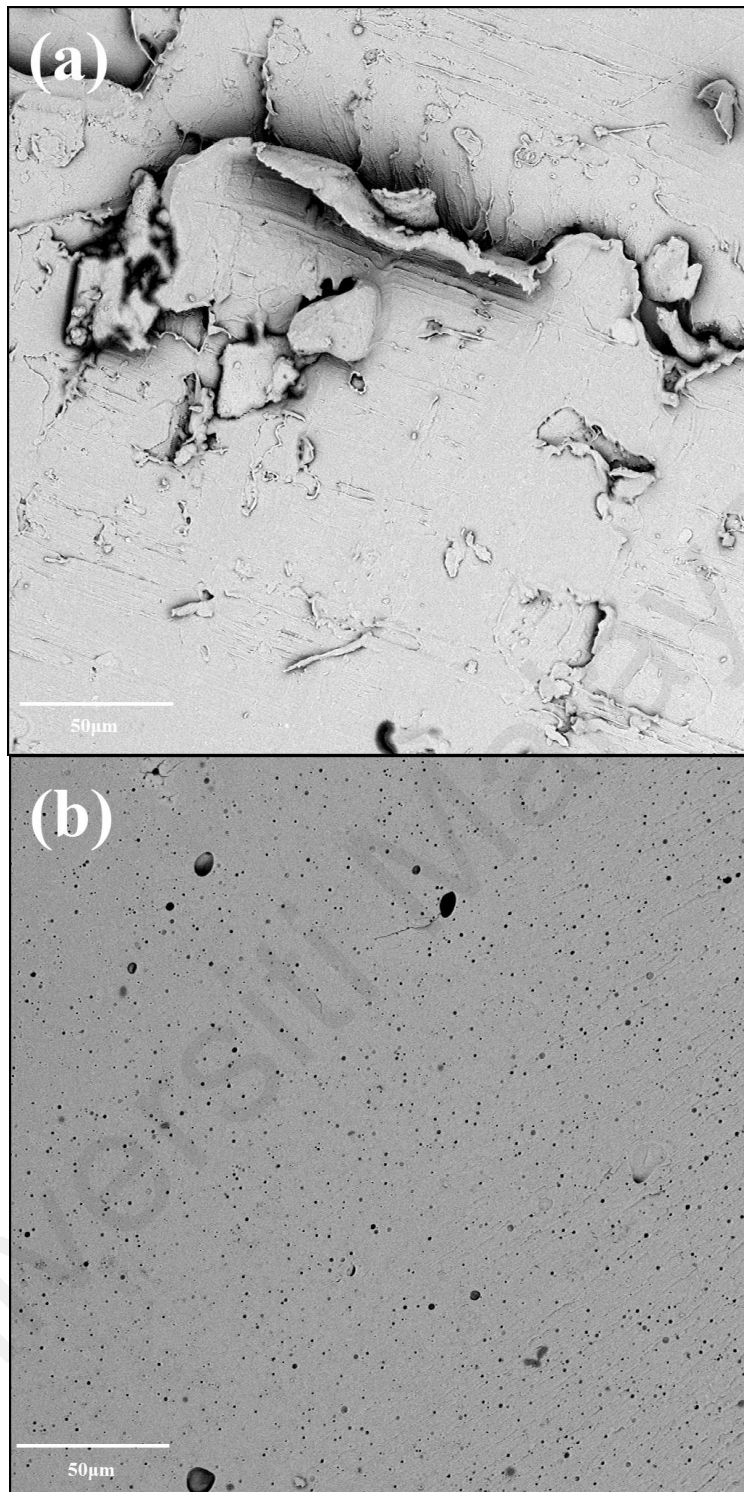


Figure 4.23: SEM cross section images of PLA-CFF₁₀₀ (a) and PLA-CFF₁₀₀IL (b)

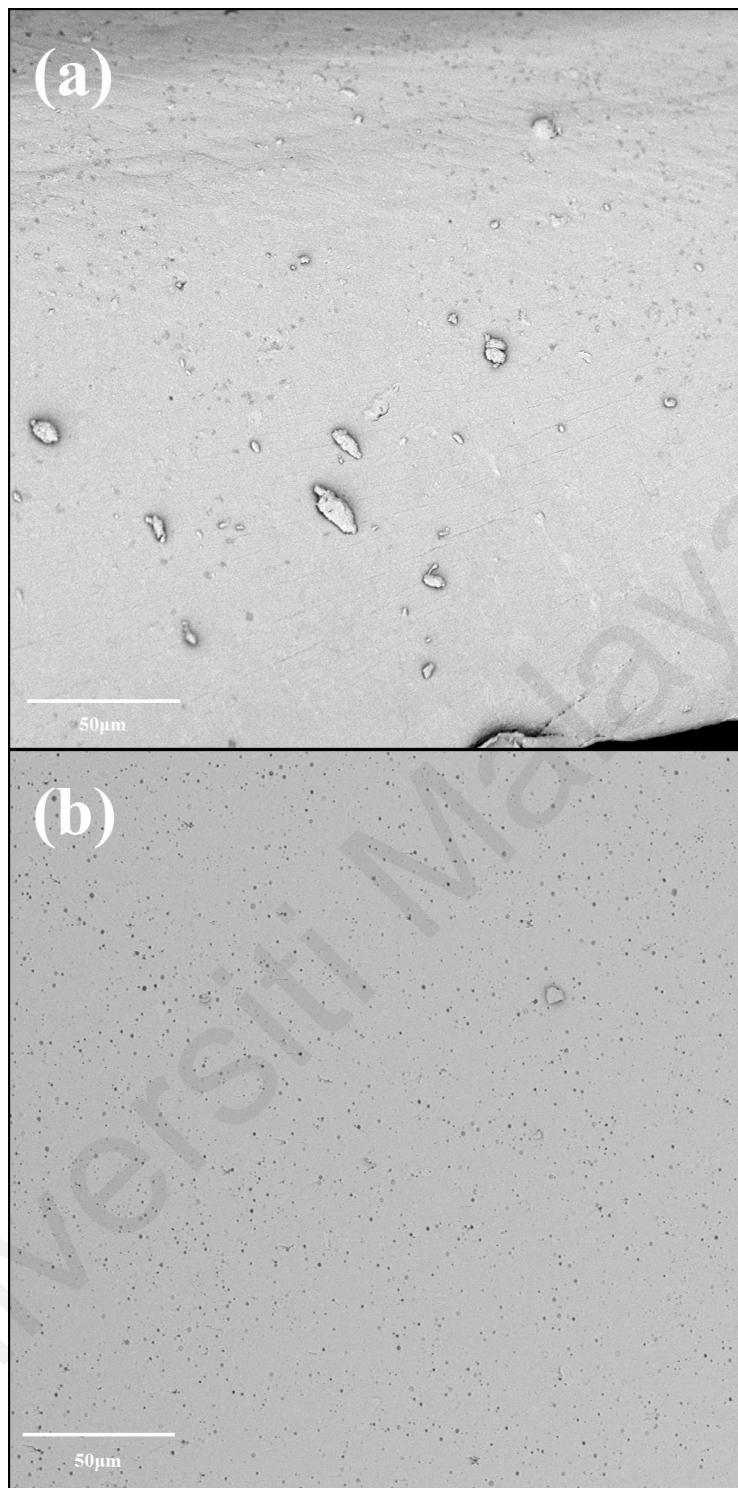


Figure 4.24: SEM cross section images of PLA-MCC₁₀₀ (a) and PLA-MCC₁₀₀IL (b)

Despite BMIMCl enhanced the fillers dispersion due to large particle sizes as seen in PLA-CFF₅₀MCC₅₀, several voids were observed in PLA-CFF₅₀MCC₅₀IL fractured cross section films. Similar observation was found in PLA-CFF₁₀₀IL, but not in PLA-MCC₁₀₀IL. Compression molding could be the reason for voids formation during the

high load compression. For instance, injection molding resulted in voids as fibers were trapped by the PLA matrix (Lam et al., 2009). Similarly, there were voids in the PLA polymer matrix around the fibers produced *via* twin-screw extruder by Huda et al. (2013). On the other hand, Aranberri et al. (2017) claimed that the presence of more voids in CFF reinforced composites was due to the hollow structure of the CFF which were preserved after the compression molding. Cheung and Lau (2007) added that moisture absorption and air permeation during fabrication process may have induced microvoids.

Although voids were barely observed in PLA composites without BMIMCl due to the surface roughness, SEM cross section images at lower resolution in Figure 4.25 described the effect of fillers to the PLA matrices. Apart from CFF particles seen in Figure 4.22a, more CFF particles were also available at lower resolution in Figure 4.25a of PLA-CFF₅₀MCC₅₀. In comparison between PLA-CFF₁₀₀ and PLA-MCC₁₀₀ at 200 μm , MCC was more dispersible than that CFF which may be due to the larger particle size of CFF. Besides, MCC reinforcement also caused the surface of PLA composite to appear rough. Several work reported agglomeration of nano-sized cellulose but the SEM images proved otherwise.

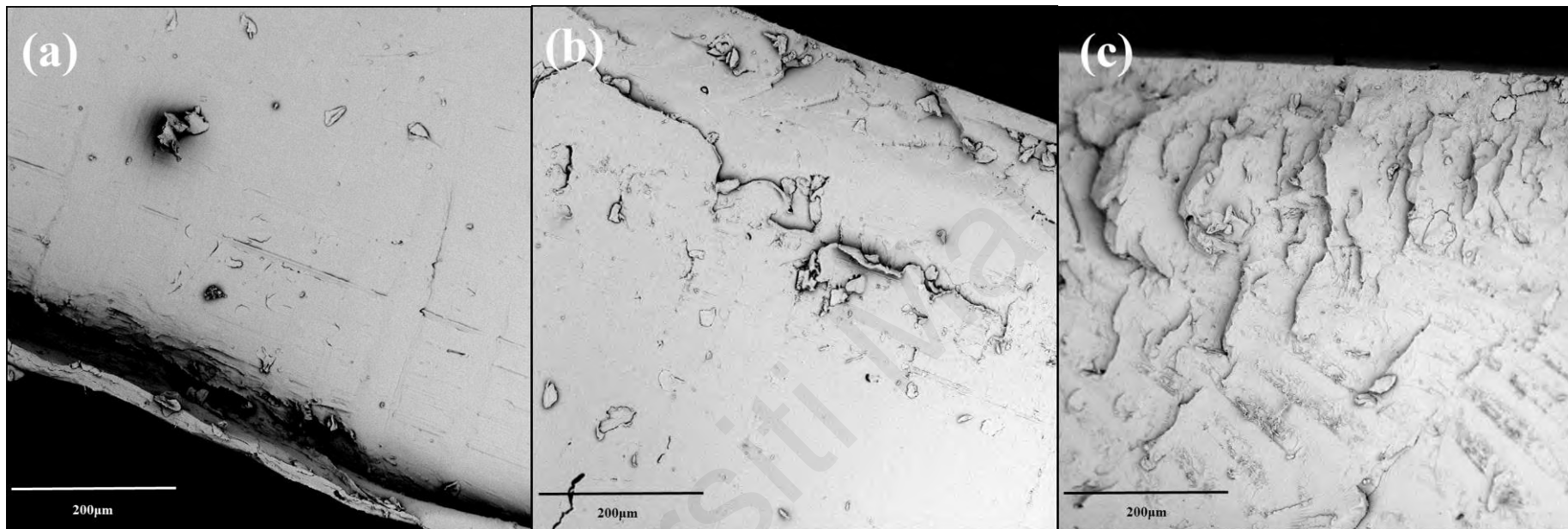


Figure 4.25: SEM cross section images of PLA-CFF₅₀MCC₅₀ (a), PLA-CFF₁₀₀ (b), and PLA-MCC₁₀₀ (c) with lower resolutions

Incorporation of BMIMCl did not only showed no phase separation in the 1 mm film thickness cross section images, but it was also an excellent solvent to dissolve CFF and MCC. Double T_g in the thermogram of PLA-MCC₁₀₀ corresponded to the MCC particles observed in the SEM image. Disintegration of MCC by the ionic liquid in PLA-MCC₁₀₀IL resulted single T_g where the particles also disappeared in the cross section image. Unlike the rough surface of dissolved polymer in ionic liquid from Elhi et al. (2016), results from SEM analysis deduced that BMIMCl was compatible with the polymers besides able to create a well dispersed homogenous film surface.

The gold coated cross section of the PLA composite films were only able to be observed *via* lower voltage magnification at 5 kV. High activation voltage of 10 kV or above resulted in excessive charging due to its non-conductivity of biopolymers. Since the composite films encountered swelling after some time and moisture content was detected in FTIR spectra, the films were considered relatively less stable for SEM analysis.

4.7 Vickers Hardness Test

Hardness mechanical test was conducted on the neat PLA and composite films using Vickers pyramidal diamond indenter. Torres (2010) defined this mechanical property as the ability for a material to resist plastic deformation with the advantages of the hardness calculations that are independent of the size of the indentation tip. The measurement was calculated by the total cross-section area of scratch groove made by the indenter where it was evaluated by the deeper the groove, the softer the material (Orozco et al., 2009). Deeper grooves obtained in BMIMCl added sample films resulted in lower Vickers hardness (HV) by at least 5 MPa as compared to PLA composites without IL as depicted in Figure 4.26. The deterioration in the mechanical properties

was as similar to the thermal stability, crystallinity index, torque viscosity, crystallization and glass transition temperatures.

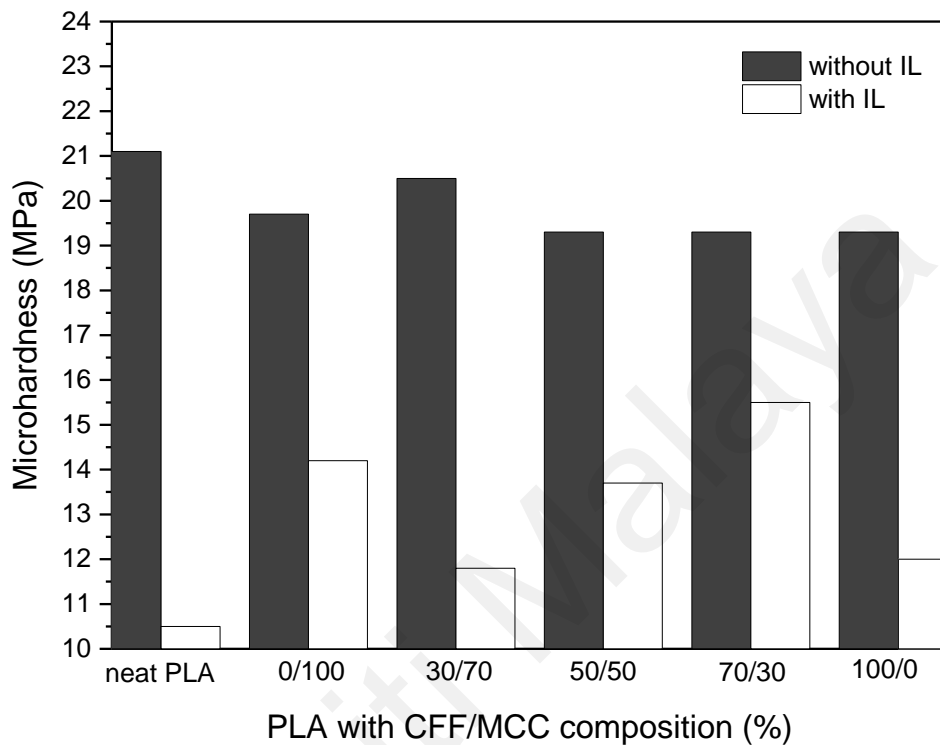


Figure 4.26: Vickers hardness test values of PLA blends with and without BMIMCl

Meanwhile, Medeiros et al. (2007) outlined that Vickers hardness number (VHN) is correlated with diametral tensile strength (DTS) as both are affected by surface wear resistance properties and the ability to maintain stability form. In fact, literature on HV testing on PLA composites was hardly found as compared to the widely adapted tensile testing. Although biomaterials and hard thin films of less than 100 nm thick such as PLA composite films are suitable for the shallow tetragonal pyramid Vickers indentation (Torres, 2010), sample films with BMIMCl were more likely to crack upon indentation due to the brittleness especially those with the HV= 10-12 MPa.

The low HV may be due to the porous structure of the composite films created by BMIMCl as seen in SEM cross section images. Higher HV in PLA-MCC₁₀₀ than PLA-CFF₁₀₀ was also due to the smaller MCC particle size than that CFF observed in SEM images, in agreement with García-Contreras et al. (2015) where reducing size of fillers increases the microhardness. Similar HV trend was not only seen in composites without IL including PLA-CFF₃₀MCC₇₀ where MCC composition was more than CFF, but also in PLA-MCC₁₀₀IL and PLA-CFF₁₀₀IL comparison. As HV and tensile strength were interconnected, reduction in tensile strength reported by Aranberri et al. (2017) was due to increasing CFF composition in PLA composites, indicating that the strength of CFF was insufficient.

In the presence of BMIMCl, PLA composites hardness raised steadily with increasing CFF composition from 30 to 70. It was presumed to be the greater dissolution efficiency of CFF in BMIMCl than MCC that created an interaction between the keratin matrices and the ionic liquid. The IL also reduced the VHN of neat PLA in PLA-IL by half and Djellali et al. (2013) claimed that decrease in Vickers hardness indicates better compatibility. No doubt that incorporation of BMIMCl transformed the double T_g in CFF and MCC reinforced composites to single T_g . The glass transition temperature depends on the cohesive energy and packing density of the polymer (El-Hadi, 2002). Single T_g , XRD pattern and SEM images suggest the presence of a single homogeneous amorphous phase.

The T_g of poly(lactic acid) is commonly known to be about 50 °C where the molecular chain in the amorphous phase of polymer begins to move over this temperature (Watanabe et al., 2004). As the BMIMCl added composite chain mobility increased with decreasing T_g , Vickers hardness values reduced. However, Calleja and Fakirov (2000) mentioned that shortening in polymer chain length could also be the

reason of declining T_g caused by the effect of BMIMCl. Apart from glass transition temperature, HV is also proportional to the crystallinity of composites (Djellali et al., 2013). This is because degrees of crystallinity and orientation affect the mechanical properties of the polymer which in turn, dependent on processing temperature and composite shear deformation respectively (Watanabe et al., 2004).

Presence of microvoids predominantly affect the mechanical surface hardness properties of composites. This is because void formation reduces polymers adhesion and causes debonding (Silverajah et al., 2012). The low microhardness, 12 MPa of PLA-CFF₁₀₀IL corresponded to its abundant empty voids observed in SEM images as compared to PLA-MCC₁₀₀IL which remained 14.2 MPa. The Vickers hardness results showed that incorporation of both fillers with larger CFF composition would enhance the composite films surface hardness.

As stated by Calleja and Fakirov (2000), high temperature compression molding depreciates the composites HV value. In the extrusion process of Baba and Özmen (2015), implementation of higher temperature (205 °C) reported only 20 MPa of VHN in PLA. On the other hand, 180 °C of melt blending and compression molding in neat PLA from Figure 4.26 resulted 21.1 MPa. Likewise, PLA film fabricated by Odahara et al. (2009) obtained only HV=15-17 MPa for the temperature and pressure of 190 °C and 30-50 MPa respectively. Concisely, CFF and MCC reinforced PLA composites in BMIMCl are most likely to be heat sensitive to cause the reduction in Vickers hardness and other mentioned characterizations.

CHAPTER 5: CONCLUSIONS

5.1 Conclusions

Fabrication of PLA composite films with CFF and MCC in BMIMCl were successful *via* high temperature measuring mixer and compression molding. Intense CH₃ rocking and C=O group of lactic acid were observed in FTIR spectra regardless of the incorporation of IL. However, addition of BMIMCl decreased the thermal stability with single stage of degradation by 100 °C as compared to PLA composites without IL. The escalation of thermal degradation corresponded to its decrease in their melting temperature. In comparison with fillers compositions, the glass transition temperature dropped as CFF/MCC ratio increased, excluding only PLA-CFF₁₀₀ and PLA-MCC₁₀₀ which shifted to higher temperature. The T_g further reduced with BMIMCl inclusion in the composites as similar to the decrease in Vickers hardness. Apart from the increase in polymer chain mobility, reduction in thermal stability and T_g were related to the shortening of chain length on solution processing with heat. Morphological study *via* SEM revealed the transformation from rough with visible filler particles in composites cross section images to smooth and porous structure upon the addition of BMIMCl in the polymer blends without phase separation. This was due to good adhesion between PLA matrix and fillers that resulted the fillers to be coated with the PLA polymer. As the pores became more abundant in the composite matrices, T_g , T_m and thermal stability decreased as seen in CFF₅₀MCC₅₀IL. Conversion of two maximum torques to single value in PLA-CFF₁₀₀IL and PLA-MCC₁₀₀IL corresponded to their double T_g to single T_g in DSC due to the compatibility enhancement by BMIMCl. Doubtlessly, the decrease in HV was also an indication of better miscibility. Although fillers with less than 10 % were hardly detectable from the ATR surface characterization, increasing CFF composition raised the films hardness and thermal stability in the presence of BMIMCl.

In contrast, absence of BMIMCl in the composites had opposite effect. This was presumed to be the greater dissolution efficiency of CFF in BMIMCl than MCC that created an interaction between the keratin matrices and the ionic liquid. An interesting contradiction in crystallinity was found where the highest χ_c value (46 %) of PLA-CFF₇₀MCC₃₀IL was the lowest in XRD, CI=17 %. PLA-CFF₇₀MCC₃₀ was recorded with the highest CI of 41 %. Increase in χ_c of PLA-CFF₇₀MCC₃₀IL was also a result from the reduction in T_c . To conclude the comparison between the fillers composition with the presence of BMIMCl, PLA-CFF₇₀MCC₃₀IL was the best ratio in obtaining moderate thermal stability, fairly low HV and single T_g , comparatively higher χ_c and porous structure with optimum compatibility and polymer chain flexibility.

5.2 Recommendations

The current fundamental studies of incorporating dissolved polymer in poly(lactic acid) matrix is rarely reported in the past literature especially with the use of ionic liquid, BMIMCl as the green solvent. Since the aim of this investigation is towards the scope of biodegradability and environmental friendliness, future medical and biological application studies are possible such as medical drug delivery in tissue engineering especially when BMIMCl is able to create porous structure in PLA composites. However, extensive toxicity studies of the composite films formed should be done as interaction between ionic liquid and the polymers may alter the functional group and surface properties of the composites. Besides, other types of ionic liquid or source of keratin waste could also be used to test on the compatibility and comparison in term of enhancement in surface morphology, mechanical and thermal properties. To further confirm the studies on their morphological and thermal properties, integrated instruments could be applied such as TGA-IR, and DSC-XRD to obtain 3-dimensional graphs to clarify its qualitative analysis with respect to temperature.

REFERENCES

- Ali, F., J. Awale, R., Mirghani, M. E. S., Anuar, H., & Samat, N. (2016). Preparation and characterization of plasticized polylactic acid/starch blend. *Jurnal Teknologi (Sciences & Engineering)*, 78(1-2), 7–12.
- Almeida, M. R., Passos, H., Pereira, M. M., Lima, Á. S., Coutinho, J. A. P., & Freire, M. G. (2014). Ionic liquids as additives to enhance the extraction of antioxidants in aqueous two-phase systems. *Separation and Purification Technology*, 128, 1–10. doi: 10.1016/j.seppur.2014.03.004
- Alsaheb, R. A. A., Aladdin, A., Othman, N. Z., Malek, R. A., Ong, M. L., Aziz, R., & Enshasy, H. A. E. (2015). Recent applications of polylactic acid in pharmaceutical and medical industries. *Journal of Chemical and Pharmaceutical Research*, 7(12), 51-63.
- Anastas, P. T., & Warner, J. C. (1998). *Green chemistry: Theory and practice*. New York: Oxford University Press.
- Aranberri, I., Montes, S., Azcune, I., Rekondo, A., & Grande, H.-J. (2017). Fully biodegradable biocomposites with high chicken feather content. *Polymers*, 9(11), 593. doi: 10.3390/polym9110593
- Auras, R., Harte, B., & Selke, S. (2004). An overview of polylactides as packaging materials. *Macromolecular Bioscience*, 4(9), 835-864. doi: 10.1002/mabi.200400043
- Baba, B. O., & Özmen, U. (2015). Preparation and mechanical characterization of chicken feather/PLA composites. *Polymer Composites*, 38(5), 837-845. doi: 10.1002/pc.23644
- Barczewski, M., Matykiewicz, D., Krygier, A., Andrzejewski, J., & Skórczewska, K. (2017). Characterization of poly(lactic acid) biocomposites filled with chestnut shell waste. *Journal of Material Cycles and Waste Management*, 20(2), 914-924. doi: 10.1007/s10163-017-0658-5
- Barone, J. R., & Schmidt, W. F. (2005). United States of America Patent No. US20050148703 A1.
- Barone, J. R., Schmidt, W. F., & Liebner, C. F. E. (2005). Thermal processed keratin films. *Journal of Applied Polymer Science*, 97, 1644–1651.

- Battegazzore, D., Noori, A., & Frache, A. (2018). Natural wastes as particle filler for poly(lactic acid)-based composites. *Journal of Composite Materials*, 002199831879131. doi: 10.1177/0021998318791316
- Běhálek, L., Maršálová, M., Lenfeld, P., Habr, J., Bobek, J., & Seidl, M. (2013). *Study of crystallization of polylactic acid composites and nanocomposites with natural fibres by DSC method*. Paper presented at the NANOCON 2013, Brno, Czech Republic.
- Broers, L., Dongen, S. v., Goederen, V. d., Ton, M., Spaen, J., Boeriu, C., & Schroën, K. (2018). Addition of chitin nanoparticles improves polylactic acid film properties. *Nanotechnology and Advanced Material Science*, 1(2), 1-8.
- Byun, Y., Whiteside, S., Thomas, R., Dharman, M., Hughes, J., & Kim, Y. T. (2012). The effect of solvent mixture on the properties of solvent cast polylactic acid (PLA) film. *Journal of Applied Polymer Science*, 124(5), 3577-3582. doi: 10.1002/app.34071
- Calleja, F. J. B., & Fakirov, S. (2000). *Microhardness of polymers*. Cambridge, United Kingdom: Cambridge University Press.
- Cañavate, J., Aymerich, J., Garrido, N., Colom, X., Macanás, J., Molins, G., . . . Carrillo, F. (2015). Properties and optimal manufacturing conditions of chicken feathers/poly(lactic acid) biocomposites. *Journal of Composite Materials*, 50(12), 1671-1683. doi: 10.1177/0021998315595534
- Carrillo, F., Rahhali, A., Canavate, J., & Colom, X. (2013). Biocomposites using waste whole chicken feathers and thermoplastic matrices. *Journal of Reinforced Plastics and Composites*, 32(19), 1419–1429.
- Chen, X., Zhuo, J., & Jiao, C. (2012). Thermal degradation characteristics of flame retardant polylactide using TG-IR. *Polymer Degradation and Stability*, 97(11), 2143-2147. doi: 10.1016/j.polymdegradstab.2012.08.016
- Cheng, S., Lau, K.-t., Liu, T., Zhao, Y., Lam, P.-M., & Yin, Y. (2009). Mechanical and thermal properties of chicken feather fiber/PLA green composites. *Composites Part B: Engineering*, 40(7), 650-654. doi: 10.1016/j.compositesb.2009.04.011
- Cheung, H.-Y., & Lau, K. T. (2007). *Study on a silkworm silk fiber / biodegradable polymer biocomposite*. Paper presented at the 16th International Conference on Composite Materials, Kyoto, Japan.
- Chiappe, C., Sanzone, A., Mendola, D., Castiglione, F., Famulari, A., Raos, G., & Mele, A. (2013). Pyrazolium- versus imidazolium-based ionic liquids: Structure,

dynamics and physicochemical properties. *The Journal of Physical Chemistry B*, 117(2), 668-676. doi: 10.1021/jp3107793

Chinta, S. K., Landage, S. M., & Krati, Y. (2013). Application of chicken feathers in technical textiles. *International Journal of Innovative Research in Science, Engineering and Technology*, 2(4), 1158-1165.

Collins, E. A., Bareš, J., & Billmeyer, F. W. (1973). *Experiments in Polymer Science*. New York, USA: John Wiley and Sons.

Darie, R. N., Pâslaru, E., Sdrobis, A., Pricope, G. M., Hitruc, G. E., Poiată, A., . . . Vasile, C. (2014). Effect of nanoclay hydrophilicity on the poly(lactic acid)/clay nanocomposites properties. *Industrial & Engineering Chemistry Research*, 53(19), 7877-7890. doi: 10.1021/ie500577m

Day, M., Nawaby, A. V., & Liao, X. (2006). A DSC study of the crystallization behaviour of polylactic acid and its nanocomposites. *Journal of Thermal Analysis and Calorimetry*, 86(3), 623-629.

Demirel, B., Yaraş, A., & ELÇİÇEK, H. (2011). Crystallization behavior of PET materials. *BAÜ Fen Bil. Enst. Dergisi Cilt*, 13(1), 26-35.

Dharaskar, S. A., Varma, M. N., Shende, D. Z., Yoo, C. K., & Wasewar, K. L. (2013a). Synthesis, characterization and application of 1-butyl-3 methylimidazolium chloride as green material for extractive desulfurization of liquid fuel. *Scientific World Journal*. doi: 10.1155/2013/395274

Dharaskar, S. A., Wasewar, K. L., Varma, M. N., Shende, D. Z., & Yoo, C. K. (2013b). Deep removal of sulfur from model liquid fuels using 1-butyl-3-methylimidazolium chloride. *Procedia Engineering*, 51, 416-422. doi: 10.1016/j.proeng.2013.01.058

Dharaskar, S. A., Wasewar, K. L., Varma, M. N., Shende, D. Z., & Yoo, C. K. (2013c). Ionic Liquids: - The novel solvent for removal of dibenzothiophene from liquid fuel. *Procedia Engineering*, 51, 314-317. doi: 10.1016/j.proeng.2013.01.042

Djellali, S., Haddaoui, N., Sadoun, T., Bergeret, A., & Grohens, Y. (2013). Structural, morphological and mechanical characteristics of polyethylene, poly(lactic acid) and poly(ethylene-co-glycidyl methacrylate) blends. *Iranian Polymer Journal*, 22(4), 245-257. doi: 10.1007/s13726-013-0126-6

Doncea, S. M., Ion, R. M., Fierascui, R. C., Bacalum, E., Bunaciu, A. A., & Aboul-Enein, H. Y. (2010). Spectral methods for historical paper analysis: Composition and age approximation. *Instrumentation Science & Technology*, 38(1), 96-106.

- Drumright, R. E., Gruber, P. R., & Henton, D. E. (2000). Polylactic acid technology. *Advanced Materials*, 12(23), 1841-1846.
- Duan, Z., Thomas, N. L., & Huang, W. (2013). Water vapour permeability of poly(lactic acid) nanocomposites. *Journal of Membrane Science*, 445, 112 - 118.
- Dutrow, B. L., & Clark, C. M. (2019). *X-ray powder diffraction (XRD)*. Retrieved from Geochemical Instrumentation and Analysis website: https://serc.carleton.edu/research_education/geochemsheets/techniques/XRD.html
- El-Hadi, A. M. (2002). *Development of a biodegradable material based on poly(3-hydroxybutyrate) PHB*. (Doctoral Dissertation, Martin-Luther University Halle-Wittenberg).
- El-Hadi, A. M. (2017). Increase the elongation at break of poly (lactic acid) composites for use in food packaging films. *Scientific Reports*, 7, 1-14. doi: 10.1038/srep46767
- Elhi, F., Aid, T., & Koel, M. (2016). *Ionic liquids as solvents for making composite materials from cellulose*. Paper presented at the Proceedings of the Estonian Academy of Sciences.
- Farran, A., Cai, C., Sandoval, M., Xu, Y., Liu, J., Hernaiz, M. J., & Linhardt, R. J. (2015). Green solvents in carbohydrate chemistry: From raw materials to fine chemicals. *Chemical Reviews*, 115(14), 6811-6853. doi: 10.1021/cr500719h
- Feng, L., & Chen, Z.-l. (2008). Research progress on dissolution and functional modification of cellulose in ionic liquids. *Journal of Molecular Liquids*, 142(1-3), 1-5. doi: 10.1016/j.molliq.2008.06.007
- Figovsky, O., & Beilin, D. (2014). *Advanced polymer concretes and compounds*. Boca Raton: Taylor & Francis.
- Fortunati, E., Armentano, I., Zhou, Q., Puglia, D., Terenzi, A., Berglund, L. A., & Kenny, J. M. (2012). Microstructure and nonisothermal cold crystallization of PLA composites based on silver nanoparticles and nanocrystalline cellulose. *Polymer Degradation and Stability*, 97(10), 2027-2036. doi: 10.1016/j.polymdegradstab.2012.03.027
- Gajria, A. M., Dave, V., Gross, R. A., & McCarthy, S. P. (1996). Miscibility and biodegradability of blends of poly(lactic acid) and poly(vinyl acetate). *Polymer*, 37(3), 437-444.

- Galimova, E. M., Akhmetov, I. G., Borisenko, V. N., Galimov, R. R., & Sakhabutdinov, A. G. (2015). The influence of the molecular weight and viscosity of solution-polymerised styrene butadiene rubber on the properties of rubber mixes and vulcanisates. *International Polymer Science and Technology*, 42(3), 7-12.
- Gallagher, W. (1997). FTIR analysis of protein structure. *Biochemistry*, 392, 1-8.
- Gao, F. (2012). *Advances in polymer nanocomposites: Types and applications*. Cambridge, UK: Elsevier Science.
- Gao, T., Xie, R., Zhang, L., Gui, H., & Huang, M. (2015). Use of rubber process analyzer for characterizing the molecular weight parameters of natural rubber. *International Journal of Polymer Science*, 2015, 1-6. doi: 10.1155/2015/517260
- García-Contreras, R., Scougall-Vilchis, R., Acosta-Torres, L., Arenas-Arrocena, M., García-Garduño, R., & de la Fuente-Hernández, J. (2015). Vickers microhardness comparison of 4 composite resins with different types of filler. *Journal Oral Of Research*, 4(5), 313-320. doi: 10.17126/joralres.2015.061
- Garcia, D. E., Carrasco, J. C., Salazar, J. P., Perez, M. A., Cancino, R. A., & Riquelme, S. (2016). Bark polyflavonoids from *Pinus radiata* as functional building-blocks for polylactic acid (PLA)-based green composites. *Express Polymer Letters*, 10(10), 835-848. doi: 10.3144/expresspolymlett.2016.78
- García, D. E., Salazar, J. P., Riquelme, S., Delgado, N., & Paczkowski, S. (2017). Condensed tannin-based polyurethane as functional modifier of PLA-composites. *Polymer-Plastics Technology and Engineering*, 57(8), 709-726. doi: 10.1080/03602559.2017.1344855
- Garkhail, S. K., Meurs, E., Van de Beld, T., & Pejis, T. (1999). Thermoplastic composites based on biopolymers and natural fibres. *ICCM12 Conference Paris July 99th*, 1(1), 1-10.
- Garlotta, D. (2001). A literature review of poly(lactic acid). *Journal of Polymers and the Environment*, 9(2), 63-84.
- Grygiel, K., Chabanne, L., Men, Y., & Yuan, J. (2014). Thiazolium-containing poly(ionic liquid)s and ionic polymers. *Macromolecular Symposia*, 342(1), 67-77. doi: 10.1002/masy.201300171
- Gu, J., & Catchmark, J. M. (2013). Polylactic acid composites incorporating casein functionalized cellulose nanowhiskers. *Journal of Biological Engineering*, 7(1), 31-41. doi: 10.1186/1754-1611-7-31

- Guo, W., Tao, J., Yang, C., Song, C., Geng, W., Li, Q., . . . Wang, S. (2012). Introduction of environmentally degradable parameters to evaluate the biodegradability of biodegradable polymers. *PLoS One*, 7(5), 38341-38346. doi: 10.1371/journal.pone.0038341
- Gupta, A., & Katiyar, V. (2017). Cellulose functionalized high molecular weight stereocomplex polylactic acid biocomposite films with improved gas barrier, thermomechanical properties. *ACS Sustainable Chemistry & Engineering*, 5(8), 6835-6844. doi: 10.1021/acssuschemeng.7b01059
- Gupta, K. M., & Jiang, J. (2015). Cellulose dissolution and regeneration in ionic liquids: A computational perspective. *Chemical Engineering Science*, 121, 180-189. doi: 10.1016/j.ces.2014.07.025
- Halász, K., & Csóka, L. (2013). Plasticized biodegradable poly(lactic acid) based composites containing cellulose in micro- and nanosize. *Journal of Engineering*, 2013, 1-9. doi: 10.1155/2013/329379
- Hameed, N., & Guo, Q. (2010). Blend films of natural wool and cellulose prepared from an ionic liquid. *Cellulose*, 17, 803–813.
- Han, J., Zhou, C., French, A. D., Han, G., & Wu, Q. (2013). Characterization of cellulose II nanoparticles regenerated from 1-butyl-3-methylimidazolium chloride. *Carbohydrate Polymers*, 94(2), 773-781. doi: 10.1016/j.carbpol.2013.02.003
- Handy, S. T. (2011). *Ionic liquids – Classes and properties*. Rijeka, Croatia: Intech.
- Hassan, E., Wei, Y., Jiao, H., & Yu, M. (2013). Dynamic mechanical properties and thermal stability of poly(lactic acid) and poly(butylene succinate) blends composites. *Journal of Fiber Bioengineering and Informatics*, 6(1), 85-94. doi: 10.3993/jfbi03201308
- Helmenstine, A. M. (2017). *Green chemistry examples*. Retrieved from Thought Co. website: <https://www.thoughtco.com/green-chemistry-examples-607649>
- Hendrick, E., & Frey, M. (2014). Increasing Surface Hydrophilicity in Poly(Lactic Acid) Electrospun Fibers by Addition of Pla-b-Peg Co-Polymers. *Journal of Engineered Fibers and Fabrics*, 9(2), 153-164.
- Herrera, N., Roch, H., Salaberria, A. M., Pino-Orellana, M. A., Labidi, J., Fernandes, S. C. M., . . . Oksman, K. (2016). Functionalized blown films of plasticized polylactic acid/chitin nanocomposite: Preparation and characterization. *Materials & Design*, 92, 846-852. doi: 10.1016/j.matdes.2015.12.083

- Herrera, N., Salaberria, A. M., Mathew, A. P., & Oksman, K. (2015). Plasticized polylactic acid nanocomposite films with cellulose and chitin nanocrystals prepared using extrusion and compression molding with two cooling rates: Effects on mechanical, thermal and optical properties. *Composites: Part A*, 83, 89–97.
- Hina, S., Zhang, Y., & Wang, H. (2015). Role of ionic liquids in dissolution and regeneration of cellulose. *Reviews on Advanced Materials Science*, 40, 215-226.
- Hishammuddin, N., & Zakaria, Z. (2016). Mechanical strength properties of chitin/polylactic acid biocomposite film. *eProceedings Chemistry*, 1(1), 31-35.
- Holm, J., & Lassi, U. (2011). Ionic Liquids in the Pretreatment of Lignocellulosic Biomass. In A. Kokorin (Ed.), *Ionic Liquids: Applications and Perspectives* (pp. 545-560): InTech.
- Huda, M., Drzal, L., Mohanty, A., & Misra, M. (2006). Chopped glass and recycled newspaper as reinforcement fibers in injection molded poly(lactic acid) (PLA) composites: A comparative study. *Composites Science and Technology*, 66(11-12), 1813-1824. doi: 10.1016/j.compscitech.2005.10.015
- Huda, M. S., Schmidt, W. F., Misra, M., & Drzal, L. T. (2013). Effect of fiber surface treatment of poultry feather fibers on the properties of their polymer matrix composites. *Journal of Applied Polymer Science*, 128(2), 1117-1124. doi: 10.1002/app.38306
- Huddleston, J. G., Visser, A. E., Reichert, W. M., Willauer, H. D., Broker, G. A., & Rogers, R. D. (2001). Characterization and comparison of hydrophilic and hydrophobic room temperature ionic liquids incorporating the imidazolium cation. *Green Chemistry*, 3, 156-164.
- Idris, A., Vijayaraghavan, R., Rana, U. A., Fredericks, D., Patti, A. F., & MacFarlane, D. R. (2013). Dissolution of feather keratin in ionic liquids. *Green Chemistry*, 15(2), 525-534. doi: 10.1039/c2gc36556a
- Inkinen, S., Hakkarainen, M., Albertsson, A. C., & Sodergard, A. (2011). From lactic acid to poly(lactic acid) (PLA): Characterization and analysis of PLA and its precursors. *Biomacromolecules*, 12(3), 523-532. doi: 10.1021/bm101302t
- Isik, M., Sardon, H., & Mecerreyes, D. (2014). Ionic liquids and cellulose: dissolution, chemical modification and preparation of new cellulosic materials. *International Journal of Molecular Sciences*, 15(7), 11922-11940. doi: 10.3390/ijms150711922

- Jawaid, M., & Swain, S. K. (2018). *Bionanocomposites for packaging application*. Switzerland: Springer.
- Jiang, H., Wang, L. B., Xu, D. J., & Liu, X. Y. (2014). Comparison of solvent-casting and melt-compounding blended biomedical (polylactide)-(polyethylene glycol) mixture as drug carrier. *Advanced Materials Research*, 1002, 99-104.
- Jouannin, C., Tourne-Peteilh, C., Darcos, V., Sharkawi, T., Devoisselle, J.-M., Gaveau, P., . . . Viau, L. (2014). Drug delivery systems based on pharmaceutically active ionic liquids and biocompatible poly(lactic acid). *Journal of Materials Chemistry B*, 2, 3133–3141.
- Kaczmarek, H., Nowicki, M., Vuković-Kwiatkowska, I., & Nowakowska, S. (2013). Crosslinked blends of poly(lactic acid) and polyacrylates: AFM, DSC and XRD studies. *Journal of Polymer Research*, 20, 91-103.
- Kakar, A., Jayamani, E., Heng, S. K., Bakri, M. K. B., & Hamdan, S. (2015). Optimization of hot press compression molding and fabrication of poly lactic acid. *Australian Journal of Basic and Applied Sciences*, 9(8), 105-112.
- Kamavaram, V., & Reddy, R. G. (2008). Thermal stabilities of di-alkylimidazolium chloride ionic liquids. *International Journal of Thermal Sciences*, 47(6), 773-777. doi: 10.1016/j.ijthermalsci.2007.06.012
- Kammiovirta, K., Jaaskelainen, A.-S., Kuutti, L., Holopainen-Mantila, U., Paananen, A., Suurnakki, A., & Orelma, H. (2016). Keratin-reinforced cellulose filaments from ionic liquid solutions. *RSC Advances*, 6, 88797–88806.
- Ke, T., Sun, S. X., & Seib, P. (2003). Blending of poly(lactic acid) and starches containing varying amylose content. *Journal of Applied Polymer Science*, 89, 3639–3646
- Ketabchi, M. R., Khalid, M., Ratnam, C. T., & Walvekar, R. (2016). Mechanical and thermal properties of polylactic acid composites reinforced with cellulose nanoparticles extracted from kenaf fibre. *Materials Research Express*, 3(12), 125301. doi: 10.1088/2053-1591/3/12/125301
- Khosa, M., & Ullah, A. (2013). A sustainable role of keratin biopolymer in green chemistry: A review. *Journal of Food Processing & Beverages*, 1(1), 1-8.
- Kock, J. W. (2006). *Physical and mechanical properties of chicken feather materials*. (Master's Thesis, Georgia Institute of Technology).

- Koh, J. J., Zhang, X., & He, C. (2018). Fully biodegradable poly(lactic acid)/starch blends: A review of toughening strategies. *International Journal of Biological Macromolecules*, *109*, 99-113. doi: 10.1016/j.ijbiomac.2017.12.048
- Kuzmina, O., Heinze, T., & Wawro, D. (2012). Blending of Cellulose and Chitosan in Alkyl Imidazolium Ionic Liquids. *ISRN Polymer Science*, *2012*, 1-9. doi: 10.5402/2012/251950
- Lam, P. M., Lau, K. T., Zhao, Y. Q., Cheng, S., & Liu, T. (2009). *Development of an eco-friendly CFF/PLA biocomposite*. Paper presented at the 17th International Conference on Composite Materials, Edinburgh, UK.
- Lee, S. H., & Yeo, S. Y. (2016). Improvement of hydrophilicity of polylactic acid (PLA) fabrics by means of a proteolytic enzyme from *Bacillus licheniformis*. *Fibers and Polymers*, *17*(8), 1154-1161. doi: 10.1007/s12221-016-5923-z
- Li, H., Cao, Z., Wu, D., Tao, G., Zhong, W., Zhu, H., . . . Liu, C. (2016). Crystallisation, mechanical properties and rheological behaviour of PLA composites reinforced by surface modified microcrystalline cellulose. *Plastics, Rubber and Composites*, *45*(4), 181-187. doi: 10.1179/1743289815y.0000000040
- Li, J., Li, J., Feng, D., Zhao, J., Sun, J., & Li, D. (2017). Comparative study on properties of polylactic acid nanocomposites with cellulose and chitin nanofibers extracted from different raw materials. *Journal of Nanomaterials*, *2017*, 1-11. doi: 10.1155/2017/7193263
- Li, S., Meng Lin, M., Toprak, M. S., Kim, D. K., & Muhammed, M. (2010). Nanocomposites of polymer and inorganic nanoparticles for optical and magnetic applications. *Nano Reviews*, *1*. doi: 10.3402/nano.v1i0.5214
- Li, S. M., Yuan, H., Yu, T., Yuan, W. Z., & Ren, J. (2009). Flame-retardancy and anti-dripping effects of intumescent flame retardant incorporating montmorillonite on poly(lactic acid). *Polymers for Advanced Technologies*, *20*(12), 1114-1120. doi: 10.1002/pat.1372
- Li, X., Qin, A., Zhao, X., Ma, B., & He, C. (2014). The plasticization mechanism of polyacrylonitrile/1-butyl-3-methylimidazolium chloride system. *Polymer*, *55*(22), 5773-5780.
- Liebeck, B. M., Hidalgo, N., Roth, G., Popescu, C., & Boker, A. (2017). Synthesis and characterization of methyl cellulose/keratin hydrolysate composite membranes. *Polymers (Basel)*, *9*(3). doi: 10.3390/polym9030091

- Lim, K., Ching, Y., & Gan, S. (2015). Effect of palm oil bio-based plasticizer on the morphological, thermal and mechanical properties of poly(vinyl chloride). *Polymers*, 7(10), 2031-2043. doi: 10.3390/polym7101498
- Liu, D. Y., Yuan, X. W., Bhattacharyya, D., & Easteal, A. J. (2010). Characterisation of solution cast cellulose nanofibre – reinforced poly(lactic acid). *Express Polymer Letters*, 4(1), 26-31. doi: 10.3144/expresspolymlett.2010.5
- Lu, Y., Chen, Y.-C., & Zhang, P.-H. (2016). Preparation and characterisation of polylactic acid (PLA)/polycaprolactone (PCL) composite microfibre membranes. *Fibres & Textiles in Eastern Europe*, 24(3), 17-25.
- Ma, Y.-Y., Qi, R.-R., Jia, S.-Y., & Wang, Z.-H. (2016). *Preparation and characterization of keratin–cellulose composite films*. Paper presented at the 2nd Annual International Conference on Advanced Material Engineering (AME 2016), Wuhan, China.
- Manavitehrani, I., Fathi, A., Badr, H., Daly, S., Negahi Shirazi, A., & Dehghani, F. (2016). Biomedical applications of biodegradable polyesters. *Polymers*, 8(1), 20. doi: 10.3390/polym8010020
- Marras, S. I., Zuburtikudis, I., & Panayiotou, C. (2010). Solution casting versus melt compounding: Effect of fabrication route on the structure and thermal behavior of poly(l-lactic acid) clay nanocomposites. *Journal of Materials Science*, 45(23), 6474-6480. doi: 10.1007/s10853-010-4735-6
- Martin, O., & Averous, L. (2001). Poly(lactic acid): Plasticization and properties of biodegradable multiphase systems. *Polymer*, 42, 6209-6219.
- Martins, M., Craveiro, R., Paiva, A., Duarte, A. R. C., & Reis, R. L. (2014). Supercritical fluid processing of natural based polymers doped with ionic liquids. *Chemical Engineering Journal*, 241, 122–130.
- Masmoudi, F., Bessadok, A., Dammak, M., Jaziri, M., & Ammar, E. (2016). Biodegradable packaging materials conception based on starch and polylactic acid (PLA) reinforced with cellulose. *Environmental Science and Pollution Research*, 23(20), 20904-20914. doi: 10.1007/s11356-016-7276-y
- Mathew, A. P., Oksman, K., & Sain, M. (2005). Mechanical properties of biodegradable composites from poly lactic acid (PLA) and microcrystalline cellulose (MCC). *Journal of Applied Polymer Science*, 97(5), 2014-2025. doi: 10.1002/app.21779

- Matsuura, Y., & Furuta, K. (2015). Properties of polyferrocenylsilane dissolved in ionic liquids. *Journal of Molecular Liquids*, 212, 671-674. doi: 10.1016/j.molliq.2015.10.022
- Mecerreyes, D. (2015). Ionic liquids as solvents and/or catalysts in polymerization. In K. Vijayakrishna, K. Manojkumar & A. Sivaramakrishna (Eds.), *Applications of ionic liquids in polymer science and technology*. New York, USA: Springer.
- Medeiros, I. S., Gomes, M., Loguercio, A., & Filho, L. R. (2007). Diametral tensile strength and Vickers hardness of a composite after storage in different solutions. *Journal of Oral Science*, 49(1), 61-66. doi: 10.2334/josnusd.49.61
- Menon, A. R. R. (1999). Melt-rheology of natural rubber modified with phosphorylated cashew nut shell liquid prepolymer - A comparative study with spindle oil. *Iranian Polymer Journal*, 8(3), 167-171.
- Mohd Asri, S. E. A., Zakaria, Z., Hassan, A., & Mohamad Haafiz, M. K. (2014). Effect of fermented chitin nanowhiskers on properties of polylactic acid biocomposite films. *The Malaysian Journal of Analytical Sciences*, 18(2), 385 - 390.
- Muller, J., Gonzalez-Martinez, C., & Chiralt, A. (2017). Combination of poly(lactic) acid and starch for biodegradable food packaging. *Materials (Basel)*, 10(8), 952-973. doi: 10.3390/ma10080952
- Murphy, C. A., & Collins, M. N. (2016). Microcrystalline cellulose reinforced polylactic acid biocomposite filaments for 3D printing. *Polymer Composites*. doi: 10.1002/pc.24069
- Na Ayutthaya, S. I., Tanpichai, S., & Wootthikanokkhan, J. (2015). Keratin extracted from chicken feather waste: Extraction, preparation, and structural characterization of the keratin and keratin/biopolymer films and electrospuns. *Journal of Polymers and the Environment*, 23(4), 506-516.
- Na Ayutthaya, S. I., & Wootthikanokkhan, J. (2013). Extraction of keratin from chicken feather and electrospinning of the keratin/PLA blends. *Advanced Materials Research*, 747, 711-714.
- Nagarajan, V., Mohanty, A. K., & Misra, M. (2016). Perspective on polylactic acid (PLA) based sustainable materials for durable applications: Focus on toughness and heat resistance. *ACS Sustainable Chemistry & Engineering*, 4, 2899-2916.
- Nanthananon, P., Seadan, M., Pivsa-Art, S., & Suttiruengwong, S. (2015). Enhanced crystallization of poly (lactic acid) through reactive aliphatic bisamide. *IOP*

Conference Series: Materials Science and Engineering, 87, 012067. doi: 10.1088/1757-899x/87/1/012067

- Nasrin, R., Biswas, S., Rashid, T. U., Afrin, S., Jahan, R. A., Haque, P., & Rahman, M. M. (2017). Preparation of chitin-PLA laminated composite for implantable application. *Bioactive Materials*, 2(4), 199-207. doi: 10.1016/j.bioactmat.2017.09.003
- Nijnenhuis, A. J., Colstee, E., Grijpma, D. W., & Pennings, A. J. (1996). High molecular weight poly(L-lactide) and poly(ethylene oxide) blends: Thermal characterization and physical properties. *Polymer*, 37(26), 5849-5857. doi: 10.1016/S0032-3861(96)00455-7
- Niroomand, F., Khosravani, A., & Younesi, H. (2016). Fabrication and properties of cellulose-nanochitosan biocomposite film using ionic liquid. *Cellulose*, 23, 1311–1324.
- Nishikawa, K., Wang, S., Katayanagi, H., Hayashi, S., Hamaguchi, H.-o., Koga, Y., & Tozaki, K.-i. (2007). Melting and freezing behaviors of prototype ionic liquids, 1-butyl-3-methylimidazolium bromide and its chloride, studied by using a nano-watt differential scanning calorimeter. *The Journal of Physical Chemistry B*, 111(18), 4894-4900. doi: 10.1021/jp0671852
- Odahara, S., Yamauchi, T., & Fukuda, T. (2009). Effects of notch shape and cyclic loading test frequency on the fatigue strength properties of poly-lactic acid. *Research reports of Sasebo National College of Technology*, 45, 11-14.
- Olsson, C. (2014). *Cellulose processing in ionic liquid based solvents*. (Doctoral Dissertation, Chalmers University of Technology).
- Orozco, V. H., Brostow, W., Chonkaew, W., & López, B. L. (2009). Preparation and characterization of poly(lactic acid)-g-maleic anhydride + starch blends. *Macromolecular Symposia*, 277(1), 69-80. doi: 10.1002/masy.200950309
- Pang, J., Liu, X., Zhang, X., Wu, Y., & Sun, R. (2013). Fabrication of Cellulose Film with Enhanced Mechanical Properties in Ionic Liquid 1-Allyl-3-methylimidazolium Chloride (AmimCl). *Materials (Basel)*, 6(4), 1270-1284. doi: 10.3390/ma6041270
- Park, K.-I. (2008). *Ionic liquids as additives for biodegradable polylactic acid*. (Doctoral Dissertation, New Jersey Institute of Technology).

- Peng, N., Lv, R., Jin, T., Na, B., Liu, H., & Zhou, H. (2017). Thermal and strain-induced phase separation in an ionic liquid plasticized polylactide. *Polymer*, *108*, 442-448. doi: 10.1016/j.polymer.2016.12.024
- Peng, X., Ren, J., Zhong, L., & Sun, R. (2011). Homogeneous synthesis of hemicellulosic succinates with high degree of substitution in ionic liquid. *Carbohydrate Polymers*, *86*(4), 1768-1774. doi: 10.1016/j.carbpol.2011.07.018
- Petersson, L., & Oksman, K. (2006). Preparation and properties of biopolymer-based nanocomposite films using microcrystalline cellulose *Cellulose Nanocomposites* (Vol. 938, pp. 132-150). Trondheim, Norway: ACS Symposium Series.
- Pillin, I., Montrelay, N., & Grohens, Y. (2006). Thermo-mechanical characterization of plasticized PLA: Is the miscibility the only significant factor? *Polymer*, *47*(13), 4676-4682. doi: 10.1016/j.polymer.2006.04.013
- Pinkert, A., Marsh, K. N., Pang, S., & Staiger, M. P. (2009). Ionic liquids and their interaction with cellulose. *Chemical Reviews*, *109*(12), 6712-6728.
- Plechkova, N. V., & Seddon, K. R. (2007). Ionic liquids: "Designer" solvents for green chemistry. In P. Tundo, A. Perosa & F. Zecchini (Eds.), *Methods and reagents for green chemistry: An introduction* (pp. 105-130). Venice, Italy: John Wiley & Sons, Inc.
- Pospiech, B. (2015). Application of phosphonium ionic liquids as ion carriers in polymer inclusion membranes (PIMs) for separation of cadmium(II) and copper(II) from aqueous solutions. *Journal of Solution Chemistry*, *44*(12), 2431-2447. doi: 10.1007/s10953-015-0413-2
- Râpă, M., Darie, R., Grosu, E., Tănase, E., Trifoi, A., Pap, T., & Vasile, C. (2015). Effect of plasticizers on melt processability and properties of PHB. *Journal of Optoelectronics and Advanced Materials*, *17*(11-12)(11), 1778-1784.
- Râpă, M., Darie, R., & Vasile, C. (2017). Influence of plasticizers over some physico-chemical properties of PLA. *Materiale Plastice*, *54*(1), 73-78.
- Ren, J., Zhang, W., Lou, F., Wang, Y., & Guo, W. (2017). Characteristics of starch-based films produced using glycerol and 1-butyl-3-methylimidazolium chloride as combined plasticizers. *Starch - Stärke*, *69*(1-2), 1600161.
- Rhim, J.-W., Mohanty, A. K., Singh, S. P., & Ng, P. K. W. (2006). Effect of the processing methods on the performance of polylactide films: Thermocompression versus solvent casting. *Journal of Applied Polymer Science*, *101*(6), 3736-3742. doi: 10.1002/app.23403

- Rosewald, M., Hou, F. Y., Mututuvvari, T., Harkins, A. L., & Tran, C. D. (2014). Cellulose-chitosan-keratin composite materials: Synthesis, immunological and antibacterial properties. *ECS Transactions*, 64(4), 499-505. doi: 10.1149/06404.0499ecst
- Salaberria, A. M., R, H. D., Andres, M. A., Fernandes, S. C. M., & Labidi, J. (2017). The antifungal activity of functionalized chitin nanocrystals in poly (lactid acid) films. *Materials (Basel)*, 10(5). doi: 10.3390/ma10050546
- Schmidt, W. F., & Jayasundera, S. (2004). Microcrystalline avian keratin protein fibers. In F. T. Wallenberger & N. E. Weston (Eds.), *Natural Fibers, Plastics and Composites* (pp. 51-66). Massachusetts: Kluwer Academic Publishers.
- Setiawan, A. H. (2015). Determination of crystallization and melting behaviour of poly-lactic acid and polypropyleneblends as a food packaging materials by differential scanning calorimeter. *International Symposium on Applied Chemistry 2015*, 16, 489-494. doi: 10.1016/j.proche.2015.12.083
- Shamsuri, A. A., & Daik, R. (2015). Applications of ionic liquids and their mixtures for preparation of advanced polymer blends and composites: A short review. *Reviews on Advanced Materials Science*, 40(1), 45-59.
- Shanks, R. A. (2014). Chemistry and structure of cellulosic fibres as reinforcements in natural fibre composites. In A. Hodzic & R. Shanks (Eds.), *Natural Fibre Composites: Materials, Processes and Properties* (pp. 66-83). United Kingdom: Woodhead Publishing Limited.
- Sharma, S., & Gupta, A. (2016). Sustainable management of keratin waste biomass: Applications and future perspectives. *Brazilian Archives of Biology and Technology*, 59(0). doi: 10.1590/1678-4324-2016150684
- Shirai, M. A., Olivato, J. B., Demiate, I. M., Müller, C. M. O., Grossmann, M. V. E., & Yamashita, F. (2016). Poly(lactic acid)/thermoplastic starch sheets: Effect of adipate esters on the morphological, mechanical and barrier properties. *Polímeros*, 26(1), 66-73. doi: 10.1590/0104-1428.2123
- Sigler, M. (2014). The effects of plastic pollution on aquatic wildlife: Current situations and future solutions. *Water, Air, & Soil Pollution*, 225(11). doi: 10.1007/s11270-014-2184-6
- Silverajah, V. S., Ibrahim, N. A., Zainuddin, N., Yunus, W. M., & Hassan, H. A. (2012). Mechanical, thermal and morphological properties of poly(lactic acid)/epoxidized palm olein blend. *Molecules*, 17(10), 11729-11747. doi: 10.3390/molecules171011729

- Singh, T., & Kumar, A. (2011). Cation-anion-water interactions in aqueous mixtures of imidazolium based ionic liquids. *Vibrational Spectroscopy*, 55(1), 119-125. doi: 10.1016/j.vibspec.2010.09.009
- Sinkiewicz, I., Sliwiska, A., Staroszczyk, H., & Kołodziejski, I. (2017). Alternative methods of preparation of soluble keratin from chicken feathers. *Waste and Biomass Valorization*, 8(4), 1043–1048.
- Sippel, P., Dietrich, V., Reuter, D., Aumüller, M., Lunkenheimer, P., Loidl, A., & Krohns, S. (2016). Impact of water on the charge transport of a glass-forming ionic liquid. *Journal of Molecular Liquids*, 223, 635-642. doi: 10.1016/j.molliq.2016.08.103
- Spiridon, I., Paduraru, O. M., Zaltariov, M. F., & Darie, R. N. (2013). Influence of keratin on polylactic acid/chitosan composite properties. Behavior upon accelerated weathering. *Industrial & Engineering Chemistry Research*, 52(29), 9822-9833. doi: 10.1021/ie400848t
- Subramani, T., Krishnan, S., Ganesan, S. K., & Nagarajan, G. (2014). Investigation of mechanical properties in polyester and phenyl-ester composites reinforced with chicken feather fiber. *International Journal of Engineering Research and Applications*, 4(12), 93-104.
- Sullivan, E. M., Moon, R. J., & Kalaitzidou, K. (2015). Processing and Characterization of Cellulose Nanocrystals/Poly(lactic acid) Nanocomposite Films. *Materials*, 8(12), 8106-8116. doi: 10.3390/ma8125447
- Sun, Z., Chen, X., Ma, X., Cui, X., Yi, Z., & Li, X. (2018). Cellulose/keratin–catechin nanocomposite hydrogel for wound hemostasis. *Journal of Materials Chemistry B*, 6(38), 6133-6141. doi: 10.1039/c8tb01109e
- Suwannakas, P., Petrchwattana, N., & Covavisaruch, S. (2016). *Bioplastic composite foam prepared from poly(lactic acid) and natural wood flour*. Paper presented at the AIP Conference Proceedings, Naples, Italy.
- Swatloski, R. P., Spear, S. K., Holbrey, J. D., & Rogers, R. D. (2002). Dissolution of cellulose with ionic liquids. *Journal of the American Chemical Society*, 124(18), 4974-4975.
- Tabi, T., Sajo, I. E., Szabo, F., Luyt, A. S., & Kovacs, J. G. (2010). Crystalline structure of annealed polylactic acid and its relation to processing. *Express Polymer Letters*, 4(10), 659-668. doi: 10.3144/expresspolymlett.2010.80

- Tanase, C. E., & Spiridon, I. (2014). PLA/chitosan/keratin composites for biomedical applications. *Materials Science and Engineering C*, 40, 242-247. doi: 10.1016/j.msec.2014.03.054
- Tang, Z., Zhang, C., Liu, X., & Zhu, J. (2012). The crystallization behavior and mechanical properties of polylactic acid in the presence of a crystal nucleating agent. *Journal of Applied Polymer Science*, 125(2), 1108-1115. doi: 10.1002/app.34799
- Tawakkal, I. S. M. A., Talib, R. A., Khalina, A., Chin, N. L., & Ibrahim, M. N. (2010). Optimisation of processing variables of kenaf derived cellulose reinforced polylactic acid. *Asian Journal of Chemistry*, 99(9), 6652-6662.
- Tee, Y. B., Talib, R. A., Abdan, K., Chin, N. L., Basha, R. K., & Yunus, K. F. M. (2014). Toughening poly(Lactic Acid) and aiding the melt-compounding with bio-sourced plasticizers. *Agriculture and Agricultural Science Procedia*, 2, 289-295. doi: 10.1016/j.aaspro.2014.11.041
- Teoh, E. L., Mariatti, M., & Chow, W. S. (2016). Thermal and flame resistant properties of poly (lactic acid)/poly (methyl methacrylate) blends containing halogen-free flame retardant. *5th International Conference on Recent Advances in Materials, Minerals and Environment (Ramm) & 2nd International Postgraduate Conference on Materials, Mineral and Polymer (Mamip)*, 19, 795-802. doi: 10.1016/j.proche.2016.03.087
- Thakur, V. K., & Thakur, M. K. (2017). *Functional biopolymers*. Switzerland: Springer International Publishing.
- Thompson, R. C., Moore, C. J., Vom Saal, F. S., & Swan, S. H. (2009). Plastics, the environment and human health: Current consensus and future trends. *Philosophical Transactions of the Royal Society B*, 364(1526), 2153-2166. doi: 10.1098/rstb.2009.0053
- Torres, J. E. R. (2010). *Hardness characteristics of unidirectional nanowire-alumina nanocomposites*. (Master's Thesis, The Florida State University).
- Tran, C. D., & Mututuvvari, T. M. (2015). Cellulose, chitosan, and keratin composite materials. Controlled drug release. *Langmuir*, 31, 1516–1526.
- Tran, C. D., & Mututuvvari, T. M. (2016). Cellulose, chitosan and keratin composite materials. Facile and recyclable synthesis, conformation and properties. *ACS Sustainable Chemistry & Engineering*, 4(3), 1850-1861. doi: 10.1021/acssuschemeng.6b00084

- Tran, C. D., Proscenc, F., Franko, M., & Benzi, G. (2016). Synthesis, structure and antimicrobial property of green composites from cellulose, wool, hair and chicken feather. *Carbohydrate Polymers*, *151*, 1269–1276.
- Trivedi, T. J., & Kumar, A. (2015). Utilization of ionic liquids for the processing of biopolymers. In S. Jose & T. Bhaskar (Eds.), *Biomass and biofuels: Advanced biorefineries for sustainable production and distribution* (pp. 127-154). Boca Raton: Taylor and Francis.
- Tshela Ntumba, Y.-H., & Prochoń, M. (2016). The effect of modified keratin on the thermal properties of a cellulosic–elastomeric material. *Journal of Thermal Analysis and Calorimetry*, *125*(3), 1151-1160. doi: 10.1007/s10973-016-5590-8
- Tuason, D. C., Amundarain, J., Krawczyk, G. R., Selinger, E., Blakemore, W. R., Modliszewski, J. J., . . . Messick, F. (2014). United States of America Patent No. US008801847 B2. F. Corporation.
- Turner, M. B., Spear, S. K., Holbrey, J. D., & Rogers, R. D. (2004). Production of bioactive cellulose films reconstituted from ionic liquids. *Biomacromolecules*, *5*(4), 1379-1384.
- Wang, H., Gurau, G., & Rogers, R. D. (2012). Ionic liquid processing of cellulose. *Chemical Society Reviews*, *41*(4), 1519-1537. doi: 10.1039/c2cs15311d
- Wang, J., Hao, S., Luo, T., Cheng, Z., Li, W., Gao, F., . . . Wang, B. (2017). Feather keratin hydrogel for wound repair: Preparation, healing effect and biocompatibility evaluation. *Colloids and Surfaces B: Biointerfaces*, *149*, 341–350.
- Wang, M., Zhao, T., Wang, G., & Zhou, J. (2014). Blend films of human hair and cellulose prepared from an ionic liquid. *Textile Research Journal*, *84*(12), 1315–1324.
- Wasewar, K. (2013). Low sulfur liquid fuel by deep desulfurization using ionic liquid. *Journal on Future Engineering and Technology*, *8*(1), 1-5. doi: 10.26634/jfet.8.1.1973
- Watanabe, Y., Iwamoto, T., Teramoto, A., Abe, K., & Ohkoshi, Y. (2004). Biodegradability of poly (L-lactic acid) functionally graded materials with hardness gradient. *Materials Transactions*, *45*(4), 1005-1009.
- Webb, H., Arnott, J., Crawford, R., & Ivanova, E. (2012). Plastic degradation and its environmental implications with special reference to poly(ethylene terephthalate). *Polymers*, *5*(1), 1-18. doi: 10.3390/polym5010001

- Welton, T. (2015). Solvents and sustainable chemistry. *Proceedings of the Royal Society of London A*, 471(2183), 20150502. doi: 10.1098/rspa.2015.0502
- Wu, J., Bai, J., Xue, Z., Liao, Y., Zhou, X., & Xie, X. (2015). Insight into glass transition of cellulose based on direct thermal processing after plasticization by ionic liquid. *Cellulose*, 22, 89–99.
- Xiao, L., Wang, B., Yang, G., & Gauthier, M. (2012). Poly(lactic acid)-based biomaterials: Synthesis, modification and applications. In D. N. Ghista (Ed.), *Biomedical Science, Engineering and Technology* (pp. 247-282): IntechOpen.
- Yaacab, N. D., Ismail, H., & Ting, S. S. (2016). Potential use of paddy straw as Filler in poly lactic acid/paddy straw powder biocomposite: Thermal and thermal properties. *Procedia Chemistry*, 19, 757-762. doi: 10.1016/j.proche.2016.03.081
- Yamamuro, O., Minamimoto, Y., Inamura, Y., Hayashi, S., & Hamaguchi, H.-o. (2006). Heat capacity and glass transition of an ionic liquid 1-butyl-3-methylimidazolium chloride. *Chemical Physics Letters*, 423(4-6), 371-375. doi: 10.1016/j.cplett.2006.03.074
- Yee, Y. Y., Ching, Y. C., Rozali, S., Hashim, N. A., & Singh, R. (2016). Preparation and characterization of poly(lactic acid)-based composite reinforced with oil palm empty fruit bunch fiber and nanosilica. *BioResources*, 11(1), 2269-2286.
- Yeh, J.-T., Yang, M.-C., Wu, C.-J., Wu, X., & Wu, C.-S. (2008). Study on the crystallization kinetic and characterization of poly(lactic acid) and poly(vinyl alcohol) blends. *Polymer-Plastics Technology and Engineering*, 47, 1289–1296.
- Yin, H.-M., Qian, J., Zhang, J., Lin, Z.-F., Li, J.-S., Xu, J.-Z., & Li, Z.-M. (2016). Engineering porous poly(lactic acid) scaffolds with high mechanical performance via a solid state extrusion/porogen leaching approach. *Polymers*, 8(6), 213. doi: 10.3390/polym8060213
- Young, J. A. (2008). Chloroform. *Journal of Chemical Education*, 85(5), 628. doi: 10.1021/ed085p628
- Zhang, F., Ren, H., & Lee, J. (2013). Study of the structural properties of microcrystalline cellulose (MCC) particles from distillers grains (DG) by XRD, FTIR and SEM. *Applied Mechanics and Materials*, 295-298, 339-344.
- Zhang, J.-F., & Sun, X. (2004). Mechanical properties of poly(lactic acid)/starch composites compatibilized by maleic anhydride. *Biomacromolecules*, 5, 1446-1451.

- Zhang, J., Wu, J., Yu, J., Zhang, X., He, J., & Zhang, J. (2017a). Application of ionic liquids for dissolving cellulose and fabricating cellulose-based materials: state of the art and future trends. *Materials Chemistry Frontiers*, 1(7), 1273-1290. doi: 10.1039/c6qm00348f
- Zhang, L., Liu, J., Sui, S. Y., Dong, C. H., Xu, J. T., & Zhu, P. (2017b). Study on the preparation and characterization of cross-linked film of human hair keratin and cellulose. *Ferroelectrics*, 521(1), 77-85. doi: 10.1080/00150193.2017.1390964
- Zhang, M., Kamavaram, V., & Reddy, R. G. (2005). Thermodynamic properties of 1-butyl-3-methylimidazolium chloride (C₄mim[Cl]) ionic liquid. *Journal of Phase Equilibria and Diffusion*, 26(2), 124-130. doi: 10.1007/s11669-005-0131-3
- Zhang, P., Peng, L., & Li, W. (2008). Application of ionic liquid [bmim]PF₆ as green plasticizer for poly(L-lactide). In S. Agarwal & A. Greiner (Eds.), *e-Polymers* (Vol. 8).
- Zhao, Y. Q., Lau, K. T., Liu, T., Cheng, S., Lam, P. M., & Li, H. L. (2008). Production of a green composite: Mixture of poly (lactic acid) and keratin fibers from chicken feathers. *Advanced Materials Research*, 47-50, 1225-1228.